University of Zurich[UZH]

Potential sources of soil organic carbon in forests of different ages in Jaun, Switzerland - assessed by lipid analysis

ESS 511 Master's Thesis

Author
Nils Mathias Güntert
16-927-329

Supervised by
Tatjana Carina Speckert

Faculty representative
PD Dr. Guido Lars Bruno Wiesenberg

06.04.2023
Department of Geography, University of Zurich

Abstract

Despite the relevance of soil organic matter (SOM) for the global carbon cycle, many gaps in knowledge persist regarding the sources of soil organic carbon (SOC), its preservation, and its transformation. Studying individual compound classes of SOM, such as *n*-alkanes and fatty acids, enables insight into the plant-soil carbon cycle. For this purpose, lipid distributions of fresh plant samples representing the carbon source materials, the partially degraded organic horizons, and the mineral topsoil were identified. Carbon (C) and nitrogen (N) concentrations, and δ^{13}C isotope values were also determined. The study took place in an alpine ecosystem in Jaun, Switzerland, consisting of forest areas that are either 40-, 55-, or 130-years-old. C concentrations showed a continuous decrease through the degradation stages from the fresh plant materials via the organic horizons to the topsoil, on average ranging between 48.7 ± 0.8 % and 6.7 ± 1.4 %. δ^{13}C values show continuous ^{13}C enrichment from the organic horizons to the topsoil, on average ranging between -27.8 ± 0.4 ‰ and -26.4 ± 0.2 ‰. Depending on the forest area, N concentrations reached maximum values either in the litter layer, Oi, or Oe horizon. A substantial decrease in N concentration can be observed from the Oe horizon to the Oa horizon and further to the topsoil. N concentrations range on average between 1.1 ± 0.3 % and 0.4 ± 0.1 %. The main findings of the lipid distributions were: (1) the importance of spruce needles which are shown as the dominant source material for SOC regarding *n*-alkanes as a biomarker, as well as the importance of spruce twigs to the soil carbon concerning fatty acids as a biomarker, (2) no significant differences in vegetative influences between the investigated areas of different forest ages regarding the molecular litter inputs, but significant differences in the lower organic horizons and the topsoil, which might be explained with differences in preservation or decomposition, (3) preferential degradation of short-chained components or preferential preservation of long-chained molecules, (4) highest degradation rate of organic material in the lower organic horizons Oe and Oa, and lower microbial turnover in the organic horizon Oi and the topsoil. However, further research is needed. Besides the investigated plant samples in this thesis, other sample types, such as spruce cones or fungi, might also contribute significantly to SOC. It would also be interesting to investigate expected climate-related changes at the molecular lipid level to incorporate new findings into future climate models.

Contents

List of Figures

List of Tables

Abbreviations

ACL	Average chain length
Alk	*n*-Alkane
A-fraction	Aliphatic hydrocarbons
a-value	Color space, greenness to redness
B-fraction	Aromatic fraction
b-value	Color space, blueness to yellowness
C	Carbon
C-fraction	Heterocompounds
CPI	Carbon preference index
DCM	Dichloromethane
FA	Fatty acid
GC	Gas chromatography
GC-FID	Gas chromatography with flame ionisation detector
GC-MS	Gas chromatography with mass spectrometry
H-fraction	Carboxylic acids
KOH	Potassium hydroxide
L-value	Lightness, darkness to lightness
N	Nitrogen
N-fraction	Neutral compounds
OEP	Odd-over-even predominance
OM	Organic matter
P-fraction	High molecular weight compounds
SOC	Soil organic carbon
SOM	Soil organic matter
TOC	Total organic carbon
TLE	Total lipid extract
TN	Total nitrogen

1 Introduction

The soil belongs to the second largest carbon sink after the ocean (Zhang et al., 2017), represents an essential short- to long-term storage medium of carbon, and is significantly important in the global carbon cycle (Thomas et al., 2021), and for climate change mitigation (Amelung et al., 2020). Soil organic matter (SOM) consists of plant and animal detritus at different stages of decay, soil microbes, and the substances they synthesize (Baldock and Skjemstad, 2000). Soils contain more than 10 times as much carbon as the entire forest biomass, and more than the atmosphere and terrestrial vegetation combined (Zhang et al., 2017). Therefore SOM dynamics and the ability of soils to store carbon through SOM management have recently received considerable attention (Lal, 2016). Despite the importance of understanding processes related to SOM, many gaps in knowledge regarding the formation, degradation and preservation of SOM persist (Schmidt et al., 2011). Investigating the transformation and conservation of different compound classes in SOM, such as lipids, can improve the general understanding of SOM dynamics (Thomas et al., 2021). Although controversial opinions exist, it can be assumed that none of the lipid variations is significantly resistant to decomposition (Schmidt et al., 2011). It is also shown that the turnover rate of SOM depends on the functional complexity where the variation of the molecularly diverse group of SOM plays an important role (Lehmann et al., 2020; Thomas et al., 2021). In recent decades, many studies have been conducted using lipids in the soil as molecular proxies for various purposes, including paleoecology and paleoclimate reconstructions (Jansen and Wiesenberg, 2017; Thomas et al., 2021). Many of these lipid compounds can be considered biomarkers because they have specific characteristics that indicate their source organisms and might be preserved after decomposition in soils and sediments (Thomas et al., 2021).

In Swiss alpine regions, pasture land is increasingly becoming abandoned for two reasons. First, maintaining pasture land is no longer profitable for farmers. Second, afforestation can be used as protection against avalanches (Hiltbrunner, 2012; García-Hernández et al., 2017). Land use change is one of the most important factors that affects carbon fluxes between the atmosphere and the terrestrial biosphere and determines whether an ecosystem is a net sink or source of atmospheric CO_2 (Hiltbrunner et al., 2013). While the deforestation of tropical rainforests increases the concentration of carbon dioxide in the atmosphere, the afforestation of abandoned pastures in the northern hemisphere generally contributes to the increasing C sequestration (Houghton, 2003). It can be assumed that after pasture land gets afforested, more carbon is accumulated and stored in aboveground plant biomass such as living trees and litter depositions (Hiltbrunner et al., 2013). Depending on different studies, soil carbon sequestration after afforestation of prior pasture lands can show either an increase, a decrease or even no effect in carbon sequestration (Hiltbrunner, 2012;

Post and Kwon, 2000; Thuille and Schulze, 2006). Carbon storage is affected by the amount of foliage input (Bowden et al., 2014), the carbon pathways, and the vegetation type (Hiltbrunner, 2012). Nevertheless, more information is needed to fully understand this complex carbon distribution and stabilization process to reconstruct the contribution of diverse plant types and plant organs to the organic material (Mueller et al., 2012).

1.1 Carbon cycle

The absorption of atmospheric carbon through photosynthesizing mechanisms of plants is a major process of terrestrial ecosystems (Van Veen et al., 1991) (Fig.1). Higher plants, such as trees and shrubs, contribute to the C input. The contribution happens through the release of organic compounds to the soil by plant root systems and the degradation of plant material, as well as by soil organisms when they die (Kögel-Knabner, 2002). The plant-soil system is a dynamic system with inputs, outputs, distributions, and storage of organic material like free extractable lipids, such as n-alkanes and fatty acids. Essential nutrients for plant growth are released through a microbial breakdown of organic matter (OM) (Kögel-Knabner, 2017). This process of decay releases a part of the carbon as CO_2 through soil respiration. Other carbon parts transform into organic compounds of higher stability, which can persist in the soil over an extended period (Thomas et al., 2021). How fast this process takes place depends on various factors, including temperature, soil moisture, soil properties, vegetation, the quantity and quality of organic material falling on the ground, and microbial and fungal activity (Kögel-Knabner, 2002; Hiltbrunner, 2012).

Prior to incorporation into the soil, plant residues can form a litter layer on the soil surface, especially in forest ecosystems (Thomas et al., 2021). Materials of plant litter provide the primary source for the formation of SOM (Kögel-Knabner, 2002). The amount of plant litter, composition and soil properties are essential for SOM formation and the humification process (Swift et al., 1979). However, microbial residues and exudates are also essential components for forming SOM (Kögel-Knabner, 2002). Nevertheless, the relative amount of soil organism residue is small and therefore plays a minor role as source material for SOM formation. A considerable amount of the organic material is incorporated into the soil as root litter and rhizodeposition (Kögel-Knabner, 2002). Because roots might contain a different wax lipid composition than the investigated plant residues in this study, root inputs may disturb the chronology of reconstruction by overprinting signals (Jansen and Wiesenberg, 2017; Lavrieux et al., 2012).

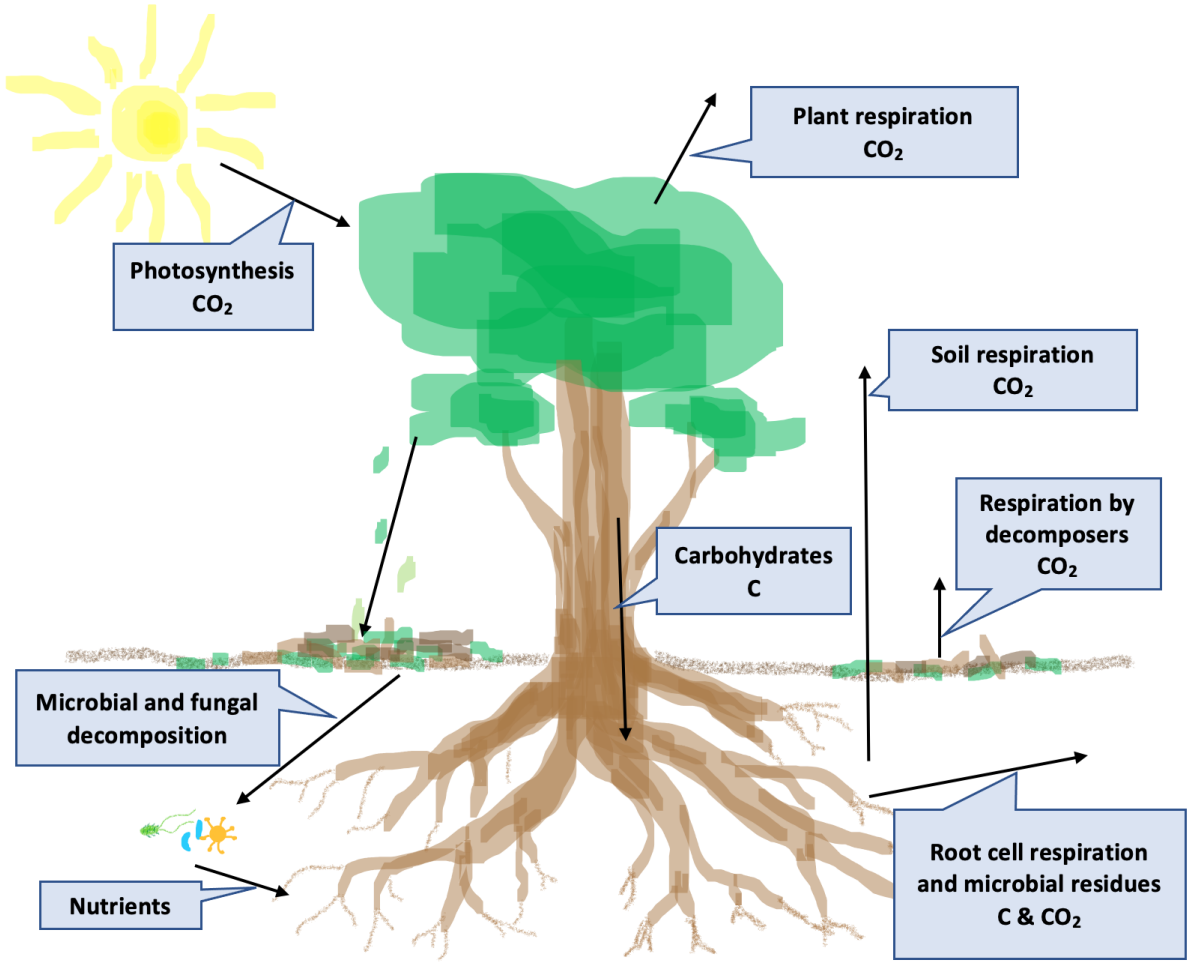

Figure 1: Carbon cycle between the atmosphere and the biosphere

1.2 Lipids as molecular proxies

Lipids belong to a heterogeneous group of organic substances, which per definition, are insoluble in water, but extractable with non-polar solvents, such as hexane (Wiesenberg et al., 2004). They are found in plants, animals, and microorganisms. In soils, lipids originate almost exclusively from plants and microorganisms, whereas soil animals play a minor role (Kögel-Knabner, 2002; Wiesenberg et al., 2004). Under certain conditions, soil lipids can provide a relatively stable carbon pool compared to other organic components such as carbohydrates, amino acids, lignin, or tannins (Lichtfouse et al., 1995; Kögel-Knabner, 2002; Wiesenberg et al., 2004). Deposited in sediment layers, molecular lipid distribution patterns can even survive millions of years because they can be resistant to chemical and microbial degradation (Huang et al., 1995). Analyses of lipids are performed frequently in plant tissues, soils, peat depositions, sediments, rocks, and oil to trace the contribution of diverse biological sources of organic matter (OM), environmental changes, and the fate of OM such as the degradation (Wiesenberg and Gocke, 2015). The implementation of lipids in soil investigations as molecular proxies, often referred to as biomarkers, is promising as

long as some constraining factors are considered, including i) variation of molecular compositions in plant-derived OM both within and between plant species, ii) variability of input pathway into the soil, and iii) the transformation and selective decomposition of some components in the soil (Jansen and Wiesenberg, 2017). A way to understand the dynamics of SOM is the analysis of the lipid distribution patterns between the living plants, the organic horizons, and the topsoil.

n-Alkanes

The primary sources of *n*-alkanes in soil are cuticular waxes of plants and their roots (Eglinton and Eglinton, 2008; Thomas et al., 2021). *n*-Alkanes are straight-chain hydrocarbons with no functional groups. Due to insolubility in water, they are more or less immobile (Marseille et al., 1999), and sequentially deposit in soil. Alkanes are extensively used as lipid biomarkers because the extraction and analysis are relatively easy compared to other compound classes. Further, they are ubiquitous in the plant-soil system with a high potential for preservation (Diefendorf and Freimuth, 2017; Thomas et al., 2021). Characteristics of plant-derived *n*-alkanes are long-chain carbon atoms between C_{25} and C_{35}, and a strong predominance of molecules with an odd number of carbon atoms (Thomas et al., 2021). Although *n*-alkanes only represent a small fraction of the total organic matter, their conservative nature allows us to assume that the source of all the organic matter in soil can be represented by *n*-alkane biomarkers (Cooper et al., 2015).

Fatty acids

Fatty acids are carboxylic acids with an aliphatic chain. They are an essential structural component of plant and animal cells and belong to a major component of the lipids of up to 70 % by weight in some microalgae species (Chen et al., 2012). Input from terrestrial higher plants is characterized by an even-over-odd carbon chain length preference from C_{22} to C_{32}, with dominant peaks of C_{26}, C_{28}, and C_{30} (Jansen et al., 2006).

1.3 Aim and research goal

This master's thesis aims to identify soil organic carbon's origin during afforestation and determine free extractable lipids composition, including *n*-alkanes and fatty acids of spruce needles, spruce twigs, bark, mosses, lichens, the organic horizons, and the topsoil. In addition, different forest ages of 40, 55, and 130 years are considered to determine differences in the lipid distribution patterns. Thereby the following research questions and hypotheses can be formulated.

- What contributes the most to soil organic carbon (SOC)?

  SOC derives from organic components that fall to the ground in the forest ecosystem, such as spruce needles and spruce twigs, bark, wood, spruce cones, mosses, lichens, grasses, and others. Therefore, it can be expected that the forest floor's most abundant component contributes the most to SOC. Because litter fall in spruce stands is mainly dominated by needles (Hågvar, 2016; Berg and Meentemeyer, 2001), spruce needles are expected to contribute the most to SOC.

- What is the role of aboveground vegetation in relation to different forest ages on SOC?

  Depending on the forest's age, the vegetation's composition changes. The same applies to the constitution of the organic components that fall to the ground and later serve as a source of SOC (Clarke et al., 2007). It can be assumed that young forests are generally composed of smaller trees, which grow closer together and thus form a denser canopy. The sunlight can barely penetrate the forest canopy, which does not favors the growth of plants on the forest floor, such as grasses and shrubs. However, moss growth could potentially be favoured under these shady conditions. In an old forest with a less dense canopy, more sunlight can reach the ground, whereby additional plant growth can be assumed on the forest floor. In addition, older spruce trees produce more spruce cones, which then might contribute as a significant source of SOC (Hågvar, 2016; Hagner, 1965). Thus, different lipid distribution patterns are expected between the forest areas of different ages due to changes in vegetation. Furthermore, stronger lipid moss signals are expected in the youngest forest area compared to the two older forest areas.

- What is the role of molecular resistance and degradation to SOC?

  Some lipid compounds, particularly long-chained n-alkanes, are relatively resistant to degradation. Although, organic matter (OM) and its lipid compounds begin to degrade in the litter layer. Degradation will then continue in the different organic horizons and the topsoil with the aid of soil microbiota and soil organisms (Thomas et al., 2021). A proportionally stronger incidence of longer-chain components is expected with increasing decomposition stages from the organic horizons to the topsoil. Consequently, the highest SOM degradation is expected in the organic horizons, as well as a subsequent decrease of decomposition in the topsoil.

2 Materials and methods

The study site is located in a sub-alpine region in Jaun, canton of Fribourg, Switzerland (Fig.2). The entire slope area was used as pasture for at least 150 years. However, this area was probably used for cattle grazing for several hundred years (Hiltbrunner et al., 2013). After the village of Jaun was threatened by severe avalanches in 1956, the eastern side of the slope was partially afforested with Norway spruce (Picea abies L.). Since the reforestation proceeded gradually over some decades, different forest areas were formed. Three sites are of interest for this thesis, a 40-, 55-, and 130-year-old forest section. The 130-year-old forest section can be considered as mature in a climax vegetation state, representing a stable forest ecosystem, whereby the 40-, and 55-year old forest sections are still developing. The different forest sections were determined by David Hiltbrunner in 2009, based on the forest management plan, forest properties observed in the field, and by identifying the precise tree stand ages with dendrochronology (Hiltbrunner et al., 2013).

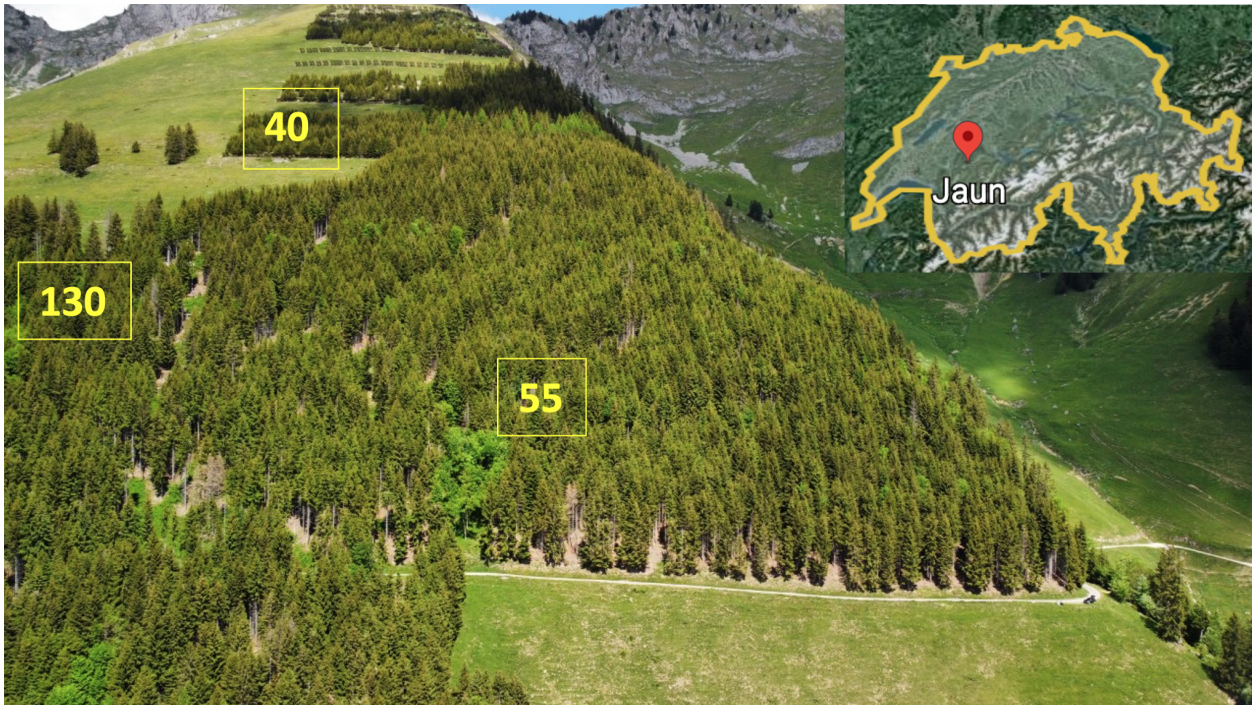

Figure 2: Study site in Jaun, Switzerland.

The investigated forest consists of a 40- 55- and 140-year old forest section (marked in yellow), drone picture provided by Guido L.B. Wiesenberg, earth.google.com acessed on 13.02.2023.

The investigated forest areas (7°15'54E; 46°37'17N) are located at an altitude from 1'450 to 1'800 m a.s.l. On average, summer and winter temperatures are 11.4°C and 0.6°C, and the mean annual precipitation is 1'250 mm. Soils in the entire study area are Eutric Cambisoils with a mean thickness of 0.8m, sitting on calcareous bedrock (Hiltbrunner et al., 2013). In the organic horizon an Oi-,

Oe-, and Oa horizon can be distinguished. The entire forest is used for forestry purposes, where a part of the produced biomass is removed from the ecosystem in the form of wood.

2.1 Sampling

For this thesis, 102 forest samples of the vegetation, the organic horizons, and the topsoil of the afforestation sequence in Jaun were investigated. The samples were collected in advance by Tatjana Carina Speckert in June 2020. Thereby, samples were taken from three different forest areas with forest ages of either 40, 55, or 130 years. Furthermore, samples were taken at three locations for each forest section to detect measurement errors and anomalies in samples or forest sections.

The vegetation is represented by aboveground plant biomass samples consisting of spruce needles, spruce twigs, bark, mosses and lichens. Spruce needles and twigs were further divided into subsamples: newly grown (less than 1-year-old), 3-years-old, and 5-years-old. Bark samples were collected on the forest ground, showing first signs of degradation, but were still considered fresh samples. Furthermore, samples were collected from the litter layer and the three organic horizons (Oi, Oe, and Oa). O horizons are layers on top of the soil with a high percentage of OM. Generally, within a forest ecosystem, three distinct organic horizons can be found. The first horizon (Oi) comprises relatively fresh and undecomposed leaves, needles, and twigs. This horizon is underlain by partially decomposed (still recognizable) plant residues (Oe), and a darker horizon of highly decomposed (unrecognizable OM) sub-horizon (Oa) (Fine et al., 2018). Although, the Oi horizon and the litter layer describe the same horizon, they where described and analyzed separately in this thesis to determine deviations due to different sampling. The material for the litter layer samples was collected over a larger area, whereas the organic horizons were sampled punctually. In addition, one topsoil sample was collected in each forest section at a soil depth of 5 cm. Mosses and lichens were collected during field work on May 26, 2022. The collected moss and lichen samples were each combined as a mixed sample regardless of the forest age and the forest area to get a small insight into the lipid distributions.

The spruce needles had to be separated from the twigs, and impurities such as rocks and mineral soil debris had to be removed from the litter layer. Some samples still had to be freeze-dried and milled using the Retsch MM 400 horizontal mill. The organic horizon and topsoil samples were already freeze-dried and milled in advance.

2.2 Elemental analysis

Small amounts of the sample material were weighed into tin capsules using the Mettler Tolero XS2015 Dual Range. These tin capsules were further analyzed using a Thermo Fisher Scientific Elemental Analyser coupled to a Delta V isotope mass spectrometer. Each sample was measured in duplicate to avoid measurement errors. The following values were evaluated: Total organic carbon (TOC), total nitrogen (TN), δ^{13}C, and δ^{15}N.

2.3 Lipid extraction and separation

After the freeze-drying and milling process, total lipids were extracted using the ultrasonic extraction method (Fig.3). Afterwards, two separation steps were applied. (1) Lipid separation into fatty acids (FA) and low polarity lipid fractions, (2) separation into aliphatic, aromatic hydrocarbons, and heterofunctionalized organic compounds. Additionally, fatty acids need to be methylated. The methods used and described in this chapter follow the detailed guideline for lipid analysis described by Wiesenberg and Gocke (Wiesenberg and Gocke, 2017).

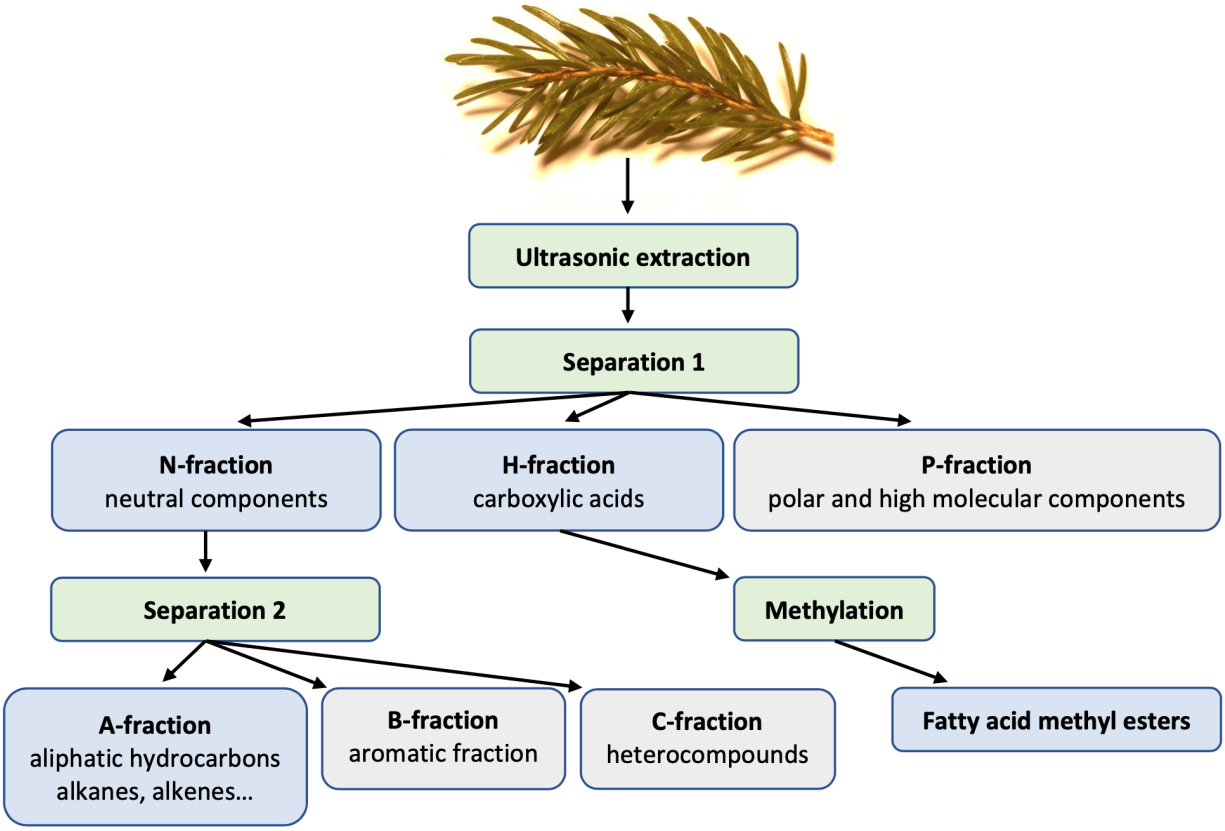

Figure 3: Schematic overview of the lipid extraction and separation methods.

Green colored boxes indicate applied methods, blue boxes indicate separated fractions further used in this work, and marked in grey boxes are the fractions which were not further used, twig photographed by N. Güntert.

2.3.1 Ultrasonic extraction

Ultrasonic extraction is a total lipid extraction method well suited for low sample quantities (Fig.4). It can be used for high-density samples, such as soils, sediments, and rocks, whereby less than 2g of sample material is required. For the extraction of plant tissues, only 0.1g of material is needed (Zink et al., 2001). Furthermore, it allows large numbers of samples to be extracted in a short period (Wiesenberg and Gocke, 2017).

With this method, the lipids contained in the finely powdered plant and soil samples were extracted. Then, the lipids were dissolved from the samples by repeated dissolution with a solvent mixture of dichloromethane (DCM) and methanol (93:7, v:v) and by subsequent ultrasonic treatment.

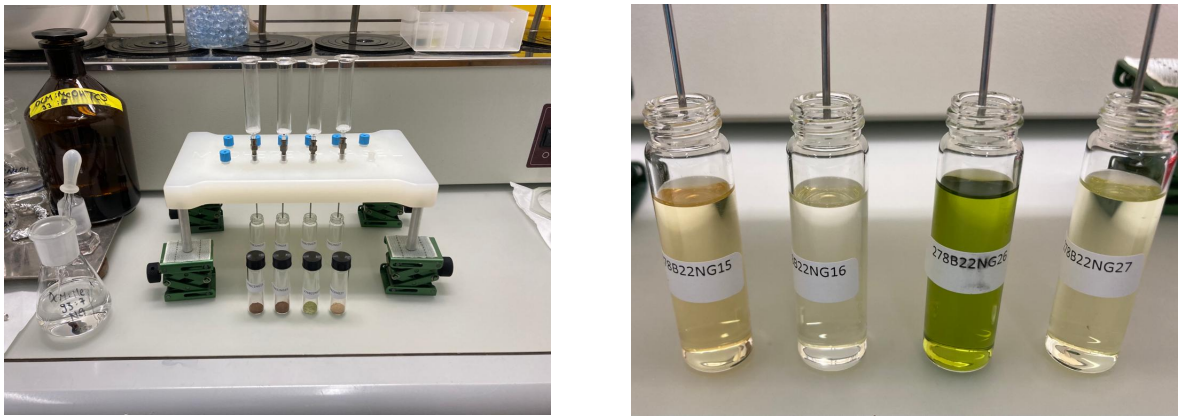

Figure 4: Lipid extraction setup.

Syringes equipped with glass filters to remove residual suspended solids from total lipid extracts (left), final total lipid extracts (right), photographed by N. Güntert.

After each run, samples were centrifuged for 2 minutes at 800g. Finally, the suspended solids settled, and the solvent containing the lipids could be removed. The procedure was repeated eight times.

2.3.2 Lipid separation into fatty acids and low polarity lipid fractions

For gas chromatography (GC) analysis, lipid extracts must be separated into fractions of different polarities. The applied method is optimized for less than 30 mg of lipid extracts obtained from plants, soils, sediments, rocks, and similar samples (Wiesenberg and Gocke, 2017).

In the first step, a glass column filled with 5 cm of KOH-coated (5%) silica gel was prepared and washed with DCM. Subsequently, the lipid extracts produced in the previous step were dissolved with pure DCM and added to the column. After repeated washing out of the column with DCM, the N-fraction (neutral components) was obtained.

In a later step, the H-fraction (carboxylic acids) is obtained. Further components of the total lipid extracts (TLE) were dissolved by adding a solvent mixture of DCM and formic acid (99:1, v:v). After a colored band has passed through the column, rinsing was performed three more times to ensure that all desired components were transferred.

The remaining P-fraction (high polar and high molecular weight components) was separated and recovered from the column by adding DCM and methanol (1:1, v:v).

2.3.3 Separation into aliphatic, aromatic hydrocarbons, and heterofunctionalized organic compounds

This method is used for the separation of aliphatic and aromatic hydrocarbons as well as other lipids. Separation of lipid extracts into fatty acid and low-polarity lipid fractions from the previously described method is recommended before splitting the hydrocarbons to avoid column overload. The sample to be separated should not exceed 20mg (Wiesenberg and Gocke, 2017).

For gas chromatography (GC) analysis, the N-fraction needs to be further separated. First, a glass column filled with 5 cm of activated silica gel was conditioned with *n*-hexane. The sample was then dissolved with a small amount (approximately 200μL) of *n*-hexane using a vortex mixer. Afterwards, the sample was transferred into the column. This step was repeated eight times. The column was then rinsed several times with *n*-hexane until the resulting A-fraction consisting of aliphatic hydrocarbons like alkanes and alkenes had been separated.

For the B-fraction (aromatic fraction), remaining residues from the N-fraction were dissolved as described for the A-fraction using a solvent mixture consisting of *n*-hexane and DCM (1:1, v:v).

Last, the C-fraction was separated. The procedure was the same as described above, but a mixture of DCM and methanol (93:7, v:v) was used.

2.3.4 Methylation of fatty acids

A critical step in gas chromatography (GC) analysis of polar lipid fractions such as fatty acids is the required methylation to obtain fatty acid methyl esters (Wang et al., 2015). Various methods exist for the derivatization of fatty acids. Silylation and methylation are widely used. However, methylated compounds are more stable and enable longer storage of the fraction (Wiesenberg and Gocke, 2017).

First, the H-fraction was dissolved in DCM using a vortex mixer. Then 50μL of internal standard ($D_{39}C_{20}$ acid) was added. Next, the samples were supplied 500μL of boron trifluide/methanol (10%, FLUKA 15716) to start the reaction. The samples were then heated for 15 minutes at 60°C. After cooling to room temperature, 500μL of millipore quality water was added, mixed with a vortex mixer, and centrifuged at 300g for 1 minute. After preparing a syringe with a glass wool filter and a 1 cm sodium sulfate layer, conditioning was performed with DCM. Then, approximately 50% of the lower organic phase of the solution was removed from the H-fraction vial and transferred to the syringe. The H-fraction was then refilled with DCM, and the process started from the beginning. This procedure was repeated 5-8 times.

2.3.5 Color measurement

The TLE from the ultrasonic extraction were differently colored (Fig.5). To conclude a possible correlation between color and sample type, the colors were measured in the L*a*b coordinate system. Since the colors of some sample types seem unique, measured total lipid L*a*b values potentially show sample type specific characteristics.

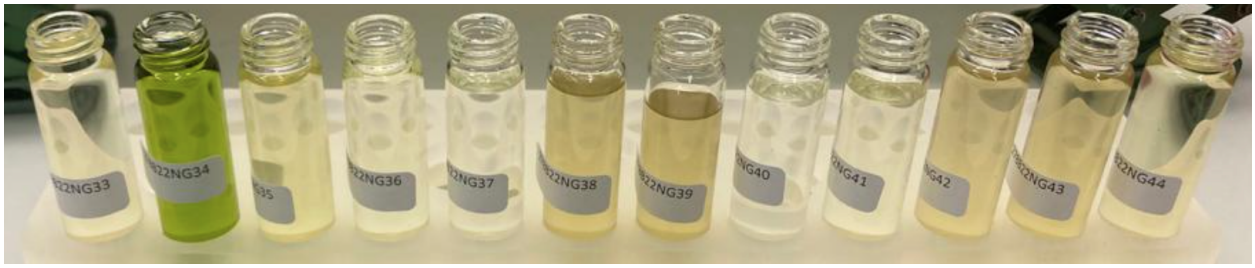

Figure 5: Total lipid extracts

Color variation of total lipid extracts obtained after ultrasonic extraction. From left to right: spruce twigs 5-years-old, spruce needles 3-years-old, spruce twigs 3-years-old, organic horizons-Oe, -Oa, -Oi, -Oe, -Oa, -Oe, -Oi, -Oi, -Oe, photographed by N. Güntert.

The L*a*b coordinate system consists of three axes. First, axis (L) represents the darkness to lightness on a scale from 0 to 100. Axis (a) represents greenness to redness, scaled from -128 to +127, and axis (b) represents blueness to yellowness, also scaled from -128 to +127 (Murali and Govindan, 2013).

The TLE were evaporated after the ultrasonic extraction and dissolved again with a vortex mixer and a small amount of DCM. This method was used to obtain complete and comparable concentrations for color measurement. The portable spectrophotometer (spectro-color by Dr. Lange) was used.

2.4 Gas chromatography and mass spectrometry

The extracted *n*-alkanes and fatty acids were analyzed by gas chromatography with flame ionization detection (GC-FID) (Agilent Technologies 7890B GC-FID system) and gas chromatography-mass spectrometry (GC-MS) (Agilent Technologies 6890N Network GC-MSD system). In this process, the mixtures of substances consisting of components with carbon chains of different chain lengths were separated chromatographically, quantified, and identified via the mass spectrometer (MS). GC analyses were performed for the A-fraction and the methylated H-fraction, following the guideline for lipid analyses by Wiesenberg and Gocke (Wiesenberg and Gocke, 2017).

Analysis of GC-FID of the aliphatic hydrocarbon fraction (N-fraction) requires adding an internal standard such as the one used here, $D_{50}C_{24}$ *n*-alkane (tetracosane, Cambridge Isotope Laboratories Inc. DLM-2209-0.5). The measurement is conducted at a concentration between 10-20μg/μL with 1μL injection at 70°C in splitless mode. Further, the injection and detection temperatures are set to 320°C. The injection temperature is kept constant for 2 min. For the oven, the temperature increases at 10°C/min until 120°C is reached and then at 5°C/min until 320°C. The final temperature remains constant for 20 min. (Wiesenberg and Gocke, 2017).

GC-FID analyses of fatty acids requires a different setting. The measurement was conducted at a concentration between 10-20μg/μL with 1μL injection at 50°C in splitless mode. Injection and detection temperatures were set to 320°C. The injection temperature was kept constant for 2 min. Oven temperature increased at 5°C/min until 120°C was reached and then at 2°C/min until 210°C and further with 3°C/min until 320°C. The final temperature remains constant for 20 min. (Wiesenberg and Gocke, 2017).

2.5 Index measurements

In geochemistry, $\delta^{13}C$ is the ratio of the stable carbon isotopes ^{13}C and ^{12}C with respect to a standard (PDB) (Eq.1). $\delta^{13}C$ values measured in plant and soil samples change over time. They depend on the primary production and the sequestration of CO_2 as the plant grows, the deposition of organic carbon, and the vegetation type. Through kinetic fractionation, biological processes such as photosynthesis preferentially take up the lighter ^{12}C isotope. However, since the lighter isotope reacts faster and is converted enzymatically more quickly, the heavier isotope ^{13}C accumulates in the organism and with increasing decomposition of organic material in the soil, causing an increase in $\delta^{13}C$ (Ladd et al., 2014).

$$\delta^{13}C = \left(\frac{\left(\frac{^{13}C}{^{12}C}\right)_{sample}}{\left(\frac{^{13}C}{^{12}C}\right)_{standard}} - 1 \right) * 1000‰ \quad (1)$$

The average chain length (ACL) of n-alkanes (Alk)(Eq.2) and fatty acids (FA)(Eq.3) is the weighted average of the different carbon chain lengths. These formulas have been adapted to component availability (Trigui et al., 2019).

$$ACL_{Alk} = \frac{21(nC_{21}) + 23(nC_{23}) + 25(nC_{25}) + 27(nC_{27}) + 29(nC_{29}) + 31(nC_{31}) + 33(nC_{33})}{nC_{21} + nC_{23} + nC_{25} + nC_{27} + nC_{29} + nC_{31} + nC_{33}} \quad (2)$$

$$ACL_{FA} = \frac{22(nC_{22}) + 24(nC_{24}) + 26(nC_{26}) + 28(nC_{28}) + 30(nC_{30}) + 32(nC_{32})}{nC_{22} + nC_{24} + nC_{26} + nC_{28} + nC_{30} + nC_{32}} \quad (3)$$

The carbon preference index (CPI) reflects the odd-over-even and the even-over-odd predominance of lipid compositions (Eq.4). It can be used as an indicator of degradation, as the decay of organic material leads to a decreasing abundance of odd-numbered compounds. High values of CPI (>10) indicate input of fresh SOC, and low values of CPI reflect degradation of SOC (Angst et al., 2016; Cranwell, 1981). The formula has been adapted to component availability.

$$CPI_{Alk} = \frac{1}{2}\left(\frac{nC_{21} + nC_{23} + ... + nC_{33}}{nC_{20} + nC_{22} + ... + nC_{32}} + \frac{nC_{21} + nC_{23} + ... + nC_{33}}{nC_{22} + nC_{24} + ... + nC_{34}}\right) \quad (4)$$

Odd-over-even predominance (OEP) can also be used as a proxy for degradation (Eq.5). Values below 5 are indicative of an enhanced state of degradation (Trigui et al., 2019; Buggle et al., 2010).

$$OEP_{Alk} = \frac{nC_{27} + nC_{29} + nC_{31} + nC_{33}}{nC_{26} + nC_{28} + nC_{30} + nC_{32}} \quad (5)$$

2.6 Statistical analysis

Fresh plant samples, organic horizon samples, and topsoil samples were collected from three areas of different forest ages and investigated for C and N concentration, δ^{13}C values, and lipid compound compositions (n-alkanes and fatty acids). Significant differences between sample types and forest ages were tested using one-way ANOVA ($p < 0.05$). Measurements were normalized to dry sample weight (μg g^{-1}), and values in figures and tables were given as average values ± SE of the

respective sample types in the different forest areas. The elemental analysis consisting of the C and N concentrations, and δ^{13}C values were measured in duplicates to detect measurement errors. Only one outlier (*n*-alkane compound C_{21} spot 40) was considered and omitted. Visualizations and statistical analysis were performed with RStudio (R Core Team, 2021).

3 Results

3.1 Elemental analysis

Carbon concentration:

Organic carbon concentrations show no significant difference between the needle, twig, and bark samples (p = 0.72), averaging 48.7 ± 0.8 % for spruce needles (needle 0 + needle 3 + needle 5), 49.0 ± 2.1 % for spruce twigs (twigs 0 + twigs 3 + twigs 5), and 48.9 ± 2.8 % for bark (Fig.6). The measured carbon concentrations decreases significantly (p = 3.76 * 10^{-24}) from the litter layer to the topsoil. Compared to the litter layer, a decreasing C concentration of 7.9 % in the Oi-, 36.6 % in the Oe-, 70.9 % in the Oa horizon, and 85.6 % in the topsoil layer can be observed. At first, only a slight decrease in C concentration in the litter layer and the Oi horizon can be observed. The measured average values are 46.8 ± 3.9 % for the litter layer and 43.1 ± 5.0 % for the Oi horizon. After that, the values drop rapidly. The average values for the C concentrations are 29.7 ± 10.2 % for the Oe horizon, 13.6 ± 10.2 % for the Oa horizon, and 6.7 ± 1.4 % for the topsoil. The C concentration in the mixed sample of moss and lichens is lower than in samples of needles, twigs, and bark and amounts to 42.9 ± 0.7 % for the moss sample, and 43.7 ± 0.03 % for the lichen sample. The differences in the measured C values between the 40-, 55-, and 130-year-old forest sections are significant for the samples of 5-year-old needles (p = 0.02), 3-year-old-twigs (p = 0.03), Oa (p = 0.03), and topsoil (p = 0.02), marked in red (Tab.1).

Nitrogen concentration:

Nitrogen concentrations show significant differences between the needle, twig, and bark samples (p = 1.15 * 10^{-20}), averaging 1.0 ± 0.2 % for spruce needles (needle 0 + needle 3 + needle 5), 0.6 ± 0.2 % for spruce twigs (twigs 0 + twigs 3 + twigs 5), and 0.8 ± 0.2 % for bark. Therefore, a decrease in N concentration can be observed from needle year 0, to needle year 3, needle year 5, branch year 0, and branch year 3 (Fig.6). The most substantial decrease of -45.1 % can be seen between newly grown twigs and the 3-year-old twigs. Between newly grown needles and 3-year-old needles a decrease in N concentration of -18.6 % can be observed. The N values in the mixed samples amounts to 1.7 ± 0.01 % for the moss sample and 1.5 ± 0.02 % for the lichen sample.

Carbon (C) concentrations in different forest areas [%]				
Sample type	40 year old forest	55 year old forest	130 year old forest	p
Spruce needle year 0	48.3 ± 0.6	48.5 ± 0.6	40.1 ± 0.6	0.45
Spruce needle year 3	48.9 ± 0.8	49.1 ± 0.5	49.2 ± 0.4	0.70
Spruce needle year 5	49.5 ± 0.8	48.3 ± 0.6	48.4 ± 0.7	0.02
Spruce twig year 0	49.2 ± 1.5	50.7 ± 1.0	49.8 ± 0.6	0.10
Spruce twig year 3	49.9 ± 0.3	49.3 ± 0.8	48.9 ± 0.5	0.03
Spruce twig year 5	48.9 ± 0.7	48.1 ± 0.8	46.0 ± 4.9	0.23
Bark	49.2 ± 0.9	49.9 ± 4.5	47.6 ± 1.4	0.36
Litter layer	48.4 ± 0.2	47.9 ± 3.3	44.1 ± 5.4	0.11
Oi	42.3 ± 7.1	46.4 ± 3.2	40.6 ± 1.7	0.12
Oe	36.1 ± 10.3	30.1 ± 6.6	22.9 ± 9.8	0.07
Oa	13.3 ± 8.4	6.3 ± 2.9	21.2 ± 11.9	0.03
Topsoil	8.5	5.8	6.0	0.02

Table 1: Carbon concentrations in forest sections of different ages.

From the litter layer to the topsoil, N concentrations decrease significantly ($p = 5.83 * 10^{-9}$). The average N concentrations are 1.1 ± 0.2 % for the litter layer, 1.0 ± 0.3 % for the Oi-, 1.1 ± 0.3 % for the Oe-, 0.6 ± 0.4 % for the Oa horizon, and 0.4 ± 0.1 % for the topsoil. Compared to the litter layer, a decrease in N concentration of 5.6 % in the Oi-, 43.2 % in the Oa horizon, 63.3 % in the topsoil, and an increase of 0.5 % in the Oe horizon can be observed. Maximum average N values have reached either in the litter layer (130-year-old forest), in the Oi horizon (55-year-old forest), or in the Oe horizon (40-year-old forest). The differences in the measured N values between the 40-, 55-, and 130-year-old forest sections are significant for Oi ($p = 0.005$), Oe ($p = 0.003$), and topsoil ($p = 0.001$), marked in red (Tab.2).

Nitrogen (N) concentrations in different forest areas [%]				
Sample type	40 year old forest	55 year old forest	130 year old forest	p
Spruce needle year 0	1.1 ± 0.1	1.1 ± 0.2	1.1 ± 0.1	0.99
Spruce needle year 3	1.0 ± 0.2	1.0 ± 0.2	1.1 ± 0.1	0.69
Spruce needle year 5	0.9 ± 0.2	0.9 ± 0.1	0.9 ± 0.1	0.83
Spruce twig year 0	0.9 ± 0.1	0.8 ± 0.1	0.8 ± 0.1	0.06
Spruce twig year 3	0.5 ± 0.1	0.5 ± 0.1	0.4 ± 0.1	0.42
Spruce twig year 5	0.3 ± 0.1	0.5 ± 0.1	0.5 ± 0.3	0.13
Bark	0.7 ± 0.2	0.7 ± 0.2	0.9 ± 0.3	0.36
Litter layer	1.1 ± 0.1	1.2 ± 0.1	0.9 ± 0.2	0.05
Oi	1.0 ± 0.2	1.2 ± 0.1	0.8 ± 0.2	0.005
Oe	1.3 ± 0.2	1.1 ± 0.2	0.8 ± 0.2	0.003
Oa	0.7 ± 0.4	0.4 ± 0.2	0.8 ± 0.3	0.17
Topsoil	0.6	0.3	0.3	0.001

Table 2: Nitrogen concentrations in forest sections of different ages.

C/N Ratio:

The C/N ratios show significant differences between the needle, twig, and bark samples ($p = 3.41 * 10^{-8}$), averaging 48.8 ± 8.7 for spruce needles (needle 0 + needle 3 + needle 5), 104.9 ± 69.2 for spruce twigs (twigs 0 + twigs 3 + twigs 5), and 69.1 ± 21.5 for bark. The C/N ratio in the mixed samples is 25.0 ± 0.5 for the moss sample, and 28.3 ± 0.4 for the lichen sample. From the litter layer to the topsoil, the measured C/N ratio decreases significantly ($p = 5.25 * 10^{-19}$). Average C/N ratios are 44.7 ± 5.5 for the litter layer, 44.8 ± 10.0 for the Oi horizon, 27.5 ± 6.2 for the Oe horizon, 21.5 ± 7.1 for the Oa horizon, and 17.9 ± 2.5 for the topsoil. Compared to the litter layer, the C/N ratio increases by 2.7 % in the Oi horizon, and decreases by 37.1 % in the Oe horizon, 50.8 % in the Oa horizon, and 59.0 % in the topsoil. The differences in the measured C/N ratio between the 40-, 55-, and 130-year-old forest sections are significant for the samples of twigs 0 ($p = 0.04$), Oi horizon ($p = 0.01$), Oa horizon ($p = 0.02$), and the topsoil ($p = 0.02$), marked in red (Tab.3).

C:N ratio in different forest areas [-]				
Sample type	40 year old forest	55 year old forest	130 year old forest	p
Spruce needle year 0	42.8 ± 5.0	44.4 ± 9.1	42.8 ± 2.8	0.87
Spruce needle year 3	50.0 ± 11.2	51.5 ± 9.9	46.0 ± 2.8	0.55
Spruce needle year 5	57.6 ± 13.9	51.4 ± 3.0	53.0 ± 1.5	0.42
Spruce twig year 0	55.7 ± 3.2	68.3 ± 11.3	62.4 ± 6.0	0.04
Spruce twig year 3	109.8 ± 25.6	101.4 ± 27.4	123.0 ± 42.5	0.53
Spruce twig year 5	151.0 ± 23.6	91.6 ± 15.6	180.8 ± 172.7	0.33
Bark	75.6 ± 27.0	72.3 ± 11.9	59.4 ± 23.1	0.41
Litter layer	45.5 ± 5.4	40.6 ± 1.2	48.0 ± 6.3	0.06
Oi	42.7 ± 4.2	38.2 ± 3.3	53.7 ± 12.7	0.01
Oe	26.9 ± 3.8	27.2 ± 2.5	28.2 ± 10.4	0.94
Oa	20.0 ± 1.9	16.9 ± 2.4	27.5 ± 9.6	0.02
Topsoil	14.9	18.6	20.2	0.02

Table 3: C/N ratios in forest sections of different ages.

$\delta^{13}C$:

δ^{13}C values show significant differences between the needle, twig, and bark samples ($p = 1.62 * 10^{-13}$). The samples average -29.6 ± 1.2 ‰ for spruce needles (needle 0 + needle 3 + needle 5), -28.3 ± 1.1 ‰ for spruce twigs (twigs 0 + twigs 3 + twigs 5), and -26.6 ± 2.1 ‰ for bark (Fig.6). From the litter layer to the topsoil, the measured δ^{13}C values increase significantly ($p = 1.04 * 10^{-9}$). Compared to the litter layer, δ^{13}C values increase by 0.3 ‰ in the Oi horizon, 0.4 ‰ in the Oe horizon, 1.0 ‰ in the Oa horizon, and 1.4 ‰ in the topsoil. The measured average values are -27.8 ± 0.4 ‰ for the litter layer, -27.6 ± 0.4 ‰ for the Oi horizon, -27.4 ± 0.5 ‰ for the Oe horizon, -26.9 ± 0.6 ‰ for the Oa horizon, and -26.4 ± 0.2 ‰ for topsoil. The δ^{13}C values in the mixed samples amounts to -29.4 ± 0.01 ‰ for the moss sample and -25.7 ± 0.04 ‰ for the lichen sample.

Measured δ^{13}C values of the different forest areas differ more in fresh and undegraded plant samples of spruce needles, spruce twigs, and bark, than in samples of the litter layer, the organic horizons, and the topsoil (Fig.6). In general, samples from the 130-year-old forest show the lowest values of δ^{13}C, and samples from the 40-years-old forest show the highest values of δ^{13}C. The δ^{13}C values for the 55-year-old forest primarily lie between the values of the other forest sections. The exception is with young twigs and bark samples, where δ^{13}C isotope values exceed those from the 40-year-old forest. Differences in δ^{13}C values between the 40-, 55-, and 130-year-old forest sections are significant for all samples of needles ($p \leq 0.0002$), twigs ($p \leq 0.0005$), and the Oa horizon ($p = 0.003$), as marked in red in the table (Tab.4).

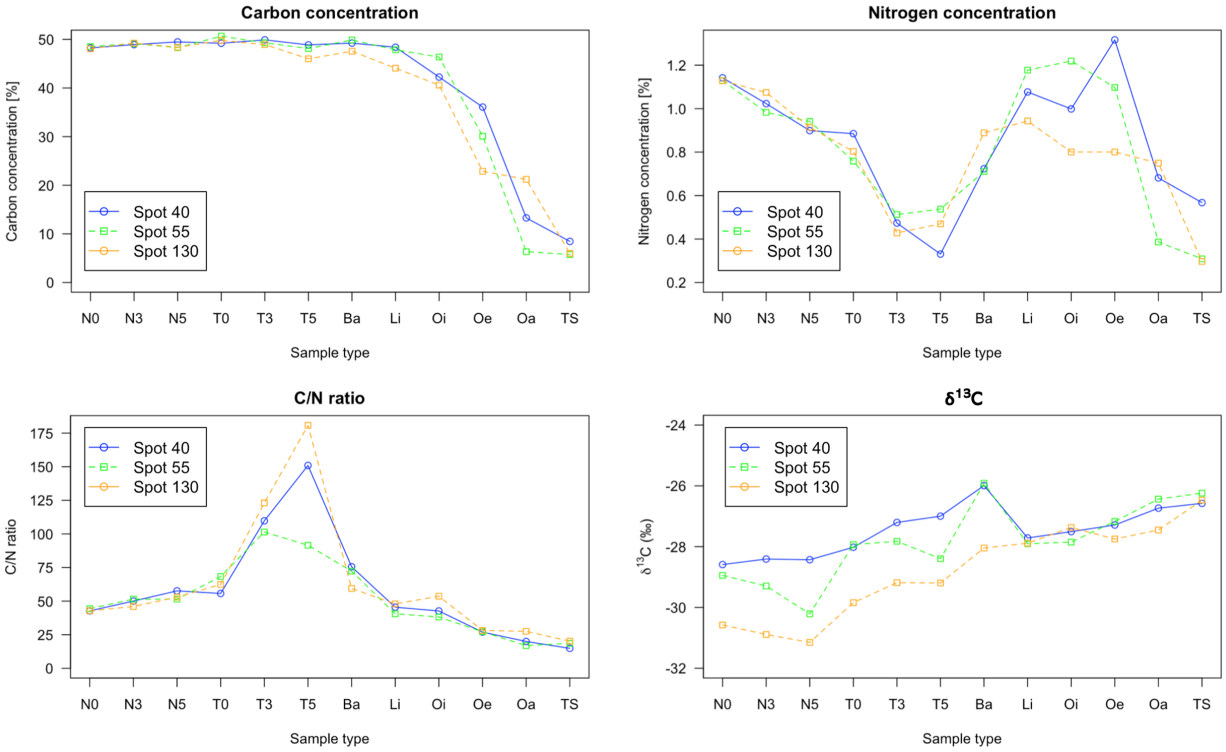

Figure 6: Carbon and nitrogen concentrations, C/N ratios and δ^{13}C values.

Results from elemental analysis for different sample types of: spruce needles = N, spruce twigs = T (less than 1 year old = 0, 3 years old = 3, 5 years old = 5), spruce bark = Ba, litter layer = Li, organic horizons-Oi, -Oe, -Oa and topsoil = TS. Measured were: carbon concentration [%], nitrogen concentration [%] and δ^{13}C [‰], calculated from the data is the C/N ratio [-].

δ^{13}C concentrations in different forest areas [‰]				
Sample type	40 year old forest	55 year old forest	130 year old forest	p
Spruce needle year 0	-28.6 ± 0.3	-29.0 ± 0.8	-30.6 ± 0.8	0.0002
Spruce needle year 3	-28.4 ± 0.3	-29.3 ± 0.6	-30.9 ± 0.8	$2 * 10^{-5}$
Spruce needle year 5	-28.4 ± 0.4	-30.2 ± 0.6	-31.2 ± 0.7	$2 * 10^{-6}$
Spruce twig year 0	-28.0 ± 0.2	-27.9 ± 0.9	-29.8 ± 0.9	0.0005
Spruce twig year 3	-27.2 ± 0.1	-27.8 ± 0.5	-29.2 ± 0.8	$7 * 10^{-5}$
Spruce twig year 5	-27.0 ± 0.2	-28.4 ± 0.6	-29.2 ± 0.4	$5 * 10^{-7}$
Bark	-26.0 ± 0.4	-25.9 ± 0.7	-28.0 ± 3.3	0.14
Litter layer	-27.7 ± 0.1	-27.9 ± 0.1	-27.9 ± 0.6	0.62
Oi	-27.5 ± 0.2	-27.9 ± 0.2	-27.4 ± 0.6	0.10
Oe	-27.3 ± 0.5	-27.2 ± 0.5	-27.8 ± 0.4	0.12
Oa	-26.7 ± 0.4	-26.4 ± 0.3	-27.5 ± 0.6	0.003
Topsoil	-26.6	-26.2	-26.47	0.11

Table 4: δ^{13}C values in forest sections of different ages.

3.2 Color measurement

Differences in the coloration of the lipid extracts could be detected with the color measurement in the L*a*b coordinate system. Differences between fresh samples of spruce needles, spruce twigs, and bark, regarding the L-value, a-value, and b-value are always significant. The same applies to differences between decomposed samples of the litter layer, the organic horizons, and the topsoil. Differences are significant for the L-values of fresh samples ($p = 2 * 10^{-6}$), and the samples from the litter layer to the topsoil ($p = 0.002$). Significant differences are also shown for the a-values of fresh samples ($p = 1.43 * 10^{-12}$), and the samples from the litter layer to the topsoil ($p = 0.008$), as well as for the b-values for fresh plant samples ($p = 0.001$), and the samples from the litter layer to the topsoil ($p = 1.71 * 10^{-6}$). The listed mean values of the individual sample types from the three forest sections are shown in the table (Tab.5).

Assigning total lipid extracts to the corresponding sample types is partially possible based on measured colors in the L*a*b coordinate system. Spruce needle samples can clearly be distinguished from other sample types based on the coloration of the total lipid extracts (Fig.7). However, it is more challenging to assign the colors to the different needle ages, since overlapping of the L*a*b coordinates occur. For all sample types, cluster formations and patterns can be detected, but some of them are highly scattered and overlap with clusters of other sample types. Since coloration depends on different lipid components, it might be possible to conclude the presence of specific lipid components based on color data. However, further investigations in this regard were not conducted.

Colour measurement			
Sample type	L- value	a- value	b- value
Spruce needle year 0	27.2 ± 1.2	-0.1 ± 0.2	1.0 ± 0.7
Spruce needle year 3	25.9 ± 2.0	0.0 ± 0.4	1.4 ± 2.0
Spruce needle year 5	27.9 ± 2.5	-0.5 ± 0.6	1.5 ± 2.0
Spruce twig year 0	30.8 ± 1.0	-1.7 ± 0.2	2.8 ± 0.7
Spruce twig year 3	30.1 ± 2.3	-1.3 ± 0.3	3.2 ± 1.9
Spruce twig year 5	30.7 ± 1.9	-1.6 ± 0.5	2.7 ± 1.0
Bark	30.5 ± 2.9	-1.3 ± 0.8	3.9 ± 1.8
Litter layer	29.1 ± 2.9	-0.6 ± 0.7	3.9 ± 1.0
Organic horizon Oi	29.7 ± 2.1	-0.6 ± 0.6	4.1 ± 0.5
Organic horizon Oe	31.6 ± 2.3	-1.5 ± 0.7	3.3 ± 1.5
Organic horizon Oa	32.8 ± 1.5	-1.2 ± 0.4	0.8 ± 1.7
Topsoil	33.6 ± 0.6	-1.2 ± 0.4	0.3 ± 1.2
Moss	18.8	0.6	2.3
Lichen	27.7	-0.2	0.1

Table 5: Color measurements of total lipid extracts.

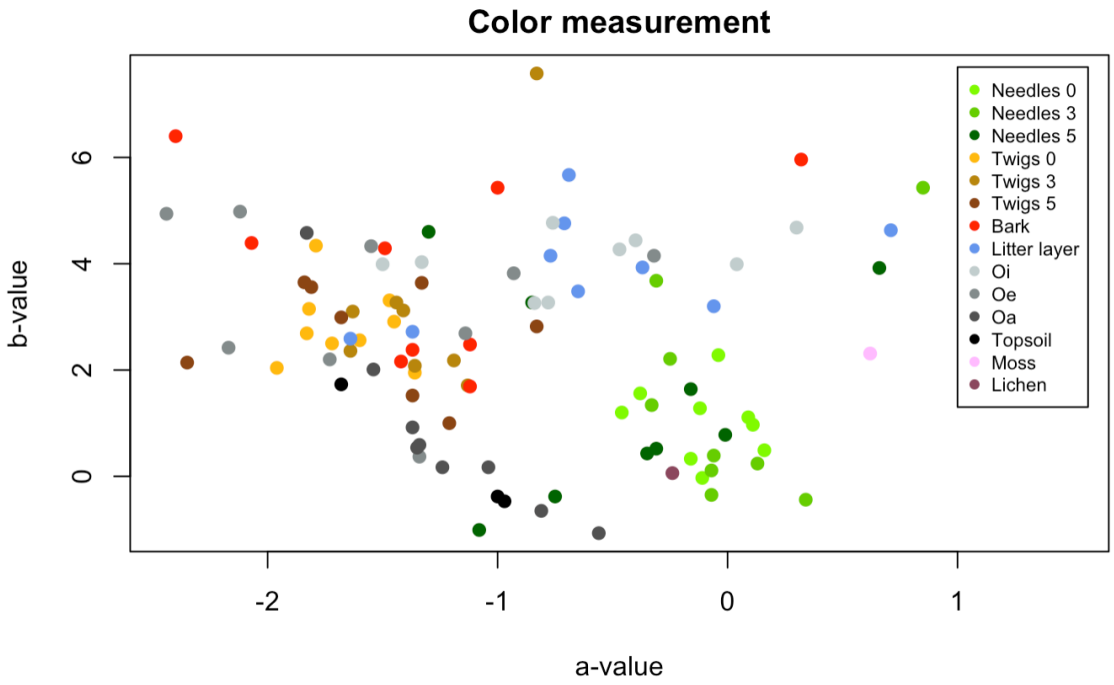

Figure 7: a- and b-values of the color measurement.

3.3 *n*-Alkanes

n-Alkane distribution in spruce needles

The *n*-alkane distribution of cuticular waxes in spruce needles consists mostly of *n*-C_{23}, *n*-C_{25}, *n*-C_{27}, *n*-C_{29}, and *n*-C_{31} hydrocarbons (Fig.8,9,10). *n*-C_{29} can be considered a dominant component, with an average concentrations ranging from 1.1 to 1.9 μg/g for maximum 1-year-old needles. Besides the mentioned carbon chain lengths, other *n*-alkanes from *n*-C_{21} to *n*-C_{33} occur. Less abundant are components below *n*-C_{21} and above *n*-C_{33}. Differences in lipid distributions between the forest areas and the needle ages can be observed.

n-Alkane distribution in spruce twigs

The most dominant hydrocarbon of *n*-alkanes in twigs is mostly *n*–C_{23}, with average concentrations ranging from 1.5 to 4.2 μg/g for twigs no older than one year. In some samples, the *n*-C_{25}, *n*-C_{29}, or *n*-C_{31} values exceed the values of *n*–C_{23} (Fig.8,9,10). High amounts of hydrocarbons can be found from *n*-C_{21} to *n*-C_{31}. Compounds below *n*-C_{21} are less abundant.

n-Alkane distribution in spruce bark

The most dominant *n*-alkane component in spruce bark is either *n*–C_{23}, with an average concentrations ranging from 0.4 to 0.9 μg/g, or *n*-C_{21}, ranging from 0.0 to 2.0 μg/g (Fig.8,9,10). In the bark sample from the 40-year-old forest section, the value of *n*-C_{21} was much higher compared to other bark samples and was omitted as an outlier. High amounts of hydrocarbons can be found from *n*-C_{21} to *n*-C_{31}. Compounds below *n*-C_{21} are scarce.

n-Alkane distribution in the litter layer

The total amount of components is less scattered in the litter layer compared to the samples of needles, branches, and bark (Fig.8,9,10). Thus, a large part of the *n*-alkanes consists of the components *n*-C_{27}, *n*-C_{29}, and *n*-C_{31}. The dominant component is always *n*–C_{29}, with an average concentrations ranging from 1.0 to 13.3 μg/g. Compounds below *n*-C_{27} are much less abundant, except for the 130-year-old forest section, where higher concentrations for the components *n*-C_{21}, *n*-C_{23}, and *n*-C_{25} could be measured.

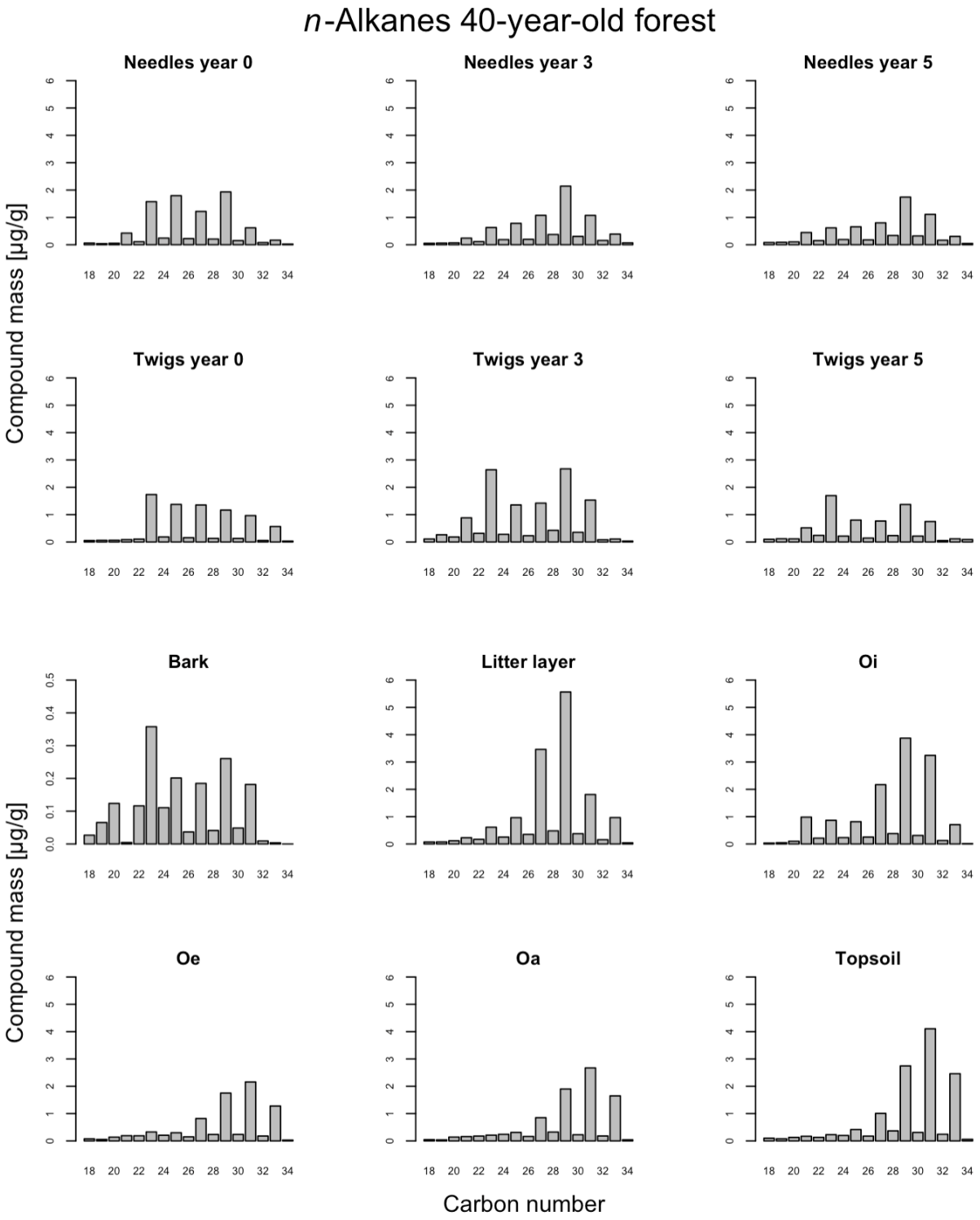

Figure 8: n-Alkane distributions in the 40-year-old forest section.

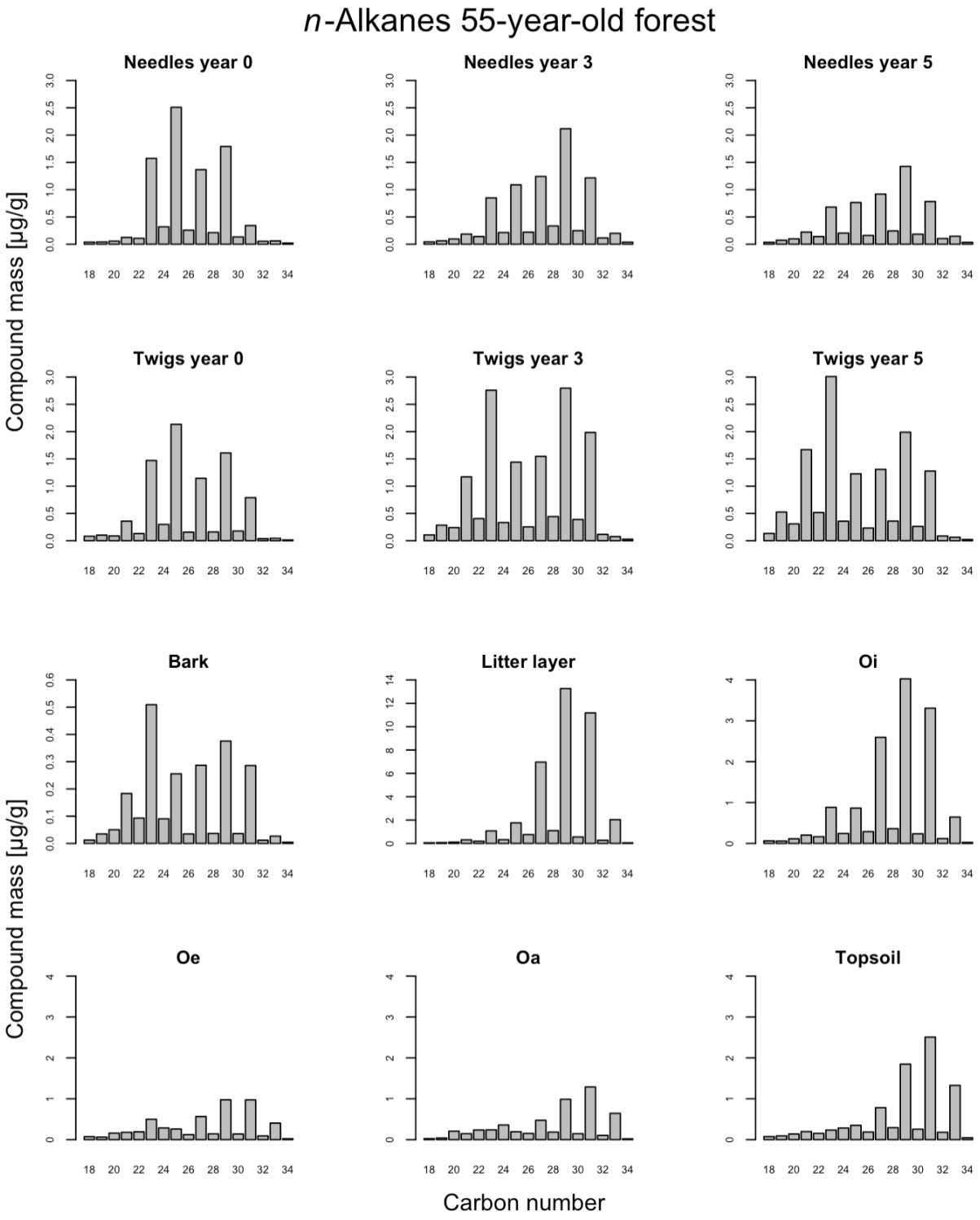

Figure 9: n-Alkane distributions in the 55-year-old forest section.

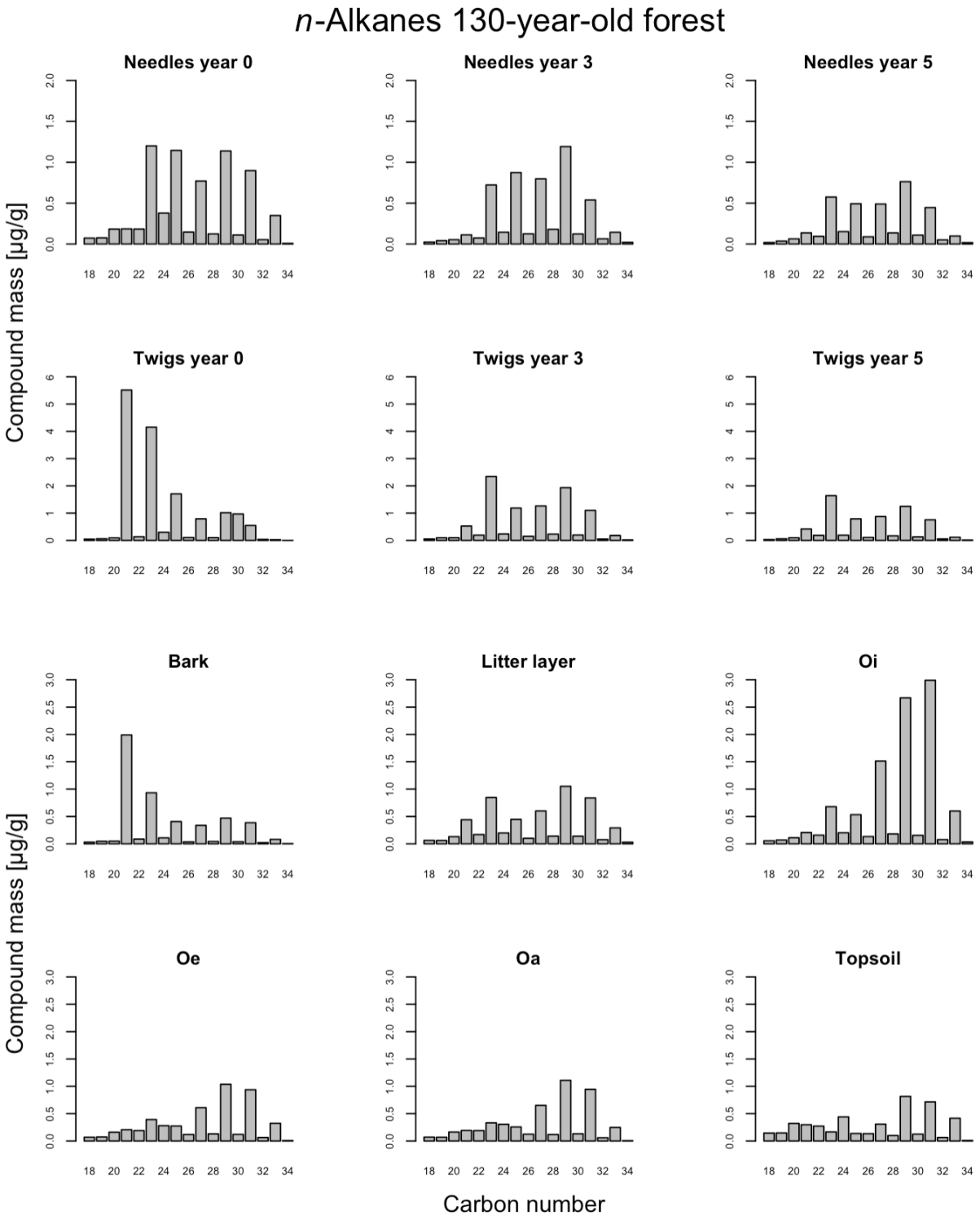

Figure 10: n-Alkane distributions in the 130-year-old forest section.

n-Alkane distribution in the organic horizons

In the organic horizons Oi, Oe, and Oa components of n-alkanes are even less scattered than in the litter horizons (Fig.8,9,10). For all three horizons, the dominant component is either n–C_{29}, with average concentrations ranging from 0.9 to 3.9 μg/g, or n–C_{31} ranging from 0.9 to 3.3 μg/g, whereby the abundance of n–C_{31} increases towards the organic horizon Oa. It can also be observed that the distribution patterns of the litter layer and the organic horizons resemble each other.

n-Alkane distribution in the topsoil

The topsoil samples show similar distribution patterns of n-alkanes as the organic horizons, where the similarity of the samples increases towards the Oa horizon (Fig.8,9,10). The most dominant component is either n–C_{29}, with an average concentrations ranging from 0.8 to 2.7 μg/g, or n–C_{31}, ranging from 0.7 to 4.1 μg/g. The highest amounts of hydrocarbons can be found for the components n–C_{29}, n–C_{31} and n–C_{33}.

n-Alkane distribution in moss

n–C_{27} is the most dominant component of the n-alkane distribution in moss (Fig.11), with a concentration of 12.0 μg/g. The second most dominant component, with a concentration of 4.4 μg/g is n–C_{29}, n–C_{31} follows with a concentration of 3.6 μg/g, and n–C_{25} with 2.9 μg/g.

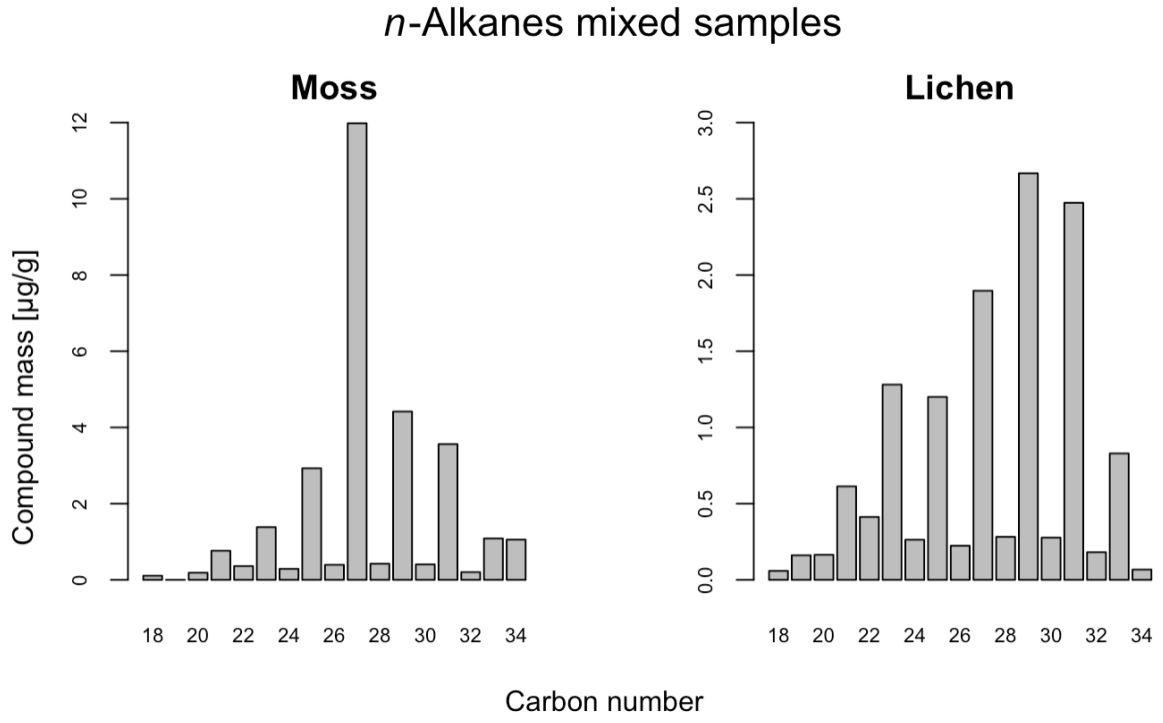

Figure 11: n-Alkane distributions for moss and lichen

n-Alkane distribution in lichen

In lichens, the most dominant component is n–C_{29}, with a concentration of 2.7 μg/g (Fig.11). n–C_{31} follows as second, with a concentration of 2.5 μg/g, and n–C_{27} with a concentration of 1.9 μg/g. Less abundant are components below n–C_{23}.

3.4 Fatty acids

Only fatty acid components with an even number of carbon atoms were evaluated. Besides carbon chain length components of C_{20}, C_{22},C_{24}, C_{26}, C_{28}, C_{30}, and C_{32}, also even-numbered diacids of carbon chain lengths of C_{20}, C_{22} and C_{24} (marked in the plots as D_{20}, D_{22}, and D_{24}) were investigated. Unlike n-alkanes, fatty acids show much higher concentrations of the individual substances (Fig.8,9,10,11,12,13,14,15).

Fatty acid distribution in spruce needles

C_{24} is always the most dominant component of fatty acids in samples of spruce needles (Fig.12,13,14), with an average concentrations ranging from 150.6 to 188.9 μg/g for the maximum 1-year-old needles. Subsequently, the second and third highest concentrations in most needle samples were measured for the components C_{22} and C_{26}. Comparatively less concentrated are the components C_{20}, C_{28}, C_{30}, and C_{32}. Compared to all other sample types, diacids are proportionally the least represented in samples of spruce needles. The concentration of the individual components decreases with increasing sample age, except for the needle samples from the 130-year-old forest. The overall distribution pattern in needle samples is approximately identical for all forest areas and all needle ages.

Fatty acid distribution in spruce twigs

C_{22} is always the dominant component of fatty acids in spruce twigs (Fig.12), with a measured average concentration between 687.6 and 1918.2 μg/g (Fig.12,13,14). Besides C_{22}, essential components in spruce twigs are only C_{20} and C_{24}. The measured concentrations of the individual components decrease with increasing sample age. Twig samples show proportionally higher concentrations of diacids compared to the needle samples.

Fatty acid distribution in spruce bark

The dominant component of fatty acids in samples of spruce bark is either C_{24} or C_{22}. Both show an average concentration ranging from 316.6 to 599.6 μg/g (Fig.12,13,14). Besides these two components, only C_{20} was detected as an essential component. Diacids in spruce bark are proportionally more abundant than in needle and twig samples.

Fatty acid distribution in the litter layer

The most dominant component of fatty acids in samples of the litter layer with an average concentration between 212.0 and 426.2 μg/g is always C_{22}, followed by C_{24} and then C_{20} (Fig.12,13,14). Other components were detected in proportionally lower quantities.

Fatty acid distribution in organic horizons

Besides one exception, the dominant component in the organic horizons is always C_{22} (Fig.12,13,14). The average concentration in the organic horizon Oi of component C_{22} was measured between 281.1 and 502.5 μg/g. In the 55-, and 130-year-old forest sections, higher concentrations for component C_{22} were measured in the organic horizon Oi compared to the the litter layer. In the 40-year-old forest section, similar values were measured for the litter layer and the Oi horizon. The compound concentrations decrease continuously from the organic horizon Oi to the organic horizon Oa. Thus, concentrations of component C_{22} were measured in the Oe horizon between 112.3 and 154.7 μg/g and in the Oa horizon between 10.7 and 27.0 μg/g. The distribution patterns of the different components are similar in all organic horizons and resemble the distribution patterns from the litter layers.

Fatty acid distribution in topsoil

The distribution patterns in the topsoil samples of the 55- and 130-year-old forest areas resemble those of the litter layers and organic horizons (Fig.12,13,14). The dominant component C_{22} was measured between 7.9 and 10.2 μg/g. In the 40-year-old forest section, component C_{24} dominates with a concentration of 9.1 μg/g. The topsoil distribution pattern of this forest area resembles the distribution pattern from the overlying Oa horizon.

Fatty acid distribution in moss and lichen

The dominant component of fatty acids in the moss and lichen samples is C_{24}, with a concentration of 45.5 μg/g for the moss sample, and 23.5 μg/g for the lichen sample. The second dominant component is C_{22}, which shows in both samples lower concentrations (Fig.15). Other essential components for both samples are C_{20}, C_{26}, and C_{28}. Diacids are proportionally most present in the lichen sample.

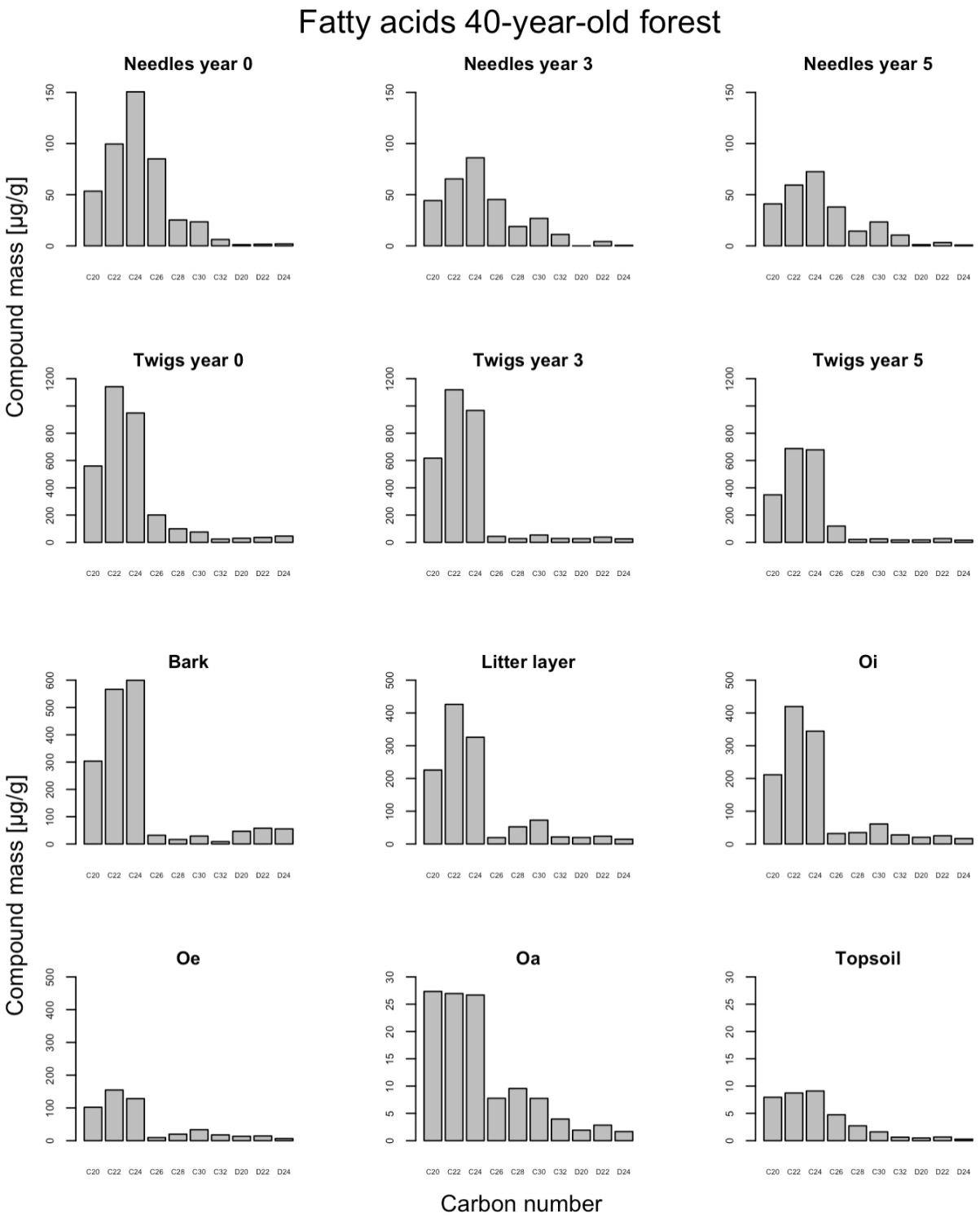

Figure 12: Fatty acid distributions in the 40-year-old forest section.

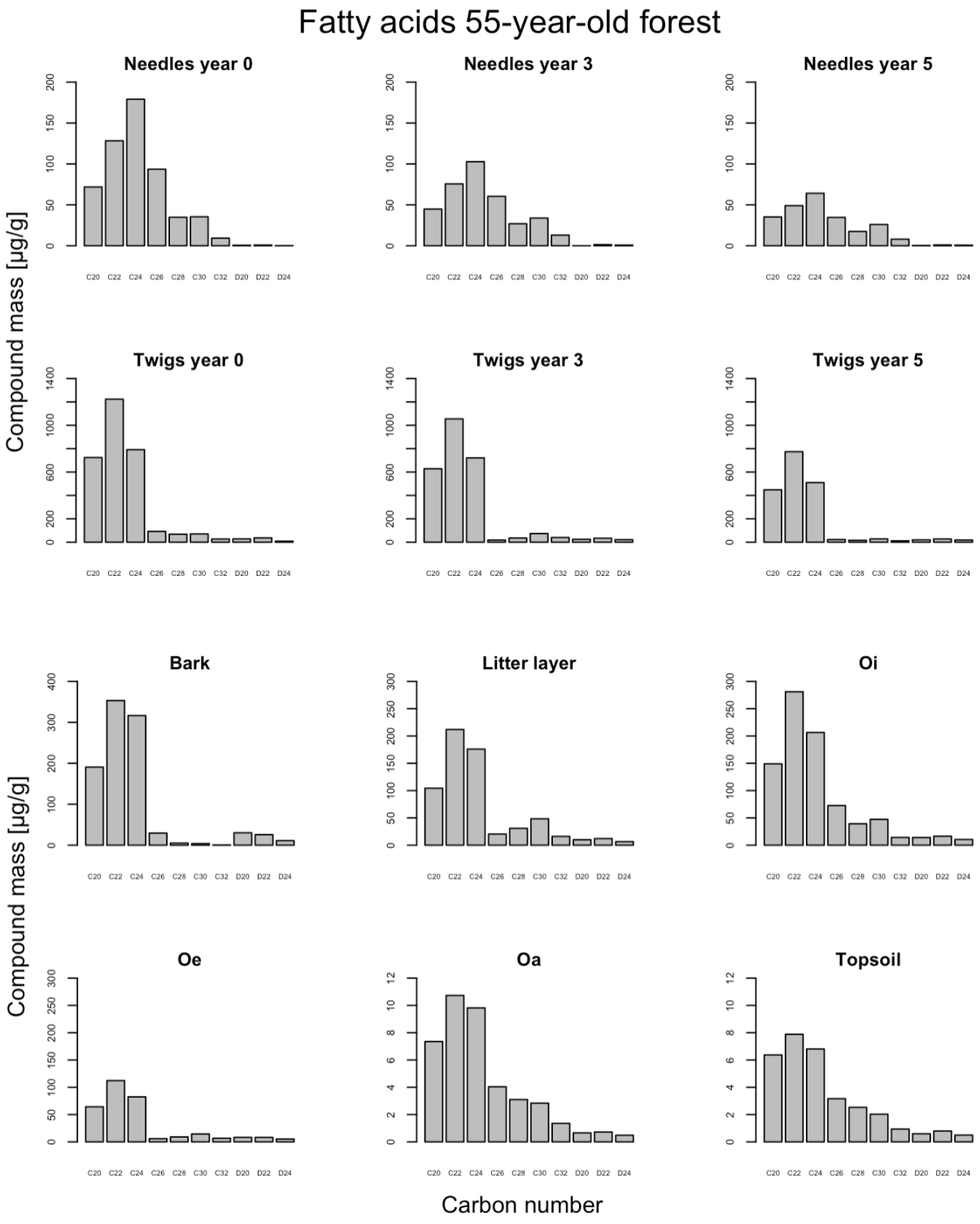

Figure 13: Fatty acid distributions in the 55-year-old forest section.

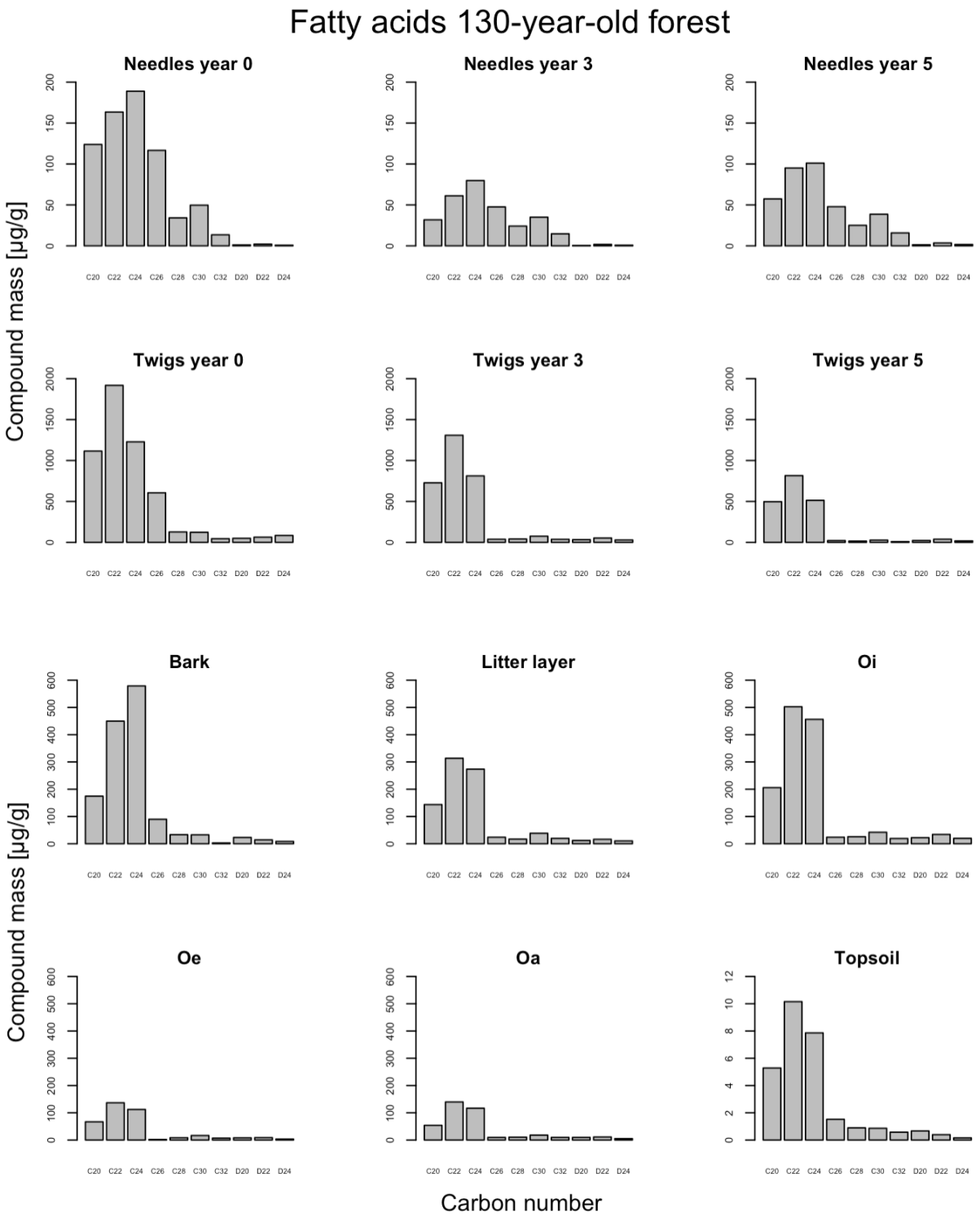

Figure 14: Fatty acid distributions in the 130-year-old forest section.

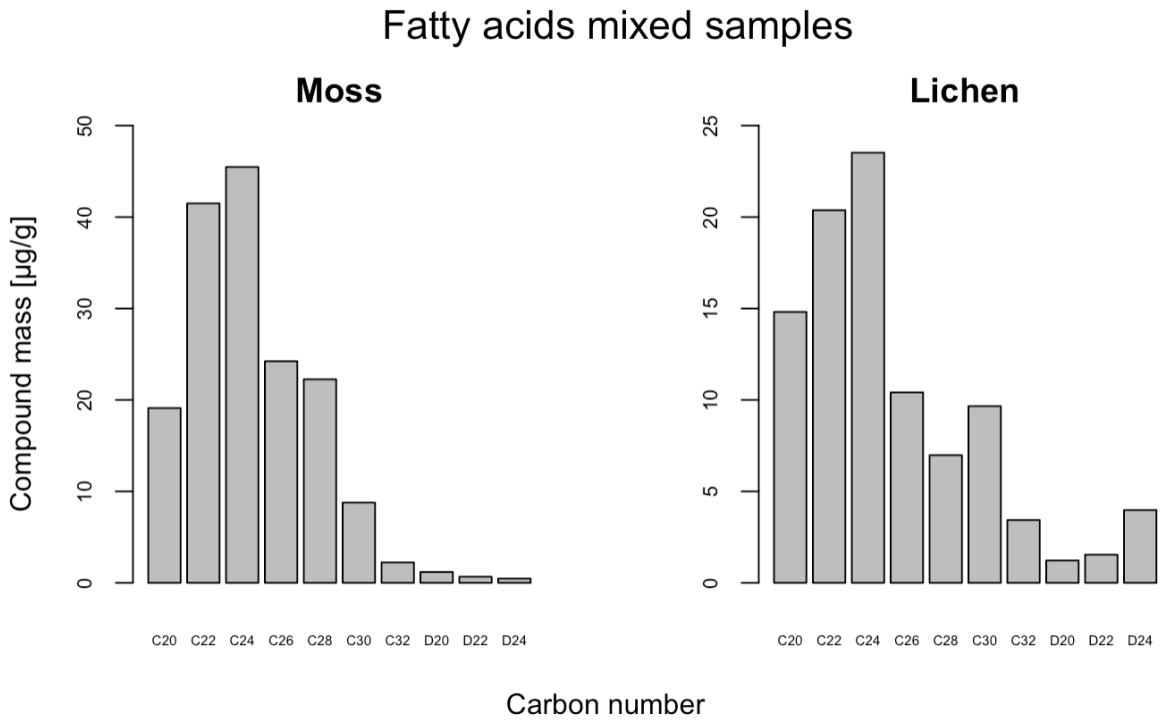

Figure 15: Fatty acid distributions of moss and lichen.

3.5 Index measurements ACL, CPI, and OEP

The measured average chain length (ACL) in n-alkanes (C_{21}-C_{34}) shows significant differences between the needle, twig, and bark samples ($p = 2 * 10^{-5}$) (Fig.16), averaging 27.2 ± 0.9 for spruce needles (needle 0 + needle 3 + needle 5), 25.8 ± 1.2 for spruce twigs (twigs 0 + twigs 3 + twigs 5), and 24.7 ± 2.8 for bark. The ACL value for the moss sample is 27.5, respectively 27.8 for the lichen sample. The measured ACL values increase significantly from the litter layer to the topsoil ($p = 0.02$). Average ACL values are 27.9 ± 1.0 for the litter layer, 27.8 ± 1.1 for the Oi horizon, 28.5 ± 0.8 for the Oe horizon, 29.0 ± 0.8 for the Oa horizon, and 29.4 ± 0.8 for the topsoil. Compared to the litter layer, the ACL in the Oi horizon decreases by -0.2 %, and increases by 2.3 % in the Oe horizon, 4.0 % in the Oa horizon, and by 5.4 % in the topsoil. The differences in the measured ACL values between the 40-, 55-, and 130-year-old forest sections are only significant for samples of the Oa horizon ($p = 0.008$), marked in red (Tab.6).

The ACL values in fatty acids (C_{22}-C_{32}) show significant differences between the needle, twig, and bark samples, ($p = 5.87 * 10^{-16}$) (Fig.16), averaging 25.1 ± 0.4 for spruce needles (needle 0 + needle 3 + needle 5), 23.4 ± 0.2 for spruce twigs (twigs 0 + twigs 3 + twigs 5), and 23.7 ± 1.2 for bark. The ACL value for the moss sample is 24.9, respectively 25.3 for the lichen sample. No significant change can be observed from the litter layer to the topsoil ($p = 0.06$). Average ACL

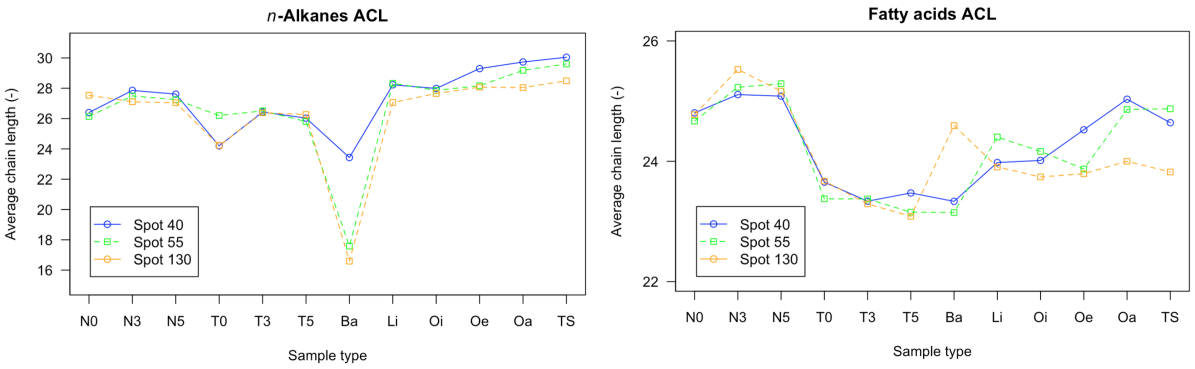

Figure 16: ACL values of different sample types for n-alkanes and fatty acids

ACL values for n-alkanes (left) and fatty acids (right) for: spruce needles = N, spruce twigs = T (less than 1-year-old = 0, 3-years-old = 3, 5-years-old = 5), spruce bark = Ba, litter layer = Li, organic horizon layers -Oi, -Oe, -Oa and topsoil = TS.

ACL_{Alk} values of different forest areas				
Sample type	40 year old forest	55 year old forest	130 year old forest	p
Spruce needle year 0	26.4 ± 0.7	26.1 ± 0.3	27.5 ± 1.8	0.35
Spruce needle year 3	27.9 ± 0.3	27.5 ± 0.3	27.1 ± 0.7	0.22
Spruce needle year 5	27.6 ± 0.6	27.3 ± 0.1	27.0 ± 0.8	0.50
Spruce twig year 0	24.2 ± 1.5	26.2 ± 0.7	24.2 ± 1.8	0.21
Spruce twig year 3	26.4 ± 0.2	26.5 ± 0.4	26.4 ± 0.6	0.93
Spruce twig year 5	26.0 ± 0.6	25.8 ± 0.8	26.3 ± 0.6	0.72
Bark	23.4 ± 3.2	26.4 ± 0.7	24.9 ± 3.8	0.95
Litter layer	28.2 ± 0.4	28.3 ± 1.6	27.1 ± 0.1	0.26
Oi	28.0 ± 0.7	27.9 ± 1.3	27.7 ± 1.5	0.94
Oe	29.3 ± 0.5	28.2 ± 0.7	28.1 ± 0.5	0.07
Oa	29.7 ± 0.4	29.2 ± 0.4	28.1 ± 0.6	0.008
Topsoil	30.1	29.6	28.5	-

Table 6: ACL_{Alk} values in forest sections of different ages.

values are 24.1 ± 0.6 for the litter layer, 24.0 ± 0.4 for the Oi horizon, 24.1 ± 0.5 for the Oe horizon, 24.6 ± 0.6 for the Oa horizon, and 24.5 ± 0.6 for the topsoil. The differences in the measured ACL values between the 40-, 55-, and 130-year-old forest sections are only significant for samples of the Oa horizon (p = 0.02), marked in red (Tab.7).

The carbon preference index CPI of n-alkanes (C_{21}-C_{34}) shows significant differences between the needle, twig, and bark samples, (p = 0.02) (Fig.17), averaging 5.4 ± 1.9 for spruce needles (needle 0 + needle 3 + needle 5), 8.7 ± 7.4 for spruce twigs (twigs 0 + twigs 3 + twigs 5), and 13.9 ± 10.9 for bark. The CPI value for the moss sample is 9.9, respectively 6.3 for the lichen sample. Significant changes in CPI values can be observed from the litter layer to the topsoil (p = 0.01). Average CPI values are 7.2 ± 3.6 for the litter layer, 7.8 ± 3.5 for the Oi horizon, 4.2 ± 1.1 for the Oe horizon, 4.0 ± 1.2 for the Oa horizon, and 4.9 ± 2.6 for the topsoil. The differences in

ACL_{FA} values of different forest areas				
Sample type	40 year old forest	55 year old forest	130 year old forest	p
Spruce needle year 0	24.8 ± 0.4	24.7 ± 0.2	24.8 ± 0.3	0.87
Spruce needle year 3	25.1 ± 0.2	25.2 ± 0.1	25.5 ± 0.6	0.37
Spruce needle year 5	25.1 ± 0.6	25.3 ± 0.2	25.2 ± 0.4	0.89
Spruce twig year 0	23.6 ± 0.1	23.4 ± 0.1	23.7 ± 0.4	0.31
Spruce twig year 3	23.3 ± 0.1	23.4 ± 0.1	23.3 ± 0.1	0.54
Spruce twig year 5	23.5 ± 0.3	23.2 ± 0.1	23.1 ± 0.2	0.09
Bark	23.3 ± 0.2	23.2 ± 0.1	24.6 ± 2.0	0.32
Litter layer	24.0 ± 0.5	24.4 ± 1.0	23.9 ± 0.2	0.61
Oi	24.0 ± 0.4	24.2 ± 0.3	23.7 ± 0.4	0.39
Oe	24.5 ± 0.6	23.9 ± 0.2	23.8 ± 0.2	0.11
Oa	25.0 ± 0.4	24.9 ± 0.1	24.0 ± 0.4	0.02
Topsoil	24.6	24.9	23.8	-

Table 7: ACL_{FA} values in forest sections of different ages.

the CPI values between the 40-, 55-, and 130-year-old forest sections are only significant for samples of the 5-year-old spruce twigs (p = 0.04), and the Oa horizon (p = 0.04), marked in red (Tab.8).

CPI_{Alk} values of different forest areas				
Sample type	40 year old forest	55 year old forest	130 year old forest	p
Spruce needle year 0	7.4 ± 1.7	7.3 ± 1.9	5.8 ± 4.1	0.73
Spruce needle year 3	4.6 ± 0.6	5.3 ± 0.9	5.3 ± 1.0	0.49
Spruce needle year 5	4.0 ± 0.3	4.5 ± 0.5	4.4 ± 1.1	0.63
Spruce twig year 0	20.5 ± 13.4	7.6 ± 1.0	13.7 ± 14.4	0.43
Spruce twig year 3	5.8 ± 0.5	6.2 ± 1.4	7.7 ± 0.9	0.12
Spruce twig year 5	5.0 ± 0.3	5.4 ± 0.6	6.6 ± 0.8	0.04
Bark	19.9 ± 14.5	5.6 ± 2.3	13.2 ± 6.5	0.43
Litter layer	6.1 ± 2.5	10.5 ± 4.3	4.9 ± 1.0	0.13
Oi	7.9 ± 2.5	7.7 ± 2.6	7.9 ± 5.9	1.00
Oe	5.2 ± 0.4	3.7 ± 1.1	3.8 ± 0.9	0.12
Oa	5.2 ± 0.7	3.1 ± 0.5	3.6 ± 1.1	0.04
Topsoil	7.3	5.0	5.0	-

Table 8: CPI_{Alk} values in forest sections of different ages.

The odd-over-even predominance OEP of *n*-alkanes (C_{26}-C_{33}) shows no significant differences between the needle, twig, and bark samples (p = 0.07) (Fig.18), averaging 5.3 ± 1.2 for spruce needles (needle 0 + needle 3 + needle 5), 6.0 ± 1.9 for spruce twigs (twigs 0 + twigs 3 + twigs 5), and 6.9 ± 3.0 for bark. The OEP value for the moss sample is 14.8, respectively 8.2 for the lichen sample. From the litter layer to the topsoil, no significant changes in OEP values can be observed (p = 0.2). Average OEP values are 8.2 ± 3.9 for the litter layer, 9.6 ± 4.3 for the Oi horizon, 6.5 ± 1.3 for the Oe horizon, 6.7 ± 1.6 for the Oa horizon and 7.3 ± 2.1 for the topsoil. The differences in the measured OEP values between the 40-, 55-, and 130-year-old forest sections are only significant for samples of the 5-year-old spruce twigs (p = 0.008), marked in red (Tab.9).

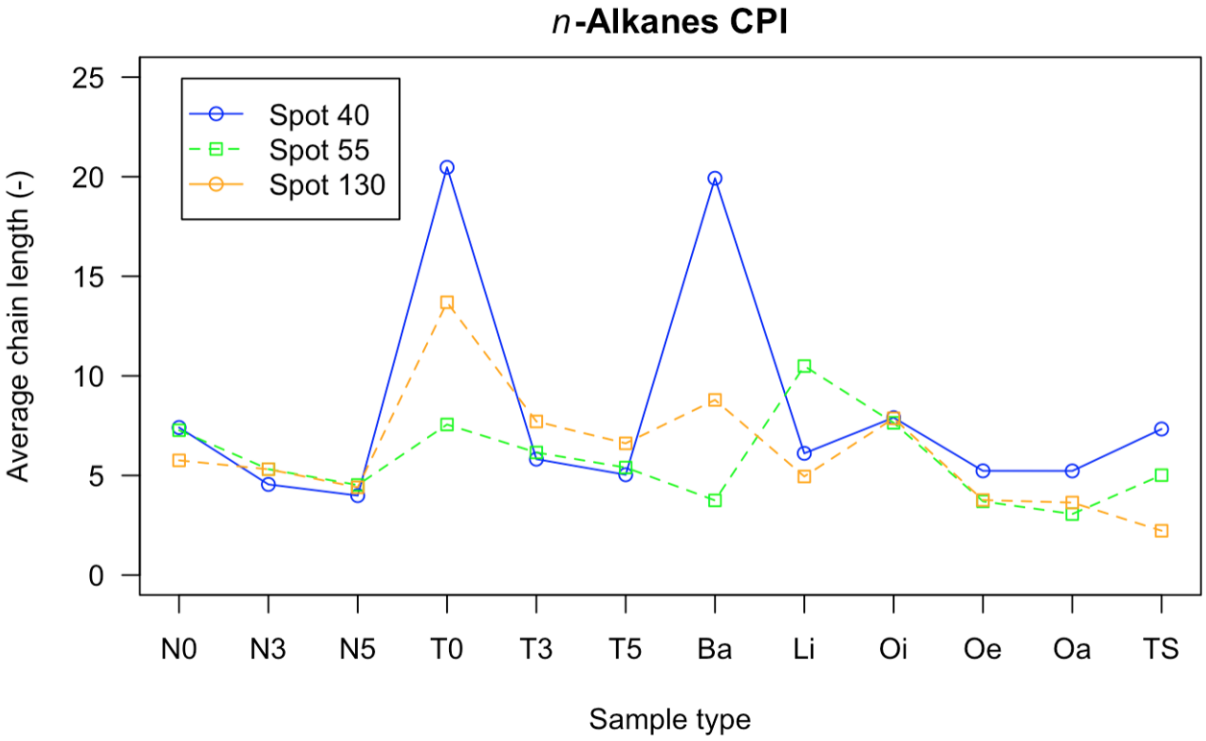

Figure 17: CPI for n-alkanes

CPI values for: spruce needles = N, spruce twigs = T (less than 1-year-old = 0, 3-years-old = 3, 5-years-old = 5), spruce bark = Ba, litter layer = Li, organic horizons -Oi, -Oe, -Oa, and topsoil = TS.

OEP_{Alk} values of different forest areas				
Sample type	40 year old forest	55 year old forest	130 year old forest	p
Spruce needle year 0	5.9 ± 0.3	5.7 ± 1.4	7.1 ± 2.0	0.47
Spruce needle year 3	4.5 ± 0.3	5.4 ± 0.9	5.2 ± 0.8	0.40
Spruce needle year 5	3.9 ± 0.2	4.8 ± 0.9	4.6 ± 0.5	0.24
Spruce twig year 0	8.6 ± 3.2	6.8 ± 1.1	4.5 ± 3.2	0.25
Spruce twig year 3	5.2 ± 0.6	5.9 ± 1.5	7.2 ± 0.3	0.09
Spruce twig year 5	4.5 ± 0.7	5.1 ± 0.5	6.5 ± 0.3	0.008
Bark	5.3 ± 1.3	8.3 ± 4.0	7.9 ± 4.5	0.54
Litter layer	7.2 ± 2.6	11.5 ± 5.4	6.0 ± 0.5	0.21
Oi	9.0 ± 2.9	9.3 ± 3.5	10.6 ± 7.2	0.92
Oe	7.3 ± 1.0	5.8 ± 0.8	6.5 ± 1.8	0.42
Oa	7.7 ± 1.0	5.8 ± 0.7	6.6 ± 2.3	0.35
Topsoil	9.4	7.1	5.3	-

Table 9: OEP_{Alk} values in forest sections of different ages.

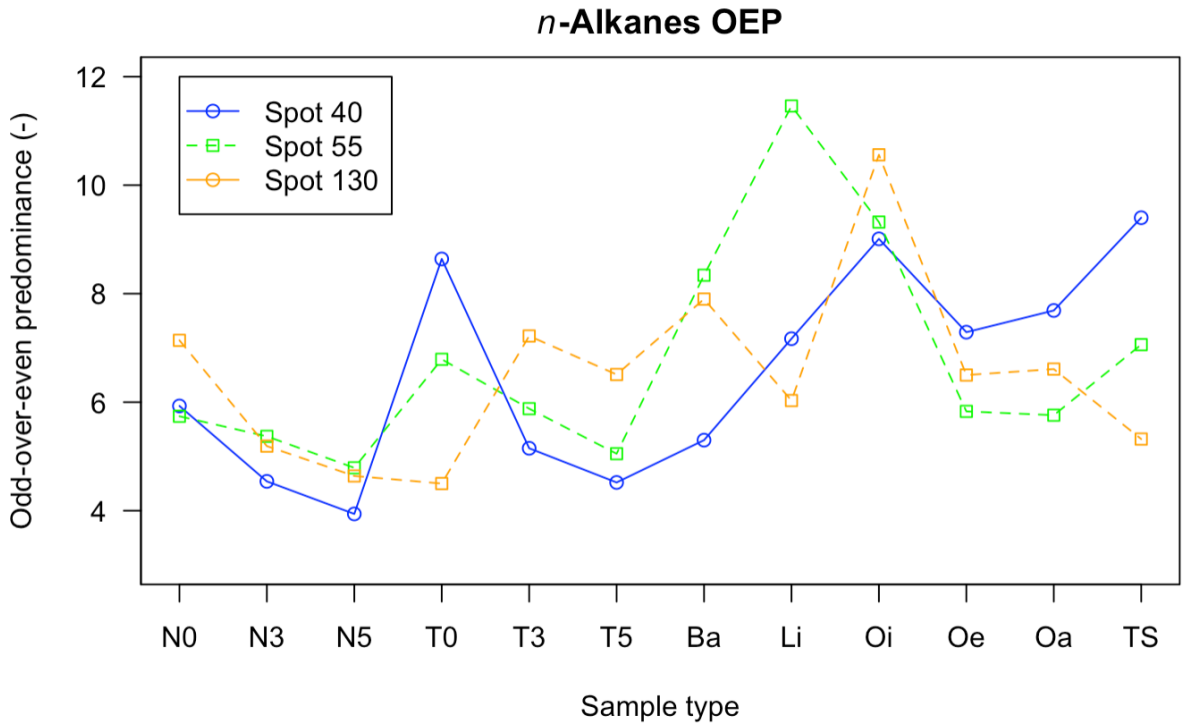

Figure 18: OEP for n-alkanes

OEP values for: spruce needles = N, spruce twigs = T (less than 1-year-old = 0, 3-years-old = 3, 5-years-old = 5), spruce bark = Ba, litter layer = Li, organic horizons -Oi, -Oe, -Oa, and topsoil = TS.

The four scatterplots of the ACL/CPI values (Fig.19) show cluster formations of the different sample types and shifts between those clusters. The x- and y-axes are identical for better comparison. The different sample types are plotted in groups, since clusters partly overlap. In the last plot (bottom right), all the ACL/CPI values from the previous plots are shown again in black (others) to get an overview of the entire distribution. Spruce needles of all ages form a distinct clustering (top left). Further, it can be observed that spruce needles of the different ages form slightly different clusters. The needles less than one-year-old (needles 0) show the most considerable scattering. Meanwhile, 3- and 5-year-old needles show lower scattering. Spruce twigs show apparent clustering (top right). Although the ACL/CPI values of the 3- and 5-year-old spruce twigs are closer to each other, a much stronger scattering can be recognized for the maximum 1-year-old the spruce twigs (twigs 0). The distribution pattern of the twigs 0 strongly resembles the distribution pattern of the bark samples (bottom left). Young twigs are proportionally most composed of bark, which may explain the convergence of these two sample types. The moss mixed sample mostly resembles the ACL/CPI values of the needle samples, whereas the lichen sample can rather be found to the right of this distribution. The distribution patterns of the litter layer (bottom left) and organic horizon Oi (bottom right) are quite similar, as they are synonyms for the same soil horizon. Furthermore,

it can be observed that the distribution patterns of the ACL/CPI values shift towards higher ACL and lower CPI values with increasing degree of decomposition in samples from the horizons Oi, Oe, Oa, to the topsoil.

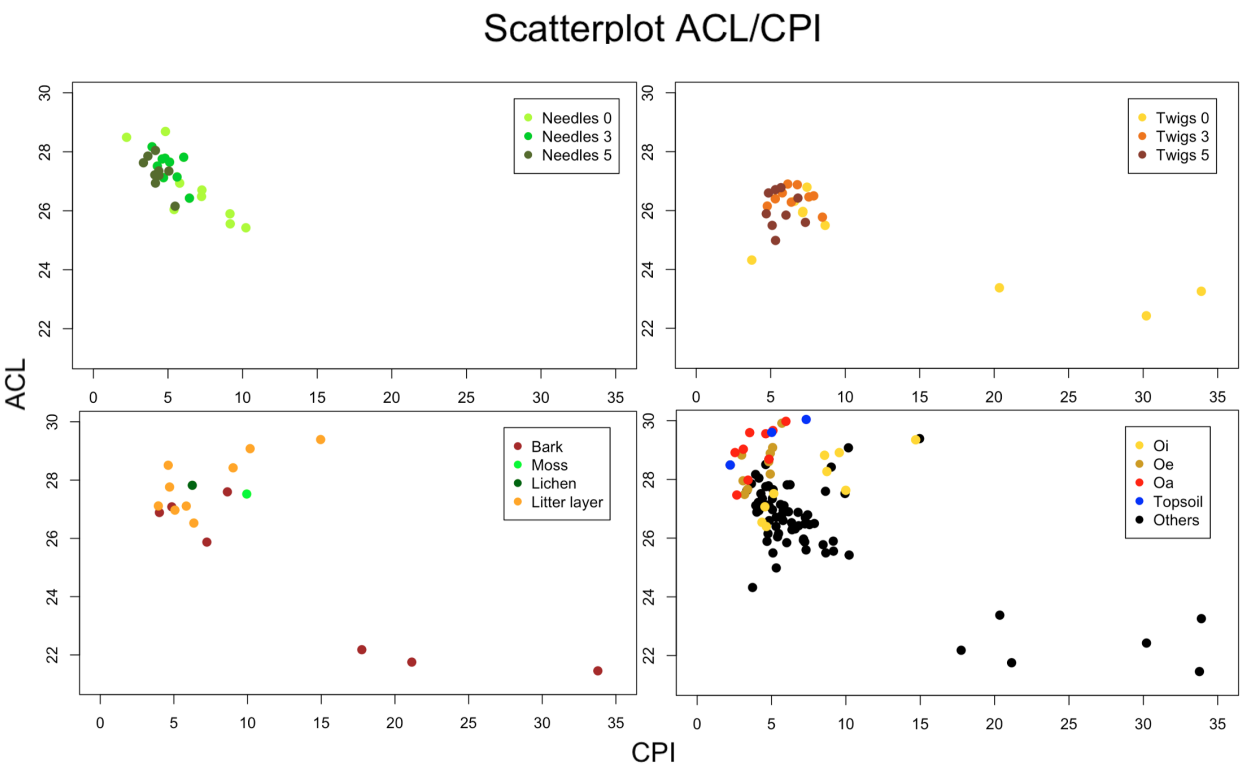

Figure 19: Scatterplot ACL/CPI

Scatterplots of different sample types. Clustering of the ACL/CPI values of the needle samples visible (top left), clustering of twig samples with three outliers (top right), values for litter layer and bark samples show cluster formation with larger scattering, and value for mosses and lichens (bottom left), clustering and clear shift toward higher ACL and lower CPI values from Oi to Oe, Oa, and topsoil samples, for better illustration all points are indicated again in black (bottom right).

4 Discussion

The aim of this master thesis was the identification of the composition of free extractable lipids, including *n*-alkanes and fatty acids in samples of fresh plant material, the organic horizons, and the topsoil, to understand the transformation of organic material from the forest biomass to the topsoil. The main findings are discussed in terms of the research questions, regarding the primary source of SOC, the differences in lipid compositions between the forest ages and vegetation, and the molecular resistance and decomposition of SOM.

4.1 What contributes the most to soil organic carbon (SOC)?

The *n*-alkane distributions in the litter layer, the organic horizons, and the topsoil are very similar from a visual point of view. Components C_{27}, C_{29}, C_{31} and C_{33} are relatively abundant in all three forest areas. However, in the 40- and 55-year-old forest sections, the dominant component changes from C_{29} in the litter layer and the Oi horizon to C_{31} in the Oe horizon, Oa horizon, and topsoil, which can also be indicated by the significant increase ($p = 0.02$) of the ACL values from the litter layer to the topsoil. In the 130-year-old forest section, the dominant component is always C_{29}, except for the Oi horizon, which shows dominance of C_{31}. Since the lipid distributions between soil samples and fresh plant samples differ significantly, clear visual assignment of plant signals in the soil is impossible. In addition, the distribution patterns within the individual plant organs sometimes differ greatly so that no general distribution pattern of spruce needles, spruce twigs, and bark could be determined. Variability of *n*-alkane distributions between plant species and between plant organs of the same species could lead to the assumption that interplant variability in general and environmental stress might be responsible for differences in the *n*-alkane distributions (Trigui et al., 2019). Leaf waxes serve as protection and belong to the plant's first barrier to the atmosphere. Therefore, it is reasonable, that their composition could be controlled and changed to some extent by environmental adaptation such as to different seasonal conditions or climatic variations (Trigui et al., 2019; Bush and McInerney, 2013). It is also visible, that the *n*-alkane distributions of the 3- and 5-year-old needle samples tend to be similar. While in the youngest needle samples for all three sites, proportionally higher concentrations of compounds C_{23} and C_{25} were measured. These changes in chemical compositions might indicate the changing physiological and biochemical properties of aging spruce needles (Camp et al., 1982). Nevertheless, certain similarities can be observed. Thus, some *n*-alkane signals of spruce needles can be detected in the litter layer, such as the identical dominant component C_{29}, or visually viewed the molecular distribution pattern itself. Similar distribution patterns can be detected between the 3- and 5-year-old needles and the litter

layer in all three forest areas. While *n*-alkane needle signals from short-chain components ($< C_{25}$) are less abundant in the litter layer, longer-chain components ($> C_{25}$) can be detected again in the litter layer. On the other hand, relatively abundant components such as C_{21}, C_{23}, and C_{25} that might occur in spruce twigs and bark cannot clearly be detected in the litter layer, the organic horizons, and the topsoil. Based on visually observed lipid distributions, it might be concluded that spruce needles play the most important role as a source of organic material in the litter layer, organic horizons, and the topsoil. Of course, not only do spruce needles contribute to soil organic carbon, but also spruce twigs, bark, mosses, lichens, and other plant components such as spruce cones or wood could affect the input. However, it is difficult to identify the investigated ones based on the molecular distributions in the organic horizons and the topsoil.

Fatty acid distributions in the litter layer, the organic horizons, and the topsoil are proportionally very similar from a visual point of view, except for the 40-year-old forest section, where patterns differ in the Oa horizon and the topsoil. Besides the mentioned exception, compound C_{22} is always dominant, followed by C_{24} and C_{20}. Also, distribution patterns within individual plant organs are very similar, so a rather characteristic distribution pattern could be determined for spruce needles, spruce twigs, and bark. The significantly stronger concentrations of fatty acid compounds in spruce twigs compared to spruce needles and the dominance of C_{22} compounds in spruce twigs could be the reason for C_{22} domination in the litter layer, the organic horizons, and the topsoil. Therefore, spruce twigs appear to play an important role for the distribution pattern of fatty acids in litter and soil samples. Another indication pointing to the importance of spruce twigs for SOC is the relatively high concentration of diacids in the litter layer, organic horizons, and topsoil, which can also be found in spruce twigs, but not as concentrated in spruce needles. However, the proportionally highest concentration of diacids can be observed in bark. But a relatively high concentration of longer-chain components (C_{26}, C_{28}, C_{30}, and C_{32}) can be detected in litter and soil samples, which cannot be observed to the same degree in spruce twig samples. For this reason, spruce needles, mosses, and lichens also play an important role, as they show proportionally higher concentrations of longer-chain components than spruce twigs. Therefore, based on visually observed fatty acid distributions, spruce twigs play a significant or even the most important role in forming the distribution pattern in litter and soil samples. However, it is shown that spruce needles, bark, and other plant components or plant species such as mosses and lichens are important as well.

While *n*-alkanes reveal a rather spruce needles dominated source of SOC, fatty acid distributions show that rather spruce twigs come into question as the primary source. On the other side, it can be observed that other plant components such as spruce needles, mosses, or lichens might also play

an essential role in the fatty acid distributions in forest floor and forest soil samples. Whether *n*-alkanes or fatty acids reflect a better proxy for the source of SOC is challanging to evaluate. However, other studies show that the litter fall in spruce stands is mainly dominated by needles (Hågvar, 2016; Berg and Meentemeyer, 2001), strengthening the credibility of *n*-alkanes as a proxy. But in certain spruce forests and years, spruce cones (not investigated in this thesis) can also contribute to a significant amount to the litterfall (Hågvar, 2016; Hagner, 1965). Both, fatty acids and *n*-alkanes can provide helpful information about the source of SOC. Hence, using both methods in conjunction with each other provides a more comprehensive understanding of the sources and dynamics of plant-soil systems.

Because soil *n*-alkanes are supposed to represent an average *n*-alkane distribution pattern of the surrounding biome (Yan et al., 2021), it can be determined, if besides the investigated plant samples other lipid signals are missing, which could be derived from other plant species or plant organs not examined in this thesis. Thereby, an *n*-alkane mixing scatter plot of ACL and CPI values for the different sample types was performed (Fig.19). Despite considerable scatter between individual sample types, significant differences could be observed ($p= 4.76*10^{-7}$), as previously described in another study (Cooper et al., 2015). Because soil and organic horizon samples do not cluster aside from the linear combination of the different plant samples, it can be suggested that the *n*-alkane distribution pattern could potentially be obtained by mixing of the investigated plant samples. Further it can be observed that no other plant signal is needed to obtain the soil *n*-alkane ACL/CPI pattern displayed in the plot (Yan et al., 2021). This can be seen from the fact that the ACL/CPI values are mostly mapped on a straight belt, starting with the fresh plant samples, and ending with the topsoil samples (bottom right). In addition, there are some outliers for the maximum 1-year-old twigs (twigs 0, top right) and bark samples (bottom left). However, these samples could possibly be assigned to the outliers of the litter layer (bottom left) and Oi horizon (bottom right). Nevertheless, this does not mean that other plant samples or plant species, which could also cluster within the linear combination, cannot be considered a source of SOC.

4.2 The role of aboveground vegetation and different forest ages on SOC

The aboveground vegetation and forest age can play an essential role in the accumulation and maintenance of SOC. The type and amount of plant litter that falls to the forest floor can significantly influence the rate of SOC accumulation, depending on the vegetation type, such as tree species, canopy cover, or human influences, such as forestry (Lal, 2005). Also, different forest ages can greatly impact SOC accumulation. Differences in soil carbon inputs and transformations likely occur in

stands of different forest ages due to changing inputs from tree and ground vegetation litter, light penetration, throughfall, as well as changing water and nutrient availability. Moreover, effects might occur due to increasing forest management treatments with advanced stand age (Clarke et al., 2007).

Long-chain *n*-alkanes of the investigated fresh plant samples all revealed a strong odd-over-even predominance (OEP), which is a characteristic of epicuticular leaf waxes of terrestrial higher plants (Trigui et al., 2019), such as Norway spruce. However, the two investigated lower plants (mosses and lichens) showed even higher OEP values. The stable carbon isotope values δ^{13}C of the investigated plant samples are between -32.2 % and -24.98 % (Fig.6), They are thus located within the typical values for C_3 plants (Hirave et al., 2020), such as spruce trees, mosses, and lichens. Samples from the organic horizons and topsoil also lie within the ranges for higher plants and C_3 plants, which confirms their contribution.

The investigated samples either derived from a 40-, 55-, or a 130-year-old forest section. In addition to the forest ages, these sites also differ in their vegetation. In the youngest 40-year-old forest section, only spruce trees are growing close to each other. In the 55- and 130-year-old forest section, also a few deciduous trees grow sporadically next to the spruce trees. In the 130-year-old forest area most broadleaf trees can be observed. Results from the elemental analysis have shown that C and N concentrations and δ^{13}C values show significant differences between the different forest ages. Differences are significant for C concentrations in the organic horizon Oa and the topsoil, for N concentrations in the organic horizons Oi and Oe and the topsoil, and for δ^{13}C values in the organic horizon Oa, and for all samples of spruce needles and twigs. ACL values from *n*-alkanes and fatty acids and CPI values have only shown significant differences between the three forest ages in the organic horizon Oa. Differences are also clearly visible in the topsoil, but the values cannot be statistically verified due to the low sample number. Since no significant differences between forest ages can be observed for the litter layer and the organic horizon Oi (except for N concentrations), it is impossible to assess how the different vegetation of the three investigated forest areas affect SOC input. Also, lipid distribution patterns of *n*-alkanes and fatty acids do not show significant differences that could be attributed to different vegetative influences. The strikingly high concentration of the *n*-alkane component C_{27} in the mixed moss sample could not be found to the same extent in the spruce needle, spruce twig, and bark samples, and cannot verify the assumption of the higher moss contribution to the youngest forest section. Visually observed lipid distributions are not showing different C_{27} values for the 40-, 55-, and 130-year-old forest sections regarding the litter layer and the organic horizon Oi. Although the *n*-alkane ACL values for the organic horizons and topsoil show no significant differences (except the Oa horizon), the ACL values are consistently

highest for the 40-year-old forest section and always lowest for the 130-year-old forest section. This observation indicates the prevailing tree diversity, which is supported by a previous study (Thomas et al., 2021) that shows that ACL values are highest for coniferous forests, lower for mixed forests, and lowest for deciduous forests. This result would also be consistent with the observations of the three investigated forest sections, with deciduous trees being most abundant in the 130-year-old forest section, less abundant in the 55-year-old forest section, and barely present in the 40-year-old forest section.

4.3 The role of molecular resistance and degradation to SOC

Until now, many gaps persist in the knowledge of the degradation and preservation of diverse SOM compound classes, such as lipids (Schmidt et al., 2011; Thomas et al., 2021). Although recent studies reveal that the persistence of SOC is caused by functional complexity (Lehmann et al., 2020), other investigations demonstrate that the molecular structure alone is not responsible for SOM stability. However, environmental and biological factors predominate (Schmidt et al., 2011).

Observed molecular lipid distributions in fresh plant biomass of spruce needle, spruce twig, and spruce bark samples were not necessarily transferred to the litter layer, the organic horizons, and the topsoil. This can be seen by the change of the average chain length (ACL) in both compound classes of *n*-alkanes and fatty acids (Fig.16), and by changes in the lipid distributions (Fig.8,9,10,12,13,14) (Marseille et al., 1999; Hirave et al., 2020). Relatively high ACL values for *n*-alkanes in the topsoil compared to the overlying organic horizons Oi, Oe, and Oa might result from preferential degradation of short-chained components or preferential preservation of long-chained molecules (Thomas et al., 2021). Regarding the fatty acids, changes in the lipid compositions (Fig.12,13,14), as well as an increase in the ACL values from fresh plant samples of spruce twigs and spruce bark to the litter layer and to the organic horizons, can be observed (Fig.16). This might be caused by preferential degradation and the production of long-chained fatty acids by oxidation of lipid components such as *n*-alkanes or *n*-alkanols (Marseille et al., 1999; Hirave et al., 2020; Amblès et al., 1994). Despite preferential degradation, identifying characteristic patterns of plant derived *n*-alkanes in soil is still possible, because primary long-chained components remain dominant (Thomas et al., 2021).

In general, OEP is considered a proxy for the preservation of leaf wax derived *n*-alkanes. Thus measured high values indicate no or little degradation of *n*-alkanes. On the other hand, low values (<5) reflect an enhanced state of degradation (Trigui et al., 2019). Observed OEP values from fresh plant samples are generally much lower than those obtained in the organic horizons and the topsoil

(Fig.18). However, decreases in the OEP values can be observed in the organic horizon Oe as well as unchanged or slightly increased values in the organic horizon Oa. The considerable decrease towards the horizons Oe and Oa meets the expectation and thus might indicate increased effects of degradation compared to the organic horizon Oi or litter layer (Trigui et al., 2019; Buggle et al., 2010). Further, OEP values in the 40-, and 55-year-old forest sections indicate lower decomposition in the topsoil. Contrary to expectation, the highest state of decomposition represented by the lowest OEP value is shown in the topsoil of the 130-year-old forest section.

The C/N ratio (Fig.6, bottom left) is an important parameter that affects the rate of degradation of organic material. When microorganisms decompose organic material, they depend on a certain balance of carbon and nitrogen to thrive. If the C/N ratio is too high, nitrogen becomes limited, and carbon consumption decelerates. Contrariwise, too low C/N ratios results in carbon limitation, lowering degradation rates. Optimal C/N ratios for microbial growth and the degradation of OM generally range between 20 and 25 (Xie et al., 2022; Mooshammer et al., 2014). Within this range, organic material tends to decompose fast. Outside of this range, the decomposition rate might become reduced. This indicates that among the fresh plant samples, spruce twigs (C/N = 104 ± 69) are the least favorable for microbial decomposition regarding the C/N ratio, followed by spruce bark (C/N = 69 ± 22), and spruce needles (C/N = 49 ± 9). On the other hand, mosses (C/N = 25) reveal an optimal composition for microbial decomposition, and lichens reveal a slightly higher ratio (C/N = 28). It is further shown that the litter layer (C/N = 45 ± 6) and Oi horizon (C/N = 45 ± 10) do not show optimal conditions for microbial decomposition. In contrast, the organic horizons Oe (C/N = 27 ± 6) is nearly in the optimal range, and Oa (C/N = 21 ± 7) is in the optimal range. The topsoil (C/N = 18 ± 3) can again be found slightly outside the optimum range. Thus, the organic horizon Oa is best suited for microbial turnover and growth, followed by the topsoil, the organic horizon Oe, and Oi. Thus, findings from the C/N ratios generally correlate with those from the OEP values.

With progressive degradation, the isotopic compositions showed continuous enrichment of ^{13}C from fresh plant samples (needles, twigs, bark, moss, and lichen) via the organic horizons (Oi, Oe, Oa) to the topsoil (Hirave et al., 2020). One exception occurs in the organic horizon Oe of the 130-year-old forest section, where a decrease in $\delta^{13}C$ values can be observed. Enrichment of the stable carbon isotope $\delta^{13}C$ occurs due to preferential microbial consumption of the lighter ^{12}C isotope, leaving a higher proportion of ^{13}C in the remaining organic matter and the soil (Meckenstock et al., 1999). As a result, with continuous degradation, $\delta^{13}C$ values increase. The highest increases of the $\delta^{13}C$ values can be observed either for the Oa horizon (40-year-old forest section), or the Oe and Oa horizons (55-year-old forest section). Thus, the degree of ^{13}C enrichment can be used as an indicator of the

turnover of SOM. Progressive decomposition from the litter to the topsoil and the highest turnover rates in the organic horizons Oa and Oe can, therefore also be observed by the $\delta^{13}C$ values. The highest decomposition rates for the 130-year-old forest section are shown in the topsoil.

The *n*-alkanes in cuticular waxes of higher plant species are reported to have strong odd-over-even predominance, resulting in CPI values above 5. In contrast, *n*-alkanes originating from bacterial activity or algae growth show low odd-over-even predominance resulting in CPI values of 1 (Cranwell et al., 1987). The fresh plant CPI values are in average always higher than 5 (spruce needle = 5.39, spruce twigs = 8.72, bark = 10.82, moss = 9.94, and lichen = 6.25) (Fig.16). The decomposition of organic material increases with advancing soil depths. Hence, the CPI values decrease rapidly and even fall below the CPI value of 5, which can be attributed to higher bacterial activity and faster degradation of lipid compounds (Angst et al., 2016). Thus, the initial CPI values for the two samples of the litter layer = 7.18 and the Oi horizon = 7.81, decrease to the values in the Oe horizon = 4.23, Oa horizon = 3.98, and finally slightly increase again in the topsoil to the value of 4.86. These results also fit the results described above.

The *n*-alkane analysis from the 40- and 55-year-old forest section shows a significant compound enrichment in the litter layer compared to the fresh plant samples. *n*-Alkane concentrations subsequently decrease strongly in the organic horizon Oi and Oe, until in the organic horizon Oa and topsoil concentrations increases again. The comparatively smaller concentrations in the Oi- and Oe-horizons might result from two combined factors: significant degradation of compounds in the overlying litter layer and further in the Oe horizon, and their insolubility in water which prevents them from migrating downwards (Marseille et al., 1999). Higher *n*-alkane concentrations in the organic horizons and the topsoil compared to the fresh plant samples have already been observed in other coniferous forests (Thomas et al., 2021). Since fresh plant samples often show low initial *n*-alkane concentrations (Thomas et al., 2021; Schäfer et al., 2016; Otto and Simpson, 2005), accumulation in lower layers becomes possible, even if degradation continues. Moreover, as waxes on spruce needles are renewed throughout the year, lipid enrichment in the organic horizons and the topsoil compared to fresh plant samples can be observed due to physical wax abrasion and subsequent lipid depositions into the soil (Thomas et al., 2021; Heinrich et al., 2015).

5 Conclusion

Lipid and elemental analysis in the different forest sections in Jaun (Switzerland) has shown significant differences between the forest ages and the lipid distributions in samples from fresh plant material to the topsoil. As expected, *n*-alkane dominant compounds and distributions revealed spruce needles as the most important carbon source for the organic horizons and the topsoil. Fatty acids, on the other hand, indicated that spruce twigs might be considered the most important source of SOC. However, it was also shown that other plant organs, such as needles and bark, or other plant species, such as mosses and lichens, might also be responsible to a greater degree for the observed lipid distributions in the organic horizons and the topsoil. Surprisingly, the assessment of fatty acids was not as expected and contradicted the statement of the *n*-alkanes. However, since spruce needles generally belong to the most abundant component of the litter layer in Norway spruce forests, this might suggest that *n*-alkanes, which identify spruce needles as the primary source of SOC, are better suited as a proxy. The *n*-alkane values of the scatterplot (ACL/CPI) indicate, that besides the investigated fresh plant sample types of spruce needles, spruce twigs, bark, mosses, and lichens, no other plant signals might be missing from the surrounding biome, to conclude the primary source of SOC. On the other hand, spruce cones (not investigated in this thesis), which in general also belong to a primary compound of the litter layer in Norway spruce forests, could also match the ACL/CPI scatterplot, and thus confirm their importance for SOC. However, further investigations of spruce cones are needed to verify this assumption.

Samples from the organic horizons and the topsoil, as well as fresh plant samples, reveal a strong odd-over-even predominance (OEP), which is indicative for higher plants, and δ^{13}C values, which lies within the range for C_3 plants. Thus, molecular signals of higher plants (such as spruce trees), and C_3 plants (such as spruce trees, mosses, and lichens), could be detected both in the fresh plant samples and in the soil. Furthermore, samples derived from the 40-, 55-, and 130-year-old forest sections partly illustrate significant differences for C-, N-, δ^{13}C-, ACL-, CPI-, and OEP values. But contrary to the expectations, since no significant differences could be observed for the litter layer, or the organic horizon Oi (except for N concentrations), it was impossible to conclude the different vegetational influences between the three forest areas of different ages. Thus, significant differences in the lower organic horizons and the topsoil might not be explainable with different litter layer inputs, but rather with processes, which are responsible for the preservation or decomposition of those components. The only indication for the prevailing tree diversity might be the *n*-alkane ACL values, which are the lowest for the 40-year-old forest section, higher for the 55-year-old forest section, and the highest for the 130-year-old forest section, regarding samples of the organic horizons and the topsoil. In fact, a previous study has shown that, that ACL values of the organic horizons

and topsoil are highest for coniferous forests, lower for mixed forests and lowest for deciduous forests (Thomas et al., 2021), which is consistent with the observations from the investigated three forest areas.

As expected, observed high ACL values for n-alkanes in the topsoil compared to the overlaying organic horizons might result from preferential degradation of short-chained components and the preferential preservation of long-chained molecules. Increasing ACL values for fatty acids from the fresh plant samples to the organic horizons might also be caused by preferential degradation, but also by the in situ production of long-chained fatty acids in the organic horizons. A considerable decrease of OEP values from the organic horizon Oi to Oe observed in all forest areas, might indicate increased effects of degradation in the Oe horizon. OEP values in the organic horizon Oa then showed no changes compared to Oe, and finally decreased in the topsoil, except for the 130-year-old forest section, where a significant increase of the OEP values can be observed. The C/N ratio reveals that the organic horizon Oa is best suited for microbial growth and decomposition rate, followed by the topsoil, the organic horizon Oe, and the Oi horizon. Continuous degradation from the organic horizons to the topsoil and highest turnover rates of SOM in the organic horizons Oa and Oe, can also be observed by increasing δ^{13}C values, as well as highest decomposition rates for the 130-year-old forest section in the topsoil. Increasing degradation rates can also be shown by rapidly decreasing CPI values in the two organic horizons Oe and Oa, and the switch from the dominant n-alkane compound C_{29} to C_{31}. Significant n-alkane enrichment of the 40-, and 55-year-old forest section in the litter layer compared to the fresh plant samples, can be observed. Subsequently, a substantial decrease in the organic horizons Oi and Oe, might result from continuous physical wax abrasion, its accumulation in the litter layer, and from significant degradation of OM in the lower organic horizons Oi and Oe.

6 Limitations

Yields of total lipid extracts (TLE) were not considered in the context of this master thesis due to an unsuccessful drying process. TLE data would have been valuable as verification for successful extraction and to complete to the rest of the results. Incomplete drying may have affected the subsequent methods of separation. Thus, some uncertainties in the results must be assumed. Another uncertainty cannot be excluded during the integration of GC-FID peak areas. Since components partially overlap, calculated peak areas and the information obtained from them about the weight distribution of the different lipid components may contain errors. In order to extend the results of this thesis, further analysis, such as measuring of lipid distributions of spruce cones, roots, wood, mycelium, and other compounds of the forest vegetation, could be helpful, as they can also be considered as a source of SOC. Another possible extension would be the measurement of shorter chain components of *n*-alkanes and fatty acids, as these can provide further information on microbial processes and could be an essential part of understanding the carbon cycle in soil.

7 Outlook

Although many studies have been conducted about the transformation of *n*-alkanes and fatty acids from plants to the soil, many gaps in knowledge persist. Since lipid distributions are highly variable, even within plant species, further studies are needed to narrow down variations. In addition, other organisms or plant organs need to be investigated for lipid distributions, such as roots, spruce cones, wood, and fungi, as these might also play a significant role in forest soil carbon input. Furthermore, due to climate change, it may be interesting to study lipid distributions in response to changing environmental parameters. This would be particularly important, if reforested ecosystems are considered as a possible carbon sink to mitigate climate change. In addition, it is unclear how SOC will behave as climate change progresses. If, in the future, more carbon is prone to escape from the soil, it would be of interest to implement this information in climate models. However, essential findings are still missing and have been ignored in climate models so far. Thus, it is crucial that further research on plant and soil lipid distributions are conducted and gathered in freely accessible databases to create transparency and to facilitate further investigations.

8 Acknowledgement

At this point, the author would like to thank all those who provided support and encouragement during this master's thesis process. First, to PD Dr. Guido L.B. Wiesenberg for his support, knowledge, and countless sketches that facilitated understanding. Further to the Soil and Biogeochemistry group, among them, Yves Brügger, Barbara Siegfried, Thomy Keller, Binyan Sun, Nadja Hertel, and Sonja Eisenring for their support and helpful discussions. A special thank goes to the supervisor of this master's thesis, Ph.D. Tatjana Carina Speckert, for her help in the laboratory, her motivation, and for making the sometimes monotonous daily lab routines bearable.

9 References

- Amblès, A., Jambu, P., Parlanti, E., Joffre, J., Riffe, C. (1994). Incorporation of natural monoacids from plant residues into an hydromorphic forest podzol. *European Journal of Soil Science, 45*(2), 175-182.

- Amelung, W., Bossio, D., Vries, W., Kögel-Knabner, I., Lehmann, J., Amundson, R., Bol, R., Collins, C., Lal, R., Leifeld, J., Minasny, B., Pan, G., Paustian, K., Rumpel, C., Sanderman, J., van Groenigen, J.W., Mooney, S., van Wesemael, B., Wander, M., Chabbi, A. (2020). Towards a global-scale soil climate mitigation strategy. *Nature Communications, 11*(1), 1-10.

- Angst, G., John, S., Mueller, C. W., Kögel-Knabner, I., Rethemeyer, J. (2016). Tracing the sources and spatial distribution of organic carbon in subsoils using a multi-biomarker approach. *Scientific Reports, 6*(1), 1-12.

- Baldock, J. A., Skjemstad, J. O. (2000). Role of the soil matrix and minerals in protecting natural organic materials against biological attack. *Organic Geochemistry, 31*(7-8), 697-710.

- Berg, B., Meentemeyer, V. (2001). Litter fall in some European coniferous forests as dependent on climate: a synthesis. *Canadian Journal of Forest Research, 31*(2), 292-301.

- Bowden, R. D., Deem, L., Plante, A. F., Peltre, C., Nadelhoffer, K., Lajtha, K. (2014). Litter input controls on soil carbon in a temperate deciduous forest. *Soil Science Society of America Journal, 78*(S1), S66-S75.

- Buggle, B., Wiesenberg, G. L. B., Glaser, B. (2010). Is there a possibility to correct fossil *n*-alkane data for postsedimentary alteration effects?. *Applied Geochemistry, 25*(7), 947-957.

- Bush, R. T., McInerney, F. A. (2013). Leaf wax *n*-alkane distributions in and across modern plants: implications for paleoecology and chemotaxonomy. *Geochimica et Cosmochimica Acta, 117*, 161-179.

- Camp, P. J., Huber, S. C., Burke, J. J., Moreland, D. E. (1982). Biochemical changes that occur during senescence of wheat leaves: I. Basis for the reduction of photosynthesis. *Plant Physiology, 70*(6), 1641-1646.

- Chen, L., Liu, T., Zhang, W., Chen, X., Wang, J. (2012). Biodiesel production from algae oil high in free fatty acids by two-step catalytic conversion. *Bioresource Technology, 111*, 208-214.

- Clarke, N., Wu, Y., Strand, L. T. (2007). Dissolved organic carbon concentrations in four Norway spruce stands of different ages. *Plant and Soil, 299*, 275-285.

- Cooper, R. J., Pedentchouk, N., Hiscock, K. M., Disdle, P., Krueger, T., Rawlins, B. G. (2015). Apportioning sources of organic matter in streambed sediments: an integrated molecular and compound-specific stable isotope approach. *Science of the Total Environment, 520*, 187-197.

- Cranwell, P. A. (1981). Diagenesis of free and bound lipids in terrestrial detritus deposited in a lacustrine sediment. *Organic Geochemistry, 3*(3), 79-89.

- Cranwell, P. A., Eglinton, G., Robinson, N. (1987). Lipids of aquatic organisms as potential contributors to lacustrine sediments—II. *Organic Geochemistry, 11*(6), 513-527.

- Diefendorf, A. F., Freimuth, E. J. (2017). Extracting the most from terrestrial plant-derived *n*-alkyl lipids and their carbon isotopes from the sedimentary record: A review. *Organic Geochemistry, 103*, 1-21.

- Eglinton, T. I., Eglinton, G. (2008). Molecular proxies for paleoclimatology. *Earth and Planetary Science Letters, 275*(1-2), 1-16.

- Fine, A. K., Schmidt, M. P., Martínez, C. E. (2018). Nitrogen-rich compounds constitute an increasing proportion of organic matter with depth in Oi-Oe-Oa-A horizons of temperate forests. *Geoderma, 323*, 1-12.

- García-Hernández, C., Ruiz-Fernández, J., Sánchez-Posada, C., Pereira, S., Oliva, M., Vieira, G. (2017). Reforestation and land use change as drivers for a decrease of avalanche damage in mid-latitude mountains (NW Spain). *Global and Planetary Change, 153*, 35-50.

- Hagner, S. (1965). Cone crop fluctuations in Scots pine and Norway spruce. *Studia forestalia Suecica, 21*, 0039-3150.

- Hågvar, S. (2016). From litter to humus in a norwegian spruce forest: Long-term studies on the decomposition of needles and cones. *Forests, 7*(9), 186.

- Heinrich, S., Dippold, M. A., Werner, C., Wiesenberg, G. L. B., Kuzyakov, Y., Glaser, B. (2015). Allocation of freshly assimilated carbon into primary and secondary metabolites after in situ ^{13}C pulse labelling of Norway spruce (*Picea abies*). *Tree Physiology, 35*(11), 1176-1191.

- Hiltbrunner, D. (2012). Turnover and stabilization of organic matter in Alpine soils: Effect of livestock grazing and reforestation (Doctoral dissertation, University of Zurich).

- Hiltbrunner, D., Zimmermann, S., Hagedorn, F. (2013). Afforestation with Norway spruce on a subalpine pasture alters carbon dynamics but only moderately affects soil carbon storage. *Biogeochemistry, 115*(1), 251-266.

- Hirave, P., Wiesenberg, G. L. B., Birkholz, A., Alewell, C. (2020). Understanding the effects of early degradation on isotopic tracers: implications for sediment source attribution using compound-specific isotope analysis (CSIA). *Biogeosciences, 17*(8), 2169-2180.

- Houghton, R. A. (2003). Revised estimates of the annual net flux of carbon to the atmosphere from changes in land use and land management 1850–2000. *Tellus B: Chemical and Physical Meteorology, 55*(2), 378-390.

- Huang, Y., Lockheart, M. J., Collister, J. W., Eglinton, G. (1995). Molecular and isotopic biogeochemistry of the Miocene Clarkia Formation: hydrocarbons and alcohols. *Organic Geochemistry, 23*(9), 785-801.

- Jansen, B., Wiesenberg, G. L. B. (2017). Opportunities and limitations related to the application of plant-derived lipid molecular proxies in soil science. *Soil, 3*(4), 211-234.

- Jansen, B., Nierop, K. G., Hageman, J. A., Cleef, A. M., Verstraten, J. M. (2006). The straight-chain lipid biomarker composition of plant species responsible for the dominant biomass production along two altitudinal transects in the Ecuadorian Andes. *Organic Geochemistry, 37*(11), 1514-1536.

- Kögel-Knabner, I. (2002). The macromolecular organic composition of plant and microbial residues as inputs to soil organic matter. *Soil Biology and Biochemistry, 34*(2), 139-162.

- Kögel-Knabner, I. (2017). The macromolecular organic composition of plant and microbial residues as inputs to soil organic matter: fourteen years on. *Soil Biology and Biochemistry, 105*, A3-A8.

- Ladd, B., Peri, P. L., Pepper, D. A., Silva, L. C., Sheil, D., Bonser, S. P., Laffan, S. W., Amelung, W., Ekblad, A., Eliasson, P., Bahamonde, H., Duarte-Guardia, S., Bird, M. (2014). Carbon isotopic signatures of soil organic matter correlate with leaf area index across woody biomes. *Journal of Ecology, 102*(6), 1606-1611.

- Lal, R. (2005). Forest soils and carbon sequestration. *Forest Ecology and Management, 220*(1-3), 242-258.

- Lal, R. (2016). Soil health and carbon management. *Food and Energy Security, 5*(4), 212-222.

- Lavrieux, M., Bréheret, J. G., Disnar, J. R., Jacob, J., Le Milbeau, C., Zocatelli, R. (2012). Preservation of an ancient grassland biomarker signature in a forest soil from the French Massif Central. *Organic Geochemistry, 51*, 1-10.

- Lehmann, J., Hansel, C. M., Kaiser, C., Kleber, M., Maher, K., Manzoni, S., Nunan, N., Reichstein, M., Schimel, J. P., Torn, M. S., Wieder, W. R., Kögel-Knabner, I. (2020). Persistence of soil organic carbon caused by functional complexity. *Nature Geoscience, 13*(8), 529-534.

- Lichtfouse, E., Dou, S., Girardin, C., Grably, M., Balesdent, J., Béhar, F., Vandenbroucke, M. (1995). Unexpected ^{13}C-enrichment of organic components from wheat crop soils: evidence for the in situ origin of soil organic matter. *Organic Geochemistry, 23*(9), 865-868.

- Marseille, F., Disnar, J. R., Guillet, B., Noack, Y. (1999). *n*-Alkanes and free fatty acids in humus and A1 horizons of soils under beech, spruce and grass in the Massif-Central (Mont-Lozère), France. *European Journal of Soil Science, 50*(3), 433-441.

- Meckenstock, R. U., Morasch, B., Warthmann, R., Schink, B., Annweiler, E., Michaelis, W., Richnow, H. H. (1999). 13C/12C isotope fractionation of aromatic hydrocarbons during microbial degradation. *Environmental Microbiology, 1*(5), 409-414.

- Mooshammer, M., Wanek, W., Hämmerle, I., Fuchslueger, L., Hofhansl, F., Knoltsch, A., Schnecker, J., Takriti, M., Watzka, M., Wild, B., Keiblinger, K, M., Zechmeister-Boltenstern, S., Richter, A. (2014). Adjustment of microbial nitrogen use efficiency to carbon: nitrogen imbalances regulates soil nitrogen cycling. *Nature Communications, 5*(1), 3694.

- Mueller, K. E., Polissar, P. J., Oleksyn, J., Freeman, K. H. (2012). Differentiating temperate tree species and their organs using lipid biomarkers in leaves, roots and soil. *Organic Geochemistry, 52*, 130-141.

- Murali, S., Govindan, V. K. (2013). Shadow detection and removal from a single image using LAB color space. *Cybernetics and Information Technologies, 13*(1), 95-103.

- Otto, A., Simpson, M. J. (2005). Degradation and preservation of vascular plant-derived biomarkers in grassland and forest soils from Western Canada. *Biogeochemistry, 74*, 377-409.

- Post, W. M., Kwon, K. C. (2000). Soil carbon sequestration and land-use change: processes and potential. *Global Change Biology, 6*(3), 317-327.

- R Core Team. (2021). A language and environment for statistical computing. R Foundation for Statistical Computing, Vienna, Austria. URL: http://www.R-project.org/.

- Schäfer, I. K., Lanny, V., Franke, J., Eglinton, T. I., Zech, M., Vysloužilová, B., Zech, R. (2016). Leaf waxes in litter and topsoils along a European transect. *Soil, 2*(4), 551-564.

- Schmidt, M. W. I., Torn, M. S., Abiven, S., Dittmar, T., Guggenberger, G., Janssens, I. A., Kleber, M., Kögel-Knabner, I., Lehmann, J., Manning, D. A. C., Nannipieri, P., Rasse, D. P., Weiner, S., Trumbore, S. E. (2011). Persistence of soil organic matter as an ecosystem property. *Nature, 478*(7367), 49-56.

- Swift, M. J., Heal, O. W., Anderson, J. M., Anderson, J. M. (1979). Decomposition in terrestrial ecosystems (Vol. 5). Univ of California Press.

- Thomas, C. L., Jansen, B., van Loon, E. E., Wiesenberg, G. L. B. (2021). Transformation of *n*-alkanes from plant to soil: a review. *Soil, 7*(2), 785-809.

- Thuille, A., Schulze, E. D. (2006). Carbon dynamics in successional and afforested spruce stands in Thuringia and the Alps. *Global Change Biology, 12*(2), 325-342.

- Trigui, Y., Wolf, D., Sahakyan, L., Hovakimyan, H., Sahakyan, K., Zech, R., Fuchs, M., Wolpert, T., Zech, M., Faust, D. (2019). First calibration and application of leaf wax *n*-alkane biomarkers in loess-paleosol sequences and modern plants and soils in Armenia. *Geosciences, 9*(6), 263.

- Van Veen, J. A., Liljeroth, E., Lekkerkerk, L. J. A., Van de Geijn, S. C. (1991). Carbon fluxes in plant-soil systems at elevated atmospheric CO_2 levels. *Ecological Applications, 1*(2), 175-181.

- Wang, J. U. N., Wu, W., Wang, X., Wang, M. I. N., Wu, F. (2015). An effective GC method for the determination of the fatty acid composition in silkworm pupae oil using a two-step methylation process. *Journal of the Serbian Chemical Society, 80*(1), 9-20.

- Wiesenberg, G. L. B., Gocke, M. I. (2017). Analysis of lipids and polycyclic aromatic hydrocarbons as indicator of past and present (micro-) biological activity, in: McGenity, T.J., N., T.K., Nogales Fernández, B. (Eds), *Hydrocarbon and Lipid Microbiology Protocols: Petroleum, Hydrocarbon and Lipid Analysis*, Springer, Berlin, Heidelberg, 61-91.

- Wiesenberg, G. L. B., Schwark, L., Schmidt, M. W. I. (2004). Improved automated extraction and separation procedure for soil lipid analyses. *European Journal of Soil Science, 55*(2), 349-356.

- Xie, Y., Zhou, L., Dai, J., Chen, J., Yang, X., Wang, X., Feng, L. (2022). Effects of the C/N ratio on the microbial community and lignocellulose degradation, during branch waste composting. *Bioprocess and Biosystems Engineering, 45*(7), 1163-1174.

- Yan, Y., Zhao, B., Xie, L., Zhu, Z. (2021). Trend reversal of soil *n*-alkane Carbon Preference Index (CPI) along the precipitation gradient and its paleoclimatic implication. *Chemical Geology, 581*, 120402.

- Zhang, Y., Zhao, M., Cui, Q., Fan, W., Qi, J., Chen, Y., Zhang, Y., Gao, K., Fan, J., Wang, G., Yan, C., Lu, H., Luo, Y., Zhang, Z., Zheng, Q., Xiao, W., Jiao, N. (2017). Processes of coastal ecosystem carbon sequestration and approaches for increasing carbon sink. *Science China Earth Sciences, 60*(5), 809-820.

- Zheng, Y., Zhou, W., Meyers, P. A., Xie, S. (2007). Lipid biomarkers in the Zoigê-Hongyuan peat deposit: Indicators of Holocene climate changes in West China. *Organic Geochemistry, 38*(11), 1927-1940.

- Zink, K. G., Leythaeuser, D., Melkonian, M., Schwark, L. (2001). Temperature dependency of long-chain alkenone distributions in recent to fossil limnic sediments and in lake waters. *Geochimica et Cosmochimica Acta, 65*(2), 253-265.

10 Appendix

Table 10: Color measurement 40-year-old forest

Spot	Sample type	L-vale	a-value	b-value
40.2	Needle 0	26.94	-0.11	-0.03
40.2	Needle 3	25.73	-0.07	-0.35
40.2	Needle 5	28.54	-0.35	0.43
40.2	Twig 0	29.45	-1.96	2.04
40.2	Twig 3	30.29	-1.19	2.18
40.2	Twig 5	30.05	-2.35	2.14
40.2	Bark	33.00	-1.42	2.16
40.2	Litter layer	30.19	-0.65	3.48
40.2	Oi	29.07	-0.47	4.27
40.2	Oe	32.26	-1.73	2.20
40.2	Oa	31.47	-1.37	0.92
40.3	Needle 0	28.85	-0.38	1.56
40.3	Needle 3	27.27	0.13	0.24
40.3	Needle 5	28.66	-0.01	0.78
40.3	Twig 0	31.17	-1.36	1.95
40.3	Twig 3	31.54	-1.64	2.36
40.3	Twig 5	33.09	-1.21	1.00
40.3	Bark	34.22	-1.49	4.29
40.3	Litter layer	29.48	-1.37	2.72
40.3	Oi	27.97	-0.40	4.44
40.3	Oe	27.38	-0.32	4.15
40.3	Oa	30.94	-1.34	0.59
40.4	Needle 0	26.60	-0.12	1.28
40.4	Needle 3	21.00	0.85	5.43
40.4	Needle 5	26.77	-0.31	0.52
40.4	Twig 0 A	30.35	-1.47	3.31
40.4	Twig 3	28.99	-1.49	5.54
40.4	Twig 5	30.03	-1.68	2.99
40.4	Bark	25.94	-2.07	4.39
40.4	Litter layer	29.62	-0.06	3.20
40.4	Oi	29.51	-0.84	3.26
40.4	Oe	31.13	-0.93	3.82
40.4	Oa	34.33	-0.56	-1.07
40	Topsoil	33.03	-1.00	-0.38

Table 11: Color measurement 55-year-old forest

Spot	Sample type	L-vale	a-value	b-value
55.2	Needle 0	27.85	-0.16	0.33
55.2	Needle 3	27.29	-0.07	0.11
55.2	Needle 5	30.68	-1.30	4.60
55.2	Twig 0	31.84	-1.82	3.15
55.2	Twig 3	30.03	-1.41	3.12
55.2	Twig 5	32.22	-1.81	3.56
55.2	Bark	32.25	-1.12	2.48
55.2	Litter layer	31.18	-0.37	3.93
55.2	Oi	26.85	0.04	3.99
55.2	Oe	31.66	-1.55	4.33
55.2	Oa	34.5	-0.81	-0.65
55.3	Needle 0	28.88	-0.46	1.20
55.3	Needle 3	25.13	-0.31	3.68
55.3	Needle 5	22.66	0.66	3.92
55.3	Twig 0	31.87	-1.60	2.56
55.3	Twig 3	25.22	-0.83	7.58
55.3	Twig 5	13.86	0.14	14.34
55.3	Bark	32.93	-1.12	1.69
55.3	Litter layer	31.41	-0.71	4.76
55.3	Oi	27.18	-0.76	4.77
55.3	Oe	32.05	-2.44	4.94
55.3	Oa	33.07	-1.35	0.54
55.4	Needle 0	27.13	0.09	1.11
55.4	Needle 3	27.43	-0.06	0.39
55.4	Needle 5	29.21	-0.75	-0.38
55.4	Twig 0 A	31.85	-1.83	2.69
55.4	Twig 3	29.75	-1.36	2.08
55.4	Twig 5	29.9	-0.83	2.82
55.4	Bark	22.41	1.19	13.91
55.4	Litter layer	30.81	-0.77	4.15
55.4	Oi	30.96	-0.78	3.27
55.4	Oe	34.33	-2.17	2.42
55.4	Oa	33.94	-1.04	0.17
55	Topsoil	33.53	-1.68	1.73

Table 12: Color measurement 130-year-old forest, moss and lichen

Spot	Sample type	L-vale	a-value	b-value
130.2	Needle 0	23.30	0.31	4.62
130.2	Needle 3	26.81	-0.25	2.21
130.2	Needle 5	30.72	-0.85	3.27
130.2	Twig 0	29.41	-1.79	4.34
130.2	Twig 3	33.57	-1.63	3.10
130.2	Twig 5	31.79	-1.84	3.65
130.2	Bark	30.05	-1.00	5.43
130.2	Litter layer	31.20	-1.64	2.59
130.2	Oi	32.59	-1.50	3.99
130.2	Oe	30.41	-1.14	2.69
130.2	Oa	31.46	-1.54	2.01
130.3	Needle 0	25.70	0.16	0.49
130.3	Needle 3	26.92	-0.33	1.34
130.3	Needle 5	26.84	-0.16	1.64
130.3	Twig 0	30.57	-1.72	2.50
130.3	Twig 3	30.30	-1.44	3.27
130.3	Twig 5	27.14	-1.33	3.64
130.3	Bark	28.80	-2.40	6.40
130.3	Litter layer	25.11	-0.69	5.67
130.3	Oi	31.04	-1.33	4.03
130.3	Oe	29.67	-2.12	4.98
130.3	Oa	31.36	-1.83	4.58
130.4	Needle 0	27.38	0.11	0.97
130.4	Needle 3	25.84	0.34	-0.44
130.4	Needle 5	27.29	-1.08	-1.01
130.4	Twig 0 A	31.01	-1.45	2.91
130.4	Twig 3	30.06	-1.13	1.71
130.4	Twig 5	31.55	-1.37	1.52
130.4	Bark	30.49	-1.37	2.38
130.4	Litter layer	23.29	0.71	4.63
130.4	Oi	31.89	0.30	4.68
130.4	Oe	35.17	-1.34	0.37
130.4	Oa	34.45	-1.24	0.17
130	Topsoil	34.29	-0.97	-0.47
Mix	Moss	18.83	0.62	2.31
Mix	Lichen	27.66	-0.24	0.06

Table 13: Elemental analysis 40-year-old forest

Spot	Sample type	C [%]	N [%]	$\delta^{13}C$ [‰]
40.2	Needle 0 A	48.32	1.16	-28.45
40.2	Needle 0 B	47.44	1.16	-28.54
40.2	Needle 3 A	48.36	0.95	-28.63
40.2	Needle 3 B	49.29	1.01	-28.39
40.2	Needle 5 A	48.98	0.95	-28.61
40.2	Needle 5 B	49.71	1.00	-28.55
40.2	Twig 0 A	48.51	0.90	-27.93
40.2	Twig 0 B	49.06	0.95	-27.88
40.2	Twig 3 A	49.95	0.52	-27.10
40.2	Twig 3 B	50.04	0.56	-27.07
40.2	Twig 5 A	47.86	0.30	-26.85
40.2	Twig 5 B	48.66	0.35	-26.77
40.2	Bark A	50.03	0.48	-25.98
40.2	Bark B	49.65	0.45	-25.75
40.2	Litter layer A	48.32	0.92	-27.86
40.2	Litter layer B	48.65	0.98	-27.70
40.2	Oi A	44.58	0.89	-27.59
40.2	Oi B	37.47	0.83	-27.67
40.2	Oe A	22.50	1.05	-27.46
40.2	Oe B	23.03	1.00	-27.52
40.2	Oa A	16.63	0.90	-27.12
40.2	Oa B	27.75	1.36	-27.10
40.3	Needle 0 A	48.85	1.28	-28.97
40.3	Needle 0 B	49.08	1.29	-28.82
40.3	Needle 3 A	48.22	1.28	-28.13
40.3	Needle 3 B	50.42	1.35	-28.08
40.3	Needle 5 A	50.27	1.07	-28.02
40.3	Needle 5 B	50.27	1.07	-27.95
40.3	Twig 0 A	50.73	0.85	-27.99
40.3	Twig 0 B	50.82	0.86	-27.99
40.3	Twig 3 A	49.76	0.53	-27.31
40.3	Twig 3 B	50.44	0.54	-27.23
40.3	Twig 5 A	49.55	0.39	-27.05
40.3	Twig 5 B	49.54	0.39	-26.97
40.3	Bark A	50.02	0.69	-26.55
40.3	Bark B	48.88	0.69	-26.48
40.3	Litter layer A	48.31	1.03	-27.77
40.3	Litter layer B	48.48	1.05	-27.72
40.3	Oi A	46.30	1.17	-27.35
40.3	Oi B	29.93	0.73	-27.65
40.3	Oe A	43.64	1.57	-27.60
40.3	Oe B	43.01	1.51	-27.80
40.3	Oa A	12.40	0.71	-26.82
40.3	Oa B	12.70	0.65	-26.71
40.4	Needle 0 A	48.05	0.95	-28.35
40.4	Needle 0 B	47.75	1.01	-28.41
40.4	Needle 3 A	48.83	0.77	-28.59
40.4	Needle 3 B	48.44	0.78	-28.64
40.4	Needle 5 A	49.29	0.67	-28.71
40.4	Needle 5 B	48.36	0.63	-28.76
40.4	Twig 0 A	49.32	0.91	-28.00
40.4	Twig 0 B	46.75	0.84	-28.33
40.4	Twig 3 A	49.55	0.36	-27.20
40.4	Twig 3 B	49.65	0.34	-27.32
40.4	Twig 5 A	49.06	0.28	-27.17
40.4	Twig 5 B	48.52	0.27	-27.18
40.4	Bark A	49.24	1.00	-25.59
40.4	Bark B	47.62	1.03	-25.59
40.4	Litter layer A	48.11	1.22	-27.63
40.4	Litter layer B	48.42	1.25	-27.61
40.4	Oi A	47.48	1.15	-27.55
40.4	Oi B	47.72	1.22	-27.22
40.4	Oe A	42.16	1.36	-26.78
40.4	Oe B	42.13	1.40	-26.57
40.4	Oa A	5.47	0.24	-26.39
40.4	Oa B	4.75	0.22	-26.27
40	Topsoil A	8.36	0.56	-26.57
40	Topsoil B	8.55	0.58	-26.58

Table 14: Elemental analysis 55-year-old forest

Spot	Sample type	C [%]	N [%]	$\delta^{13}C$ [‰]
55.2	Needle 0 A	48.21	0.85	-29.15
55.2	Needle O B	48.73	0.89	-29.06
55.2	Needle 3 A	48.81	0.79	-29.64
55.2	Needle 3 B	48.61	0.74	-29.56
55.2	Needle 5 A	49.33	0.90	-29.40
55.2	Needle 5 B	48.87	0.91	-29.55
55.2	Twig 0 A	49.22	0.58	-28.37
55.2	Twig O B	51.42	0.64	-28.41
55.2	Twig 3 A	49.65	0.36	-28.08
55.2	Twig 3 B	49.54	0.37	-27.96
55.2	Twig 5 A	48.24	0.44	-27.78
55.2	Twig 5 B	48.50	0.43	-27.77
55.2	Bark A	47.92	0.54	-26.30
55.2	Bark B	47.94	0.57	-26.17
55.2	Litter layer A	44.33	1.13	-28.04
55.2	Litter layer B	44.16	1.10	-28.10
55.2	Oi A	48.03	1.11	-27.91
55.2	Oi B	47.77	1.16	-28.10
55.2	Oe A	31.58	1.11	-27.69
55.2	Oe B	31.96	1.04	-27.83
55.2	Oa A	3.13	0.20	-26.37
55.2	Oa B	2.82	0.15	-26.34
55.3	Needle 0 A	48.62	1.30	-27.97
55.3	Needle O B	49.31	1.35	-28.04
55.3	Needle 3 A	49.72	1.14	-28.47
55.3	Needle 3 B	49.77	1.16	-28.48
55.3	Needle 5 A	48.44	0.94	-30.43
55.3	Needle 5 B	48.27	0.99	-30.40
55.3	Twig 0 A	51.26	0.84	-26.91
55.3	Twig O B	51.74	0.88	-26.77
55.3	Twig 3 A	50.39	0.59	-27.19
55.3	Twig 3 B	49.28	0.60	-27.17
55.3	Twig 5 A	48.92	0.59	-28.41
55.3	Twig 5 B	48.32	0.59	-28.40
55.3	Bark A	45.59	0.66	-26.51
55.3	Bark B	46.62	0.66	-26.34
55.3	Litter layer A	48.42	1.16	-27.88
55.3	Litter layer B	49.11	1.22	-27.84
55.3	Oi A	48.89	1.38	-27.86
55.3	Oi B	48.80	1.32	-27.82
55.3	Oe A	36.46	1.31	-27.30
55.3	Oe B	36.46	1.31	-26.95
55.3	Oa A	6.06	0.36	-26.24
55.3	Oa B	7.40	0.35	-26.18
55.4	Needle 0 A	47.68	1.24	-29.71
55.4	Needle O B	48.57	1.14	-29.74
55.4	Needle 3 A	48.78	1.08	-29.76
55.4	Needle 3 B	49.08	0.99	-29.85
55.4	Needle 5 A	47.39	1.01	-30.80
55.4	Needle 5 B	47.52	0.90	-30.70
55.4	Twig 0 A	49.73	0.86	-28.63
55.4	Twig O B	50.59	0.75	-28.51
55.4	Twig 3 A	48.79	0.62	-28.26
55.4	Twig 3 B	48.16	0.53	-28.29
55.4	Twig 5 A	48.09	0.64	-28.99
55.4	Twig 5 B	46.69	0.53	-29.03
55.4	Bark A	55.29	0.92	-24.99
55.4	Bark B	55.85	0.91	-25.19
55.4	Litter layer A	48.25	1.19	-27.80
55.4	Litter layer B	52.97	1.25	-27.77
55.4	Oi A	42.31	1.20	-27.68
55.4	Oi B	42.37	1.14	-27.73
55.4	Oe A	21.78	0.92	-26.60
55.4	Oe B	22.23	0.89	-26.65
55.4	Oa A	9.21	0.61	-26.70
55.4	Oa B	9.44	0.63	-26.79
55	Topsoil A	6.31	0.32	-26.36
55	Topsoil B	5.19	0.29	-26.12

Table 15: Elemental analysis 130-year-old forest, moss and lichen

Spot	Sample type	C [%]	N [%]	$\delta^{13}C$ [‰]
130.2	Needle 0 A	47.81	1.12	-31.21
130.2	Needle 0 B	47.87	1.07	-31.18
130.2	Needle 3 A	48.86	1.00	-31.41
130.2	Needle 3 B	48.87	1.03	-31.40
130.2	Needle 5 A	48.10	0.93	-31.36
130.2	Needle 5 B	48.76	0.95	-31.24
130.2	Twig 0 A	50.27	0.81	-30.51
130.2	Twig 0 B	49.57	0.79	-30.52
130.2	Twig 3 A	48.25	0.51	-29.63
130.2	Twig 3 B	48.69	0.49	-29.93
130.2	Twig 5 A	48.69	0.12	-29.43
130.2	Twig 5 B	48.57	0.12	-29.50
130.2	Bark A	48.62	0.53	-25.41
130.2	Bark B	48.82	0.57	-25.11
130.2	Litter layer A	37.03	0.66	-27.23
130.2	Litter layer B	37.25	0.67	-26.99
130.2	Oi A	41.36	0.76	-26.74
130.2	Oi B	40.74	0.77	-26.87
130.2	Oe A	31.18	0.76	-28.23
130.2	Oe B	31.16	0.77	-28.13
130.2	Oa A	21.26	0.56	-28.12
130.2	Oa B	21.31	0.59	-28.12
130.3	Needle 0 A	47.30	1.13	-31.02
130.3	Needle 0 B	47.87	1.03	-30.92
130.3	Needle 3 A	49.18	1.06	-31.42
130.3	Needle 3 B	48.93	1.03	-31.48
130.3	Needle 5 A	49.05	0.92	-31.89
130.3	Needle 5 B	48.89	0.91	-31.81
130.3	Twig 0 A	49.40	0.90	-30.33
130.3	Twig O B	48.95	0.79	-30.29
130.3	Twig 3 A	48.86	0.49	-29.62
130.3	Twig 3 B	49.73	0.49	-29.69
130.3	Twig 5 A	44.51	0.65	-29.44
130.3	Twig 5 B	48.71	0.61	-29.45
130.3	Bark A	45.41	1.14	-32.23
130.3	Bark B	46.15	1.16	-32.22
130.3	Litter layer A	47.34	1.03	-28.31
130.3	Litter layer B	47.56	1.05	-28.45
130.3	Oi A	42.22	1.08	-27.19
130.3	Oi B	42.01	1.06	-27.25
130.3	Oe A	27.37	1.08	-27.82
130.3	Oe B	26.47	1.06	-27.81
130.3	Oa A	38.21	1.29	-27.38
130.3	Oa B	30.26	1.06	-27.61
130.4	Needle 0 A	48.94	1.28	-29.55
130.4	Needle O B	48.66	1.13	-29.58
130.4	Needle 3 A	49.67	1.21	-29.80
130.4	Needle 3 B	49.84	1.11	-29.83
130.4	Needle 5 A	48.36	0.87	-30.35
130.4	Needle 5 B	47.13	0.90	-30.26
130.4	Twig 0 A	50.50	0.85	-28.51
130.4	Twig O B	50.07	0.69	-28.89
130.4	Twig 3 A	48.87	0.35	-28.10
130.4	Twig 3 B	49.21	0.24	-28.14
130.4	Twig 5 A	48.88	0.68	-28.50
130.4	Twig 5 B	36.70	0.64	-28.86
130.4	Bark A	48.27	0.95	-26.63
130.4	Bark B	48.11	0.99	-26.68
130.4	Litter layer A	47.24	1.17	-28.22
130.4	Litter layer B	47.98	1.07	-28.12
130.4	Oi A	39.24	0.60	-28.00
130.4	Oi B	38.02	0.54	-28.17
130.4	Oe A	10.86	0.60	-27.29
130.4	Oe B	10.17	0.54	-27.22
130.4	Oa A	8.56	0.50	-26.91
130.4	Oa B	7.74	0.51	-26.58
130	Topsoil A	5.93	0.28	-26.42
130	Topsoil B	6.05	0.31	-26.53
Mix	Moss A	43.41	1.71	-29.38
Mix	Moss B	42.37	1.72	-29.36
Mix	Lichen A	43.71	1.53	-25.62
Mix	Lichen B	43.67	1.56	-25.68

Table 16: n-Alkanes 40-year-old forest [μg g^{-1}]

Spot	Sample	C18	C19	C20	C21	C22	C23	C24	C25	C26	C27	C28	C29	C30	C31	C32	C33	C34
40.2	Needle 0	0.077	0.044	0.068	1.013	0.102	0.821	0.180	1.318	0.203	1.230	0.213	2.328	0.202	0.750	0.139	0.340	0.000
40.2	Needle 3	0.021	0.035	0.049	0.439	0.102	0.581	0.150	0.731	0.162	0.934	0.284	1.860	0.292	1.024	0.141	0.416	0.034
40.2	Needle 5	0.081	0.114	0.144	1.006	0.219	0.735	0.192	0.665	0.187	0.891	0.308	1.526	0.320	1.046	0.193	0.448	0.057
40.2	Twig 0	0.016	0.054	0.080	0.000	0.127	2.632	0.187	2.106	0.209	2.345	0.162	1.436	0.142	0.578	0.062	0.072	0.040
40.2	Twig 3	0.125	0.457	0.314	1.605	0.513	4.095	0.360	1.795	0.312	2.189	0.583	3.911	0.455	2.106	0.113	0.319	0.051
40.2	Twig 5	0.073	0.150	0.166	0.830	0.359	2.273	0.252	0.913	0.176	0.849	0.267	1.418	0.260	0.962	0.067	0.166	0.226
40.2	Bark	0.036	0.105	0.044	0.000	0.175	0.146	0.150	0.230	0.053	0.276	0.065	0.411	0.072	0.280	0.026	0.000	0.000
40.2	Litter	0.045	0.077	0.131	0.262	0.204	0.759	0.373	1.997	0.783	8.789	0.990	13.547	0.679	3.123	0.265	2.074	0.057
40.2	Oi	0.035	0.041	0.086	2.399	0.142	0.717	0.202	0.755	0.293	2.551	0.422	4.396	0.286	3.426	0.136	0.974	0.000
40.2	Oe	0.126	0.072	0.192	0.210	0.231	0.315	0.337	0.347	0.211	1.116	0.361	2.496	0.304	3.441	0.255	2.457	0.057
40.2	Oa	0.106	0.074	0.245	0.233	0.268	0.316	0.375	0.492	0.226	1.329	0.444	2.863	0.325	4.118	0.291	3.086	0.067
40.3	Needle 0	0.072	0.041	0.053	0.141	0.124	1.066	0.248	1.409	0.239	1.254	0.271	2.017	0.167	0.628	0.052	0.161	0.052
40.3	Needle 3	0.069	0.069	0.080	0.147	0.124	0.614	0.212	0.590	0.187	0.818	0.383	2.026	0.321	1.169	0.166	0.428	0.077
40.3	Needle 5	0.075	0.071	0.075	0.155	0.105	0.484	0.199	0.569	0.180	0.745	0.397	2.019	0.308	1.071	0.137	0.000	0.035
40.3	Twig 0	0.054	0.071	0.042	0.259	0.102	1.622	0.202	1.001	0.125	0.879	0.142	1.100	0.126	0.501	0.028	0.044	0.021
40.3	Twig 3	0.109	0.166	0.134	0.543	0.240	2.073	0.261	1.075	0.200	1.018	0.361	1.987	0.292	1.234	0.065	0.005	0.025
40.3	Twig 5	0.095	0.078	0.041	0.237	0.102	1.073	0.133	0.487	0.084	0.502	0.138	0.873	0.108	0.020	0.031	0.009	0.023
40.3	Bark	0.043	0.088	0.322	0.000	0.166	0.897	0.175	0.359	0.053	0.258	0.054	0.334	0.070	0.238	0.000	0.000	0.000
40.3	Litter	0.061	0.056	0.101	0.191	0.153	0.384	0.183	0.393	0.148	0.799	0.261	1.823	0.235	1.306	0.107	0.441	0.042
40.3	Oi	0.031	0.058	0.112	0.297	0.302	0.961	0.262	0.895	0.274	2.565	0.404	5.134	0.366	4.743	0.155	1.146	0.039
40.3	Oe	0.026	0.041	0.089	0.149	0.146	0.363	0.162	0.229	0.093	0.493	0.131	1.027	0.157	1.312	0.121	0.754	0.000
40.3	Oa	0.005	0.003	0.009	0.008	0.010	0.011	0.013	0.013	0.007	0.033	0.011	0.076	0.011	0.101	0.008	0.053	0.000
40.4	Needle 0	0.034	0.034	0.044	0.122	0.107	2.839	0.303	2.657	0.230	1.171	0.142	1.450	0.086	0.480	0.050	0.000	0.023
40.4	Needle 3	0.071	0.077	0.078	0.139	0.117	0.696	0.198	1.025	0.244	1.475	0.458	2.542	0.300	1.027	0.164	0.324	0.096
40.4	Needle 5	0.092	0.084	0.097	0.179	0.129	0.634	0.179	0.735	0.168	0.767	0.313	1.682	0.340	1.215	0.165	0.466	0.047
40.4	Twig 0	0.089	0.058	0.067	0.000	0.085	0.951	0.167	1.015	0.137	0.834	0.089	0.965	0.121	1.818	0.078	1.578	0.037
40.4	Twig 3	0.093	0.170	0.102	0.503	0.199	1.756	0.216	1.193	0.175	1.056	0.333	2.126	0.315	1.256	0.066	0.000	0.026
40.4	Twig 5	0.124	0.125	0.133	0.485	0.262	1.739	0.263	1.002	0.168	0.950	0.293	1.823	0.279	1.263	0.058	0.170	0.022
40.4	Bark	0.002	0.003	0.005	0.013	0.008	0.030	0.007	0.015	0.003	0.021	0.004	0.036	0.004	0.027	0.002	0.011	0.000
40.4	Litter	0.113	0.094	0.118	0.232	0.151	0.701	0.199	0.502	0.124	0.802	0.191	1.323	0.217	1.005	0.099	0.384	0.027
40.4	Oi	0.033	0.040	0.104	0.253	0.196	0.922	0.235	0.798	0.191	1.396	0.314	2.094	0.287	1.561	0.090	0.000	0.000
40.4	Oe	0.075	0.050	0.133	0.215	0.188	0.306	0.126	0.322	0.143	0.847	0.219	1.731	0.255	1.722	0.160	0.619	0.033
40.4	Oa	0.025	0.038	0.167	0.236	0.253	0.306	0.338	0.427	0.258	1.190	0.518	2.764	0.342	3.801	0.246	1.811	0.057
40	Topsoil	0.099	0.078	0.128	0.170	0.130	0.229	0.199	0.416	0.176	1.007	0.368	2.745	0.310	4.106	0.244	2.460	0.058

Table 17: n-Alkanes 55-year-old forest [μg g^{-1}]

Spot	Sample	C18	C19	C20	C21	C22	C23	C24	C25	C26	C27	C28	C29	C30	C31	C32	C33	C34
55.2	Needle 0	0.027	0.032	0.049	0.126	0.088	1.426	0.256	2.004	0.221	1.278	0.208	1.680	0.137	0.575	0.057	0.178	0.022
55.2	Needle 3	0.047	0.063	0.075	0.179	0.124	0.894	0.180	1.066	0.194	1.171	0.291	2.143	0.247	1.515	0.126	0.409	0.041
55.2	Needle 5	0.016	0.044	0.062	0.188	0.113	0.686	0.180	0.659	0.127	0.580	0.200	0.990	0.172	0.611	0.066	0.260	0.033
55.2	Twig 0	0.060	0.064	0.098	0.430	0.124	2.497	0.241	1.341	0.123	0.921	0.124	1.159	0.118	0.617	0.028	0.000	0.000
55.2	Twig 3	0.124	0.177	0.139	0.658	0.261	2.920	0.279	1.496	0.214	1.526	0.321	2.348	0.194	1.683	0.083	0.227	0.033
55.2	Twig 5	0.019	0.083	0.117	0.723	0.291	2.485	0.278	1.163	0.166	0.992	0.236	1.375	0.207	0.961	0.056	0.156	0.022
55.2	Bark	0.014	0.040	0.054	0.134	0.085	0.318	0.114	0.183	0.047	0.336	0.056	0.422	0.059	0.231	0.030	0.080	0.013
55.2	Litter	0.094	0.120	0.155	0.556	0.257	1.902	0.261	1.408	0.170	1.386	0.231	1.689	0.194	1.006	0.108	0.400	0.038
55.2	Oi	0.052	0.065	0.129	0.249	0.169	1.140	0.198	0.349	0.076	0.579	0.107	0.657	0.119	0.526	0.062	0.185	0.000
55.2	Oe	0.063	0.063	0.137	0.200	0.184	0.559	0.296	0.224	0.102	0.454	0.115	0.743	0.113	0.617	0.077	0.236	0.000
55.2	Oa	0.018	0.033	0.170	0.139	0.218	0.171	0.344	0.160	0.130	0.356	0.139	0.747	0.109	0.879	0.074	0.373	0.026
55.3	Needle 0	0.053	0.053	0.072	0.147	0.151	1.529	0.390	2.585	0.344	1.526	0.278	2.243	0.177	0.000	0.090	0.000	0.040
55.3	Needle 3	0.062	0.105	0.126	0.272	0.185	0.767	0.240	1.092	0.303	1.527	0.491	2.689	0.331	1.371	0.151	0.000	0.072
55.3	Needle 5	0.056	0.126	0.110	0.329	0.164	0.681	0.200	0.723	0.189	1.110	0.303	1.740	0.223	0.968	0.180	0.000	0.070
55.3	Twig 0	0.113	0.167	0.095	0.398	0.146	1.760	0.215	1.157	0.160	0.992	0.196	1.721	0.228	0.773	0.041	0.083	0.023
55.3	Twig 3	0.170	0.628	0.456	2.502	0.766	3.958	0.484	1.653	0.366	1.793	0.716	3.868	0.739	3.040	0.214	0.000	0.051
55.3	Twig 5	0.304	1.395	0.617	3.717	0.930	5.045	0.489	1.521	0.333	1.726	0.542	2.657	0.366	1.728	0.123	0.032	0.042
55.3	Bark	0.023	0.065	0.097	0.416	0.194	1.210	0.157	0.584	0.058	0.525	0.054	0.705	0.050	0.626	0.005	0.000	0.000
55.3	Litter	0.034	0.048	0.094	0.213	0.162	0.845	0.317	1.768	0.745	7.569	0.879	15.628	0.552	17.216	0.372	3.184	0.058
55.3	Oi	0.027	0.046	0.094	0.185	0.171	0.644	0.228	1.096	0.209	2.613	0.215	2.667	0.210	2.708	0.101	0.488	0.025
55.3	Oe	0.070	0.056	0.106	0.184	0.156	0.697	0.199	0.328	0.121	0.661	0.149	1.197	0.160	1.200	0.113	0.499	0.040
55.3	Oa	0.023	0.048	0.251	0.170	0.277	0.393	0.413	0.237	0.181	0.589	0.224	1.182	0.182	1.468	0.132	0.764	0.037
55.4	Needle 0	0.035	0.038	0.047	0.099	0.085	1.763	0.310	2.940	0.206	1.294	0.151	1.452	0.085	0.450	0.014	0.000	0.000
55.4	Needle 3	0.017	0.017	0.087	0.105	0.112	0.885	0.221	1.107	0.163	1.027	0.222	1.517	0.169	0.760	0.069	0.189	0.000
55.4	Needle 5	0.032	0.045	0.122	0.149	0.142	0.672	0.231	0.912	0.166	1.066	0.228	1.549	0.156	0.768	0.066	0.178	0.000
55.4	Twig 0	0.074	0.075	0.070	0.248	0.124	0.155	0.440	3.904	0.185	1.517	0.163	1.947	0.185	0.978	0.042	0.050	0.020
55.4	Twig 3	0.024	0.047	0.126	0.350	0.190	1.397	0.237	1.172	0.181	1.318	0.290	2.171	0.236	1.229	0.050	0.000	0.000
55.4	Twig 5	0.078	0.097	0.192	0.567	0.326	1.496	0.306	0.996	0.197	1.206	0.302	1.936	0.211	1.139	0.080	0.000	0.000
55.4	Bark	0.000	0.000	0.000	0.000	0.000	0.000	0.000	0.000	0.000	0.000	0.000	0.000	0.000	0.000	0.000	0.000	0.000
55.4	Litter	0.045	0.046	0.086	0.153	0.156	0.474	0.378	2.114	1.361	11.935	2.182	22.459	0.920	15.310	0.331	2.525	0.068
55.4	Oi	0.111	0.065	0.117	0.179	0.152	0.864	0.306	1.150	0.581	4.594	0.762	8.754	0.381	6.690	0.195	1.261	0.047
55.4	Oe	0.088	0.067	0.236	0.155	0.233	0.238	0.364	0.228	0.146	0.582	0.161	0.982	0.142	1.101	0.084	0.478	0.030
55.4	Oa	0.036	0.041	0.196	0.130	0.213	0.155	0.321	0.184	0.143	0.476	0.192	1.033	0.147	1.520	0.107	0.794	0.000
55	Topsoil	0.075	0.092	0.138	0.197	0.153	0.235	0.285	0.350	0.186	0.781	0.293	1.846	0.256	2.509	0.181	1.326	0.046

Table 18: n-Alkanes 130-year-old forest, moss and lichen [μg g^{-1}]

Spot	Sample	C18	C19	C20	C21	C22	C23	C24	C25	C26	C27	C28	C29	C30	C31	C32	C33	C34
130.2	Needle 0	0.024	0.031	0.041	0.096	0.077	3.130	0.381	2.982	0.156	0.949	0.116	1.094	0.081	0.450	0.038	0.179	0.000
130.2	Needle 3	0.021	0.058	0.063	0.142	0.099	1.189	0.187	0.918	0.088	0.501	0.121	0.844	0.089	0.524	0.040	0.199	0.031
130.2	Needle 5	0.021	0.049	0.073	0.150	0.101	1.037	0.188	0.790	0.081	0.429	0.108	0.631	0.086	0.390	0.040	0.133	0.021
130.2	Twig 0	0.026	0.064	0.088	0.539	0.164	7.685	0.569	3.139	0.105	0.728	0.068	0.944	2.667	0.510	0.017	0.000	0.000
130.2	Twig 3	0.058	0.108	0.100	0.625	0.202	3.207	0.302	1.306	0.130	1.150	0.195	1.776	0.165	0.937	0.035	0.121	0.000
130.2	Twig 5	0.033	0.069	0.094	0.529	0.182	2.177	0.207	0.791	0.101	0.796	0.153	1.160	0.112	0.648	0.033	0.000	0.000
130.2	Bark	0.064	0.104	0.085	5.832	0.168	1.948	0.197	0.743	0.033	0.182	0.028	0.202	0.026	0.106	0.015	0.000	0.000
130.2	Litter	0.037	0.059	0.126	0.223	0.173	0.699	0.220	0.307	0.086	0.425	0.110	0.804	0.101	0.544	0.054	0.221	0.028
130.2	Oi	0.077	0.094	0.148	0.267	0.181	0.868	0.238	0.438	0.076	0.437	0.096	0.914	0.095	0.454	0.033	0.117	0.027
130.2	Oe	0.043	0.057	0.122	0.167	0.151	0.306	0.240	0.146	0.090	0.333	0.088	0.678	0.102	0.567	0.048	0.198	0.000
130.2	Oa	0.056	0.070	0.155	0.193	0.184	0.291	0.317	0.197	0.116	0.435	0.078	0.858	0.128	0.545	0.050	0.000	0.000
130.3	Needle 0	0.145	0.148	0.322	0.298	0.272	0.166	0.442	0.138	0.134	0.308	0.100	0.816	0.126	0.715	0.064	0.416	0.009
130.3	Needle 3	0.020	0.036	0.049	0.109	0.063	0.372	0.107	0.462	0.099	0.583	0.168	0.992	0.134	0.572	0.079	0.232	0.032
130.3	Needle 5	0.012	0.023	0.044	0.078	0.062	0.199	0.125	0.174	0.071	0.345	0.111	0.565	0.092	0.397	0.042	0.000	0.000
130.3	Twig 0	0.039	0.037	0.109	0.308	0.121	1.584	0.150	0.727	0.091	0.669	0.106	0.896	0.114	0.564	0.043	0.073	0.000
130.3	Twig 3	0.038	0.069	0.096	0.449	0.189	1.468	0.202	0.933	0.149	1.242	0.219	1.763	0.189	1.160	0.063	0.230	0.020
130.3	Twig 5	0.019	0.056	0.080	0.379	0.185	1.157	0.192	0.616	0.104	0.862	0.172	1.173	0.136	0.854	0.085	0.202	0.019
130.3	Bark	0.000	0.000	0.000	0.000	0.000	0.000	0.000	0.000	0.000	0.000	0.000	0.000	0.000	0.000	0.000	0.000	0.000
130.3	Litter	0.046	0.064	0.113	0.272	0.168	1.009	0.191	0.549	0.098	0.615	0.148	1.115	0.147	0.704	0.076	0.263	0.021
130.3	Oi	0.042	0.068	0.099	0.198	0.161	0.679	0.172	0.378	0.078	0.461	0.104	0.738	0.090	0.612	0.038	0.160	0.036
130.3	Oe	0.107	0.098	0.178	0.260	0.213	0.512	0.318	0.319	0.121	0.553	0.128	0.952	0.135	0.778	0.078	0.275	0.000
130.3	Oa	0.109	0.089	0.149	0.223	0.184	0.399	0.286	0.256	0.110	0.464	0.121	0.965	0.140	0.764	0.071	0.291	0.000
130.4	Needle 0	0.049	0.050	0.187	0.164	0.202	0.305	0.314	0.316	0.148	1.056	0.157	1.505	0.128	1.528	0.059	0.452	0.017
130.4	Needle 3	0.032	0.031	0.048	0.088	0.060	0.608	0.138	1.242	0.189	1.308	0.252	1.741	0.149	0.522	0.073	0.000	0.000
130.4	Needle 5	0.024	0.037	0.074	0.181	0.119	0.489	0.143	0.515	0.114	0.695	0.190	1.094	0.149	0.551	0.072	0.161	0.032
130.4	Twig 0	0.066	0.080	0.081	15.694	0.119	3.190	0.178	1.257	0.120	0.978	0.125	1.205	0.130	0.570	0.047	0.000	0.000
130.4	Twig 3	0.059	0.111	0.096	0.507	0.184	2.356	0.201	1.316	0.171	1.402	0.272	2.262	0.233	1.209	0.049	0.185	0.030
130.4	Twig 5	0.037	0.052	0.114	0.344	0.184	1.587	0.172	0.965	0.122	0.965	0.177	1.415	0.140	0.768	0.045	0.145	0.021
130.4	Bark	0.026	0.032	0.060	0.141	0.092	0.853	0.129	0.481	0.072	0.830	0.098	1.208	0.085	1.053	0.047	0.243	0.011
130.4	Litter	0.105	0.061	0.153	0.826	0.168	0.830	0.183	0.485	0.119	0.762	0.163	1.236	0.169	1.268	0.098	0.389	0.038
130.4	Oi	0.046	0.046	0.085	0.152	0.134	0.489	0.196	0.783	0.244	3.641	0.344	6.356	0.280	7.905	0.160	1.521	0.036
130.4	Oe	0.059	0.066	0.183	0.192	0.207	0.359	0.282	0.357	0.146	0.941	0.174	1.483	0.128	1.470	0.066	0.498	0.022
130.4	Oa	0.049	0.050	0.187	0.164	0.202	0.305	0.314	0.316	0.148	1.056	0.157	1.505	0.128	1.528	0.059	0.452	0.017
130	Topsoil	0.145	0.148	0.322	0.298	0.272	0.166	0.442	0.138	0.134	0.308	0.100	0.816	0.126	0.715	0.064	0.416	0.009
Mix	Moss	0.108	0.000	0.187	0.764	0.361	1.384	0.289	2.928	0.394	11.982	0.423	4.418	0.406	3.562	0.203	1.086	1.055
Mix	Lichen	0.059	0.161	0.164	0.613	0.413	1.281	0.263	1.200	0.224	1.897	0.282	2.668	0.277	2.474	0.181	0.829	0.067

Table 19: Fatty acids 40-year-old forest [μg g^{-1}]

Spot	Sample type	C20	C22	C24	C26	C28	C30	C32	D20	D22	D24
40.2	Needle 0	12.662	18.637	20.215	8.948	6.009	8.329	2.970	1.053	1.332	3.433
40.2	Needle 3	52.787	75.305	88.934	42.013	19.103	25.763	11.122	0.000	2.857	0.000
40.2	Needle 5	58.816	77.523	72.989	22.674	10.975	15.429	6.628	3.502	6.246	2.338
40.2	Twig 0	584.140	1208.466	933.473	46.751	103.630	125.818	39.087	36.973	39.744	20.133
40.2	Twig 3	854.427	1404.449	1027.512	13.807	31.006	76.295	47.985	38.659	49.538	33.193
40.2	Twig 5	409.881	794.924	724.901	9.326	10.589	22.664	27.560	23.875	35.890	31.166
40.2	Bark	174.050	276.141	238.820	7.374	4.400	8.459	1.721	24.437	22.258	9.703
40.2	Litter	276.730	512.249	387.991	17.361	120.148	141.745	26.911	26.023	33.163	22.975
40.2	Oi	139.070	270.585	205.450	21.678	48.020	67.635	23.007	13.548	18.442	11.532
40.2	Oe	45.346	62.260	58.374	23.856	20.373	22.714	12.906	5.246	8.093	5.686
40.2	Oa	33.831	38.267	34.509	13.822	8.701	7.363	4.159	2.522	3.006	1.705
40.3	Needle 0	68.116	149.705	184.605	84.909	25.936	23.733	5.880	1.304	2.312	1.672
40.3	Needle 3	36.572	59.743	72.673	34.450	13.955	21.518	9.596	0.000	8.131	0.000
40.3	Needle 5	29.387	57.023	78.202	53.715	17.423	28.457	11.103	0.000	1.544	0.000
40.3	Twig 0	862.209	1541.017	1424.494	522.225	110.621	48.610	17.931	33.422	45.816	3.751
40.3	Twig 3	523.770	967.432	1023.301	76.603	29.152	40.591	17.883	20.481	30.503	18.754
40.3	Twig 5	350.412	746.167	828.247	322.847	36.807	26.710	10.952	16.298	25.462	1.902
40.3	Bark	205.063	343.089	406.832	64.931	5.326	5.228	2.087	26.958	31.040	64.670
40.3	Litter	304.293	569.509	435.568	19.744	22.044	50.507	23.530	26.061	30.366	16.161
40.3	Oi	238.557	452.458	364.770	40.074	30.165	54.242	25.497	23.139	27.345	18.914
40.3	Oe	84.068	179.906	140.782	2.881	16.567	39.608	18.754	11.551	11.913	4.214
40.3	Oa	27.824	28.393	31.664	0.409	12.198	10.164	5.086	2.475	4.005	2.483
40.4	Needle 0	79.553	130.262	246.823	161.068	43.803	38.279	9.859	1.123	1.071	0.662
40.4	Needle 3	43.384	61.202	96.646	59.439	23.627	33.171	12.610	0.000	1.648	1.483
40.4	Needle 5	34.905	43.591	66.267	37.414	14.703	26.099	13.787	0.000	1.781	0.000
40.4	Twig 0	233.189	673.341	486.602	32.939	83.952	52.372	14.610	19.552	21.919	114.065
40.4	Twig 3	473.435	984.374	851.197	41.539	22.786	44.784	19.175	22.865	34.734	24.331
40.4	Twig 5	285.271	521.814	481.872	25.371	16.157	25.962	13.575	13.510	22.291	14.735
40.4	Bark	531.574	1080.030	1153.010	23.123	39.487	73.253	21.998	88.140	119.701	91.542
40.4	Litter	96.122	196.914	153.696	21.648	14.970	25.700	13.940	7.374	7.541	4.192
40.4	Oi	256.318	535.778	462.775	33.658	26.305	61.233	34.258	24.438	29.242	18.945
40.4	Oe	176.628	221.916	185.739	1.700	22.488	38.405	21.313	23.634	23.217	9.489
40.4	Oa	20.366	14.197	13.869	9.082	7.781	5.706	2.619	0.774	1.522	0.823
40	Topsoil	7.951	8.729	9.100	4.745	2.722	1.617	0.633	0.488	0.670	0.281

Table 20: Fatty acids 55-year-old forest [μg g^{-1}]

Spot	Sample type	C20	C22	C24	C26	C28	C30	C32	D20	D22	D24
55.2	Needle 0	30.842	55.294	77.419	39.159	9.959	9.704	3.048	0.000	0.694	0.431
55.2	Needle 3	32.277	70.574	111.378	69.685	27.111	26.109	11.259	0.000	0.000	0.000
55.2	Needle 5	22.764	42.142	68.885	36.943	12.986	21.556	7.187	0.866	1.727	1.212
55.2	Twig 0	256.357	524.487	339.751	32.491	30.542	20.943	7.831	9.752	11.749	1.361
55.2	Twig 3	442.633	892.053	607.270	9.005	29.545	46.105	25.308	17.765	24.653	13.979
55.2	Twig 5	256.173	558.466	402.006	8.887	12.345	20.340	10.527	10.307	17.228	9.586
55.2	Bark	60.414	166.469	130.173	1.314	4.050	6.109	0.874	11.335	14.297	8.861
55.2	Litter	101.992	226.323	186.017	33.795	15.299	32.478	16.891	11.785	14.410	8.457
55.2	Oi	174.051	319.631	218.871	191.557	46.380	53.431	13.669	13.926	17.820	7.747
55.2	Oe	58.824	108.401	73.655	2.717	6.339	12.831	5.757	6.759	6.879	2.628
55.2	Oa	4.491	5.458	5.027	2.628	1.861	1.602	0.752	0.000	0.000	0.000
55.3	Needle 0	77.316	135.736	202.080	106.833	34.613	32.779	10.489	0.000	0.000	0.000
55.3	Needle 3	55.000	79.689	100.308	59.036	26.341	37.400	16.844	0.000	2.594	1.428
55.3	Needle 5	37.885	47.286	57.933	32.363	16.734	18.326	6.904	0.000	0.000	0.000
55.3	Twig 0	887.566	1514.670	1255.953	176.979	87.276	87.370	32.730	30.410	46.528	2.413
55.3	Twig 3	839.552	1357.745	1092.038	32.781	47.751	103.602	60.089	31.874	44.675	30.831
55.3	Twig 5	719.109	1204.352	843.582	8.532	22.808	37.982	13.859	30.828	40.995	30.592
55.3	Bark	301.317	553.079	494.835	56.337	3.646	5.523	0.743	19.113	26.739	15.458
55.3	Litter	132.152	279.962	220.838	9.726	13.658	29.736	16.610	11.759	14.359	7.197
55.3	Oi	119.522	239.281	196.602	8.777	23.180	33.247	15.004	10.920	12.970	15.004
55.3	Oe	104.740	179.823	133.685	6.118	15.515	23.671	11.505	13.429	13.662	11.505
55.3	Oa	7.033	9.923	8.349	3.553	2.683	2.244	1.083	0.497	0.562	0.250
55.4	Needle 0	107.386	193.801	257.767	134.724	59.810	63.772	14.219	1.812	1.895	0.000
55.4	Needle 3	47.107	76.703	96.499	52.548	27.305	38.027	10.939	0.000	1.304	0.999
55.4	Needle 5	44.910	57.669	65.642	34.647	22.785	37.936	9.994	0.000	1.178	0.943
55.4	Twig 0	1029.421	1631.577	779.086	66.362	86.594	103.465	40.341	43.598	51.762	22.288
55.4	Twig 3	602.081	914.884	464.918	12.704	28.758	71.107	34.388	24.475	32.302	19.001
55.4	Twig 5	368.678	560.086	283.518	48.697	12.338	25.345	10.446	18.010	23.363	15.077
55.4	Bark	210.604	340.215	324.791	30.927	7.578	0.000	0.000	60.578	36.295	9.032
55.4	Litter	79.043	129.574	121.229	17.621	63.677	82.780	14.844	6.254	7.658	3.903
55.4	Oi	153.543	284.461	204.215	17.332	48.154	55.172	13.980	17.350	18.652	8.665
55.4	Oe	29.364	48.641	40.173	8.813	5.238	6.948	2.883	4.643	4.238	1.712
55.4	Oa	10.534	16.813	16.080	5.934	4.768	4.670	2.232	1.486	1.607	1.217
55	Topsoil	6.370	7.884	6.809	3.168	2.533	2.030	0.938	0.595	0.798	0.497

Table 21: Fatty acids 130-year-old forest, moss and lichen [μg g^{-1}]

Spot	Sample type	C20	C22	C24	C26	C28	C30	C32	D20	D22	D24
130.2	Needle 0	157.158	184.156	179.073	102.896	4.158	49.348	13.146	2.154	2.519	1.256
130.2	Needle 3	-	-	-	-	-	-	-	-	-	-
130.2	Needle 5	54.038	93.720	95.548	43.730	25.414	41.189	16.505	1.522	4.502	1.688
130.2	Twig 0	627.478	1256.836	724.947	122.475	90.529	89.340	32.012	29.449	42.753	17.444
130.2	Twig 3	514.608	989.918	547.638	42.670	35.414	57.482	32.774	24.650	40.430	20.342
130.2	Twig 5	164.602	309.718	164.921	12.359	7.089	12.020	5.072	7.296	13.335	5.806
130.2	Bark	237.987	618.766	854.986	117.876	5.347	3.072	0.000	33.309	8.227	2.720
130.2	Litter	166.253	355.979	317.700	16.367	12.637	33.125	19.211	15.347	20.487	14.154
130.2	Oi	144.664	368.679	418.212	27.836	15.293	26.318	14.030	17.946	28.435	18.320
130.2	Oe	54.687	115.487	96.528	0.948	5.188	14.233	6.302	6.422	7.176	2.796
130.2	Oa	32.436	70.306	64.524	14.614	8.337	13.388	7.856	7.619	8.793	3.455
130.3	Needle 0	127.039	156.923	204.720	131.392	51.232	61.643	18.314	1.113	2.019	1.086
130.3	Needle 3	29.794	52.515	71.229	44.133	22.738	42.432	19.592	0.831	1.958	0.831
130.3	Needle 5	21.586	31.200	38.027	20.114	10.375	17.262	9.603	0.962	1.120	0.943
130.3	Twig 0	808.138	1274.745	699.253	28.668	76.495	88.635	33.303	31.992	40.509	59.599
130.3	Twig 3	522.724	881.183	469.754	15.966	20.495	51.600	21.840	24.117	40.688	19.693
130.3	Twig 5	441.052	737.015	377.215	14.193	8.710	19.864	3.143	22.209	38.283	10.474
130.3	Bark	16.655	31.153	23.619	19.649	52.759	50.834	4.402	1.436	1.927	0.505
130.3	Litter	56.494	138.533	122.230	23.302	11.097	22.539	10.254	4.274	7.636	4.314
130.3	Oi	213.573	527.684	406.669	14.041	17.531	33.076	20.316	21.734	34.199	18.984
130.3	Oe	61.193	127.818	101.905	1.899	6.881	13.367	6.365	8.175	8.868	3.524
130.3	Oa	65.966	194.203	157.717	2.210	10.546	20.352	10.727	10.680	12.729	6.735
130.4	Needle 0	87.416	149.363	182.965	115.669	47.130	38.108	8.973	0.000	1.654	0.000
130.4	Needle 3	33.854	69.811	88.320	50.956	25.538	27.559	9.754	0.000	1.550	0.787
130.4	Needle 5	39.045	65.314	68.569	31.812	14.318	18.719	5.469	0.000	1.409	0.636
130.4	Twig 0	794.989	1304.877	1032.016	1059.455	86.962	67.179	23.748	37.161	43.586	91.133
130.4	Twig 3	417.710	745.889	607.140	16.945	25.908	40.981	19.244	16.595	24.981	18.179
130.4	Twig 5	388.241	583.389	484.467	16.801	14.096	22.803	9.400	15.496	25.174	18.947
130.4	Bark	94.407	249.740	279.284	42.014	8.077	11.390	1.487	11.463	18.244	13.599
130.4	Litter	64.615	132.732	107.380	8.255	10.161	20.978	9.820	4.046	4.496	2.202
130.4	Oi	53.261	108.601	87.843	5.963	18.669	24.913	4.118	4.701	5.507	2.300
130.4	Oe	17.869	30.093	25.979	0.838	4.675	5.570	1.191	1.603	1.610	0.712
130.4	Oa	9.395	14.824	11.133	2.240	1.918	2.085	0.521	0.871	0.803	0.000
130	Topsoil	5.285	10.153	7.861	1.521	0.896	0.863	0.578	0.666	0.392	0.158
Mix	Moss	19.114	41.493	45.477	24.231	22.258	8.777	2.233	1.186	0.669	0.470
Mix	Lichen	14.813	20.375	23.519	10.413	6.980	9.660	3.435	1.222	1.541	3.980

11 Personal declaration

I hereby declare that the submitted Thesis is the result of my own, independent work. All external sources are explicitly acknowledged in the Thesis.

Murten, 06^{th} of April

Nils Güntert